Instrumentation of the Maumee River Crossing

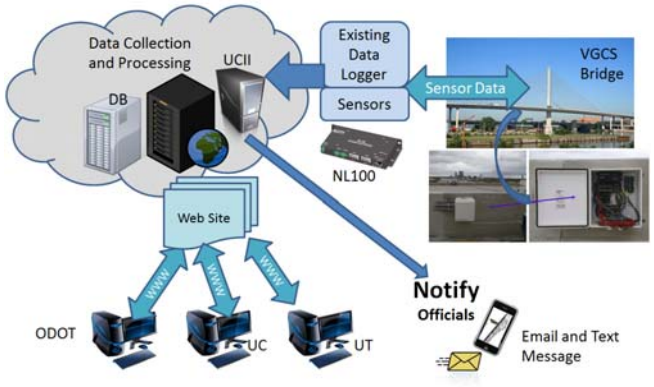

Arthur J. Helmicki, Victor J. Hunt
University of Cincinnati
Infrastructure Institute

Douglas K. Nims
University of Toledo

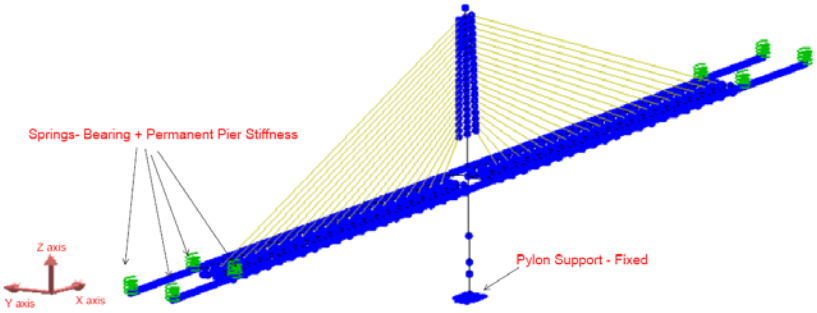

for the
Ohio Department of Transportation
Office of Research and Development

and the

Federal Highway Administration

State Job Number 426354

March, 2012

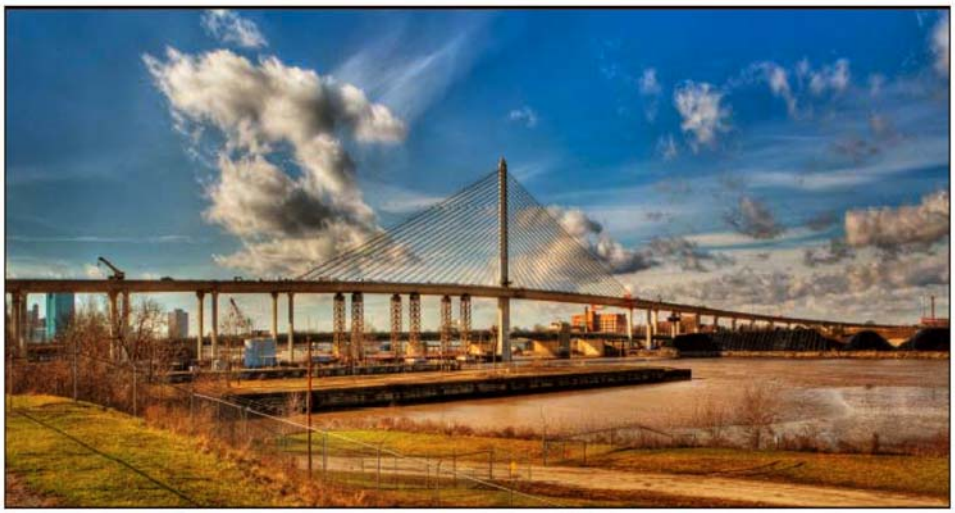

RESEARCH & DEVELOPMENT

1. Report No.	2. Government Accession No.	3. Recipient's Catalog No.
FHWA/OH-2012/2		

4. Title and subtitle	5. Report Date
Instrumentation of the Maumee River Crossing	**March 2012**
	6. Performing Organization Code

7. Author(s)	8. Performing Organization Report No.
Arthur Helmicki, Victor Hunt, Douglas Nims	10. Work Unit No. (TRAIS)

9. Performing Organization Name and Address	11. Contract or Grant No.
University of Cincinnati **Infrastructure Institute** **ML 0030** **Cincinnati, OH 45221-0030**	**426354**

12. Sponsoring Agency Name and Address	13. Type of Report and Period Covered
Ohio Department of Transportation **1980 West Broad Street** **Columbus, Ohio 43223**	**Final Report**
	14. Sponsoring Agency Code

15. Supplementary Notes

Prepared in cooperation with the U.S. Department of Transportation, Federal Highway Administration

16. Abstract

This project has focused on the instrumentation, monitoring and testing of the main span unit of the VGCS, one of Ohio's first long-span, cable-stayed bridges and one of only a few dozen such bridges in service in the nation. This effort looked at five main areas: (1) health monitoring; assessment of the changes in force distribution and bridge condition during erection and early service, (2) verification of design assumptions during erection, (3) investigation of the unique design features which have been incorporated into the VGCS, (4) investigation into the unique erection features and sequencing which will be used during its construction, and (5) investigation of stay cable vibration which is a general, unresolved issue for bridges of this type.

The purpose of this and associated documents is to outline the completed scientific study, which happened to consist primarily of two phases. The first phase (Nims, 2002), contracted at the District level, included the initial structural analysis, modeling, instrumentation package design for the monitor, and casting into the segments of the embedded sensors. The goal of this first phase was to capture the critical instrumentation issues associated with this construction project and to develop a detailed instrumentation and testing in close consultation with ODOT officials, bridge designers, and construction contractors.

The second phase (Helmicki, 2003), contracted through Central Office, included permanent instrumentation operated through a computer controlled, digital data acquisition system located on-site and accessible tele-remotely via direct fiber optic internet connection, field calibration of a main span finite element model using truckload and modal field tests; verification of various design assumptions and erection load conditions; creation of a database of measurements for use as a supplement to the designer's maintenance manual to provide guidance for conducting future maintenance, and determination of vibration performance of stay cable damping system under wind and rain-induced excitation.

The goal of the second phase was to finish the monitor installation begun in the first phase, establish a baseline concept of structural behavior and performance by utilizing a combination of field tests and ambient monitoring, capturing the overall structural concept by calibration of the finite element models, and finally benchmarking the condition of the structure by comparison of the above with its design values.

17. Key Words		18. Distribution Statement
Bridge Monitoring	Condition Assessment	No restrictions. This document is available to the public through the National Technical Information Service, Springfield, Virginia 22161
Truckload Test	Modal Test	
Load Rating	Nondestructive Evaluation	
Structural Identification		

19. Security Classif. (of this report)	20. Security Classif. (of this page)	21. No. of Pages	22. Price
Unclassified	Unclassified		

Instrumentation of the Maumee River Crossing

Arthur J Helmicki, Ph.D.
Professor, University of Cincinnati Infrastructure Institute, School of Electronic and Computing Systems, University of Cincinnati, Cincinnati, OH 45221-0030

Victor J Hunt, Ph.D.
Research Associate Professor, University of Cincinnati Infrastructure Institute, School of Electronic and Computing Systems, University of Cincinnati, Cincinnati, OH 45221-0030

Douglas K. Nims, Ph.D.
Associate Professor, Dept. of Civil Engineering, University of Toledo, Toledo, OH 43606-3390

Report # UC-CII 12/3
University of Cincinnati Infrastructure Institute
College of Engineering
Cincinnati, OH 45221-0071

March 2012

A Report to Sponsors:
U.S. Department of Transportation
Federal Highway Administration
and
Ohio Department of Transportation
State Job No. 426354
Contract No. 20359

Prepared in cooperation with the Ohio Department of Transportation and the
U.S. Department of Transportation, Federal Highway Administration

Acknowledgements

The authors would like to acknowledge the Ohio Department of Transportation (ODOT) and the Federal Highway Administration (FHWA) for their cooperation and funding of this project. Without the assistance of forward thinking agencies such as these, development of new technologies and methods would advance at a much slower rate. Special thanks go to ODOT personnel at the district office in Bowling Green and the main office in Columbus for help with design plans, analysis reports, truck support, coordination, etc. The authors specifically acknowledge the support, advice, and direction of Jeff Baker, Mike Gramza, Rich Martinko, Dan Meyer, Hiram Crabtree, Tim Keller, Mike Loeffler, Mike Brokaw, and Chris Weiss. Throughout the project, the management and tradespersons provided support, insight into the construction process and patience as the instrumentation was installed and data collected. Finally, without the support of numerous people at the district level in coordinating field support for the testing, this project could not have been a success. Though they are too numerous to name individually, their support is gratefully acknowledged. Matt Shamis of Ohio FHWA has also extended his confidence and support for this project for which we are grateful. We also acknowledge the valuable input provided by FHWA Headquarters, the Turner-Fairbank Highway Research Center, and the Office of Research at Washington, D.C.

The work documented within this report is largely the result of a combined effort of many people. Those include Scott Kangas, Parag Nimse, Shashank Chauhan, Kyle Bosworth, Balram Chamariai, Robert Sexton, Robert Ward, Bryan Wright, Chong Qiao, and many others.

Veterans' Glass City Skyway (VGCS) Final Report

The organization of VGCS final report is presented herein as follows:

Chapter 1: Introduction and Objectives

In 2002, the Ohio Department of Transportation began undertaking the construction of the Maumee River Crossing (MRC) in Toledo, OH, a monumental project by any standard. Upon its opening to traffic service in 2007, the bridge was renamed the Veteran's Glass City Skyway (VGCS) to better represent the city in which it was built and the hard work and service of its people.

Chapter 2: Proposed and Implementation Plans

The services to be provided under this phase of the research project cover the initial activities leading up to the installation of the monitor instrumentation and the installation of the embedded sensors.

Chapter 3: Preliminary Design

A health monitoring system for the bridge was designed, planned, and implemented for the Veteran's Glass City Skyway bridge, with data collection and archival throughout its construction and ultimately an automated, user-friendly interface on a dedicated website. The primary criteria for selecting the instrumented segments were the predicted stresses and rating factors using the analytical data provided by the designer. Bridge Plans Addendum and Construction Contract Bid Documents were developed to document the monitor design. A total of 64 vibrating wire strain gages were installed in eight segments at four cross sections to monitor the long-term behavior of this bridge.

Chapter 4: Bridge Modeling and Analysis

The chapter objective was to use the measured response of the bridge against construction live loads and programmed truck load tests to develop a field calibrated finite element model of the bridge simulating the end of construction and initial in-service behavior. This field calibrated model captures baseline information of the bridge before it was opened to traffic (Parag S Nimse, 2007).

Chapter 5: Analytical and Experimental Stress during Construction of the VGCS

This chapter compares the experimental stresses derived from the health monitoring strain gages during the life of the I-280 Veteran's Glass City Skyway to the calculated stresses that were anticipated during design. It focuses on the comparison for construction events since the largest change in strain occurred during the main span construction, and reviewed in-depth the strain gage and analytical data (Chong Qiao, 2009; Yi, 2010; Gupta 2011).

Chapter 6: Monitoring of the VGCS: Vibrating Wire Strain Gage Testing.

This chapter is related to the health and monitoring of the VGCS cable stay bridge. It was to confirm that vibrating wire strain gages installed in the bridge, as well as the rest of the data collection system, worked properly during construction when data was being collected; and to perform a chain calibration on the entire data acquisition system and confirmed the validity of the field results (Kyle Bosworth, 2007).

Chapter 7: Study of Temperature Gradients

It involved studying temperature gradients within the concrete box girders to preliminarily assess the consistency of VGCS response with that of the AASHTO design code (Kyle Bosworth, 2007).

Chapter 8: A Baseline Truck Test to Calibrate a Baseline Model

This chapter covers the designing and executing a truck test, performing the initial data reduction and assessment of the bridge response. Prior construction, load tests performed on the VGCS, were studied; and output from the progressively-calibrated Larsa computer model was utilized to establish baseline data that confirms the Larsa model (Kyle Bosworth thesis, 2007). After construction, testing was performed to determine the elastic bridge response using truck load tests whereby a number of heavily loaded vehicles are driven across the structure in an attempt to determine bridge response under design loads and to accurately predict live load response for the bridge. It will include a final calibration based on end of construction; truck load tests to complete the model calibration and serve as baseline information which can be referenced in the future model (Parag S Nimse, 2007).
Also a final nondestructive load testing method is preformed, in which a final Truck load test is compared to the first truck load test (Feng, X 2010).

Chapter 9: Delta Frame Monitoring and Calibration

This chapter focuses on instrumentation and monitoring system that will collect strain data for selected loading conditions in the critical regions of the delta frames in a form that can be used to validate the analyses. A study was used to confirm the analysis by determining the magnitude of the tensile strains in the critical sections in the bottom chord of delta frame and to determine its adequacy and compliance with the crack control requirements. The finite element model for the bridge was specifically calibrated for the delta frame from casting through stay stressing, simulating the end of construction baseline behavior (Parag S Nimse, 2007). This chapter deals with measuring the changes in strain in the delta frame lower chord due to two events: the tensioning of the DF-4 tendon and the stressing of the stay. The long term and short term strains caused by the stressing of the stay were examined (Bryan W. Wright, and Parag S Nimse, 2007). In addition, the hydraulic truck cranes (from Terex Demag 1998) used for segment installation were repositioned from the tip of the cantilever to the opposing side of the final gap to capture the liveload response for the instrumented delta frame (Robert J. Ward, and Parag S Nimse, 2007).

Chapter 10: Use Intermediate Construction Live Loads for Progressive Calibration

This chapter addresses the use the measured response of the bridge against construction live loads and programmed truck load tests to develop a field calibrated finite element model of the bridge simulating the end of construction and initial in-service behavior (Parag S Nimse, 2007).

Chapter 11: Strains in the Bottom Slab

This chapter examines two areas of tensile stress concentration in the concrete segments of a large segmental twin box girder prestressed concrete cable stayed bridge. They are the experimental studies of the tensile stresses in the bottom slab of the delta frame segments due to final post-tensioning and the stresses in the bottom chord of the delta frame due to final post-tensioning and the stressing of the stay (Bryan W. Wright, 2007).

This chapter investigates the transverse bending of the bottom slab. Results of the finite element analyses generated by the construction engineer and the designer were compared with data collected at various construction stages to determine whether the predicted levels of stress occurred (Robert J. Ward, 2007).

This chapter also focuses on the additional Strain Measurements that were required in the cantilever span in the bottom slab in the strain concentration regions between the bottom slab and the walls at two locations in span 28 (Robert J. Ward, and Parag S Nimse, 2007).

Chapter 12: Long Term Analytical and Experimental Stress Comparison

Data from the installed vibrating wire strain gages has been collected since the casting date of each segment. A method of assembling the time line was developed, a Matlab program was written to combine the strain time history line for the data of one strain gage, and the experimental stresses were compared to analytical stresses calculated by the contractor. This study verifies that the instrumented segments of VGCS behave as expected for the period studied.

Chapter 13: Experimental Load Rating followed by AASHTO Bridge Evaluation Manual

In another aspect of this study, the allowable stress (ASR) load rating method was used to evaluate the inventory load rating factor for analytical and experimental stresses. This work utilized results obtained from both models, long term monitoring results and truckload testing. The analytical and experimental influence lines have a good fit. Therefore, the load rating values in the analytical and experimental results are in agreement. Of the instrumented segments, the lowest inventory rating of 1.5 for an HS25 lane load was found to occur for positive moment in the southern span at the bottom of Segment 2741. The calculated load rating from the analytical and the experimental tests should be close to what was intended in the design.

Chapter 14: Stay Vibration

This chapter focuses on the stay testing program that was employed on this project (Kangas, 2009). Several experiments were performed during various stages of construction to determine the capability of using traditional vibration techniques to estimate cable tensions with the non-traditional cable sheathing system of this structure. (Dr. Hemicki and Dr. Hunt, and Kangas, 2010)

Chapter 15: Modal Analysis

This chapter focuses on the operational modal analysis program that was employed on this project (Chauhan, 2008). The magnitude and direction of structural vibrations may be monitored/measured at critical locations through the use of mounted accelerometers to identify the characteristic modal shapes and frequencies of the bridge.

Chapter 16: Website Design and Documentation

This chapter focuses on the long term instrumentation package, data collection system and web site which is used to monitor and evaluate the long term environmental effects on the structure. This system provided the ability to plot strain and temperature information about the bridge in a data-form which can easily be plotted over periods of time for multiple locations. The data collection and warehousing of gage readings means not only can officials do further analysis of the bridges health but a historical archive of bridge performance is recorded. High speed connectivity allows for frequent data collection which enables close to real time monitoring of the bridge and conditions like cold weather or icing. This also allows for a close to real time model of the bridge for possible fault detection and the ability to automatically send warning notifications.

Chapter 17: Conclusions and Future Work.

A general increase in understanding of the inspection, maintenance, and bridge management issues associated with cable-stayed bridges by key personnel in the state (at universities, ODOT, and in industry) (Dr. Nims and Hamdallah, 2010).

References and Appendices

Chapter 1 Introduction and Objectives

1.1 Significance of this Structure in Ohio

In 2002, the Ohio Department of Transportation began undertaking the construction of the Maumee River Crossing in Toledo, OH, a monumental project by any standard. Upon its opening to traffic service in 2007, the bridge was renamed the Veteran's Glass City Skyway (VGCS) to better represent the city in which it was built and the hard work and service of its people. This structure (see Figure 1.1)consists of 56 approach spans (totaling 7,273') and a main span unit of 1,525', from expansion joint to expansion joint, crossing the Maumee River for an overall bridge length of 8,798'. The structure is of pre-cast segmental concrete design with a deck system nearly 120' wide carrying three lanes of traffic in each direction. The main support tower is 379'-3" above the waterline and the main span unit sits more than 120' above the river.

The design specifications require the structure to be able to carry Michigan Grain Train Truck loadings in addition to the standard AASHTO HS25-44 and alternate military live loadings. The construction plans called for a portion of the erection to occur directly over the existing I-280 interstate in a staged fashion making use of temporary pier columns so as allow continued use of the interstate during erection.

Now completed, this structure is a key transportation link along the I-280/75/90/80 (see Figure 1.2) corridor in the northwestern part of the state, a highly visible monument for the City of Toledo (see Figure 1.3), the surrounding communities and the state, and represents a significant investment of state resources.

The main span unit of the VGCS is one of Ohio's first long-span, cable-stayed bridges and one of only a few dozen such bridges in service in the nation at this writing. As such, this structure is vastly different from the types of structures that are currently in the Ohio bridge inventory. In fact, bridges of this design type, together with the set of associated construction technologies necessary to build them, have been used extensively around the world only for the past 2 decades.

1.2 Significance of Monitoring and Testing this Structure in Ohio

Because of the relative novelty of the cable stayed bridge design, it is important that issues related to maintenance and bridge management be addressed early on with an effective

bridge monitoring system so that long-term bridge behavior, as well as any changes in bridge condition, can be tracked through the use of a longitudinal study beginning during bridge construction. Such an approach will capture certain critical design, construction, maintenance, and performance parameters that cannot be captured or quantified visually.

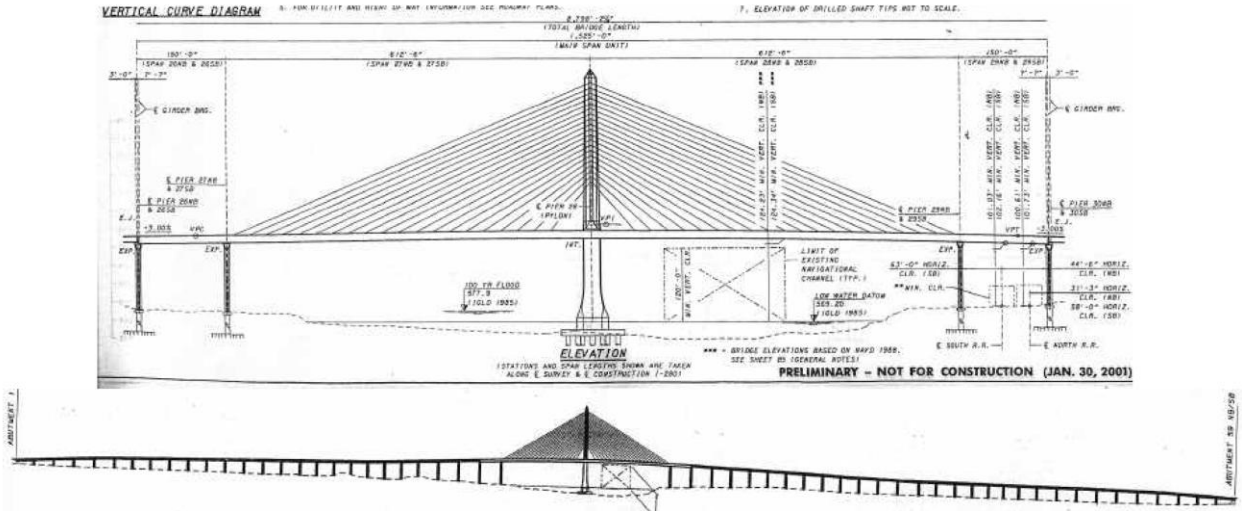

Figure 1.1 Plan and Elevation Views of MRC/VGCS (Nims, 2002)

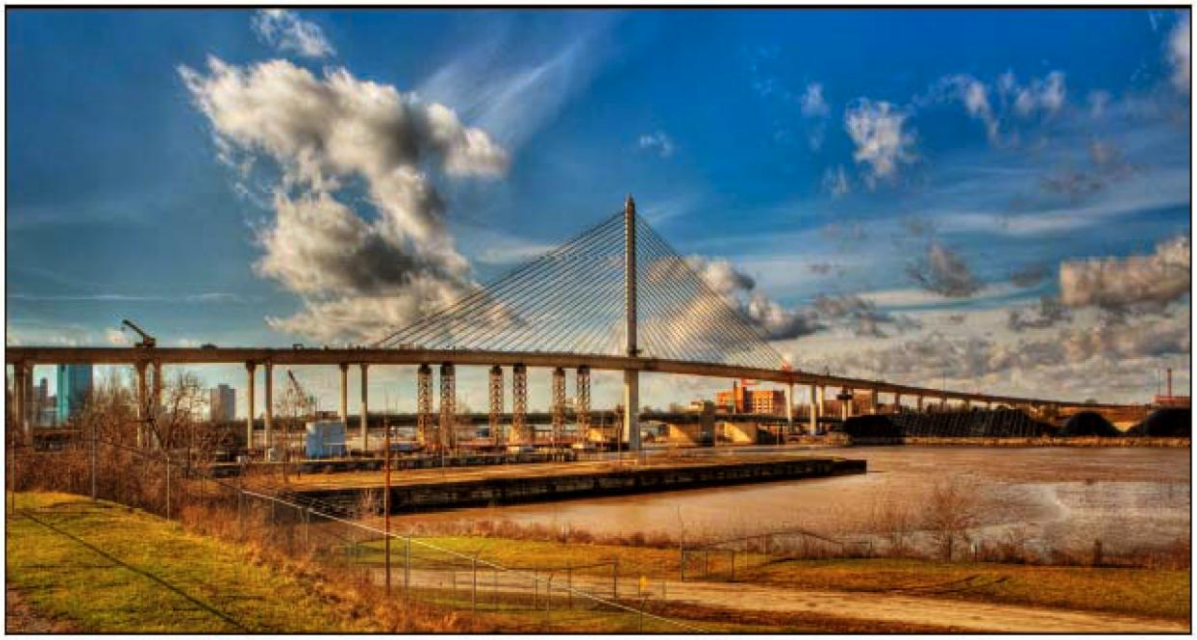

Figure 1.2 Artistic Rendering of VGCS (Nims, 2002)

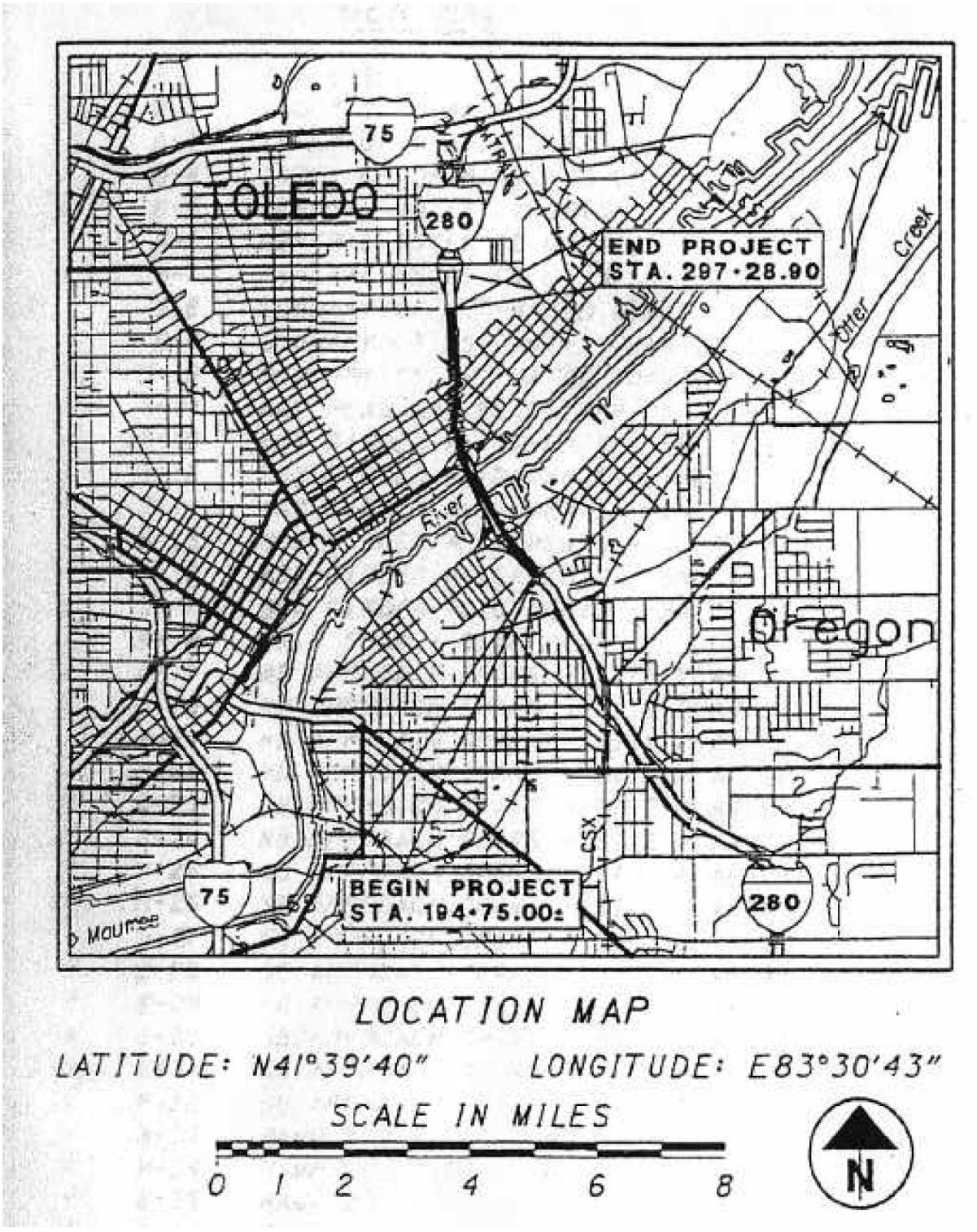

Figure 1.3 Location of VGCS (Nims, 2002)

Over the past decade, ODOT has supported numerous projects aimed at investigating bridge behavior through instrumentation, nondestructive field testing, and structural modeling/identification. These projects have revealed the advantages of incorporating monitoring and testing in dealing with a wide variety of maintenance and management issues covering dozens of bridges of various types (e.g., steel girder, truss, concrete, etc.) throughout the state. The key feature of this approach is that it provides a solid, objective database of information that can be put to a variety of uses including: verification of design assumptions and analyses, monitoring of construction processes and methods, tracking of bridge responses at key locations for rating, support of inspection and maintenance practices, long term monitoring of structural behavior, etc.

1.3 Objectives for this Project and its Phases

The size, complexity, and relative novelty of the VGCS make it an ideal candidate for the application of instrumented monitoring techniques. The instrumentation suites, sampling rates, data acquisition hardware, communications network/bandwidth requirements, etc. utilized for such a monitor are a direct function of the objectives for the monitor. A comprehensive instrumentation system that addresses all the wishes for data may be prohibitively expensive. Therefore, tradeoffs must be made in order to optimize the cost-benefit ratio.

In the case of the VGCS, the design of an instrumentation package focused on five main areas: (1) health monitoring; assessment of the changes in force distribution and bridge condition during erection and early service, (2) verification of design assumptions during erection, (3) investigation of the unique design features which have been incorporated into the VGCS, (4) investigation into the unique erection features and sequencing which will be used during its construction, and (5) investigation of stay cable vibration which is a general, unresolved issue for bridges of this type. Correspondingly, a scientific study focusing on these aspects of performance of the VGCS will add great value to the understanding of this specific structure as well as the general characteristics of the cable-stayed bridge type.

The purpose of this and associated documents is to outline the completed scientific study, which happened to consist primarily of two phases. The first phase (Nims, 2002), contracted at the District level, included the initial structural analysis, modeling, instrumentation package design for the monitor, and casting into the segments of the embedded sensors. The goal

of this first phase was to capture the critical instrumentation issues associated with this construction project and to develop a detailed instrumentation and testing in close consultation with ODOT officials, bridge designers, and construction contractors.

The second phase (Helmicki, 2003), contracted through Central Office, included permanent instrumentation operated through a computer controlled, digital data acquisition system located on-site and accessible tele-remotely via direct fiber optic internet connection, field calibration of a main span finite element model using truckload and modal field tests; verification of various design assumptions and erection load conditions; creation of a database of measurements for use as a supplement to the designer's maintenance manual to provide guidance for conducting future maintenance, and determination of vibration performance of stay cable damping system under wind and rain-induced excitation. The goal of the second phase was to finish the monitor installation begun in the first phase, establish a baseline concept of structural behavior and performance by utilizing a combination of field tests and ambient monitoring, capturing the overall structural concept by calibration of the finite element models, and finally benchmarking the condition of the structure by comparison of the above with its design values.

1.4 Expected Benefits and Deliverables of this Project

The primary benefit of the overall project has been a bridge management process for the VGCS bridge in particular and cable-stayed bridges in Ohio in general. This process will help these bridges reach their 100-year lives economically. Specific benefits include:

- Health monitoring of the bridge during construction, as changes primarily due to creep shrinkage and relaxation occur, and early service as the bridge responds to live load.
- Verification of the performance of the bridge during construction.
- Formation of a team with the knowledge and personnel to support ODOT's efforts to effectively manage cable-stayed bridges.
- A general increase in understanding of the inspection, maintenance, and bridge management issues associated with cable-stayed bridges by key personnel in the state (at universities, ODOT, and in industry).
- Calibrated analytical FE models of the VGCS main span system complete with analysis/simulation results indicating all critical load carrying members and load paths. These

models will be used by university researchers and ODOT officials for a variety of purposes: Modeling results will be used as a theoretical gauge against which field measurements will be compared in order to determine if the structure is behaving as predicted. These, in turn, can be used for verification of design assumptions, monitoring of construction processes, augmentation of routine inspection and maintenance activities, information to support management and decision making, etc. In addition, modeling results can be used by ODOT to simulate and rate the structure under special loading conditions such as in the case when overload permits are requested.

- The development of field ready monitoring strategies, together with an instrumentation plan, aimed at supporting inspection, maintenance and management activities and reducing life-cycle costs associated with the VGCS. The first step in supporting these long-term objectives was the training session in December 2011. Further, activities to continue this training are recommend.

- Examination of the stay cable vibration and damping.

- A detailed instrumentation of the VGCS's critical locations with instrumentation protection suitable for long-term, reliable operation over the next 3-5 years. This instrumentation plan will be configured so that future truck-loading tests can be run intermittently at ODOT's discretion and so that long-term environmental monitoring can be run continuously in an automated mode.

- Provision of a solid, objective database of information that can be put to a variety of uses such as: verification of design assumptions and analyses, monitoring of construction processes and methods, a baseline truck-load test, ambient vibration tests, and long-term environmental monitoring. These will form a baseline for continued health monitoring of the main span on into its service life. This information is presented on the VGCS website.

- A detailed analysis of all data obtained from field testing operations to reveal member/connection load carrying capacities at all instrumented locations, structural performance at all instrumented locations during erection, characteristics of stay cable vibration characteristics, etc.

- Development and presentation of a training component for ODOT personnel (Central Office and District) to read and analyze data. Program shall also be designed to train ODOT personnel to carry on data collection for the design life of the structure.

- Recommendations for a health monitoring program coordinated with any maintenance manual prepared for the bridge.

- A detailed, written reporting of all activities and findings obtained by researchers in the course of conducting this project, including a detailed explanation of how "lessons learned" from this structure can be applied to other cable stay bridges.

1.5 Research Results and Conclusions

Based on the discussion above, this project sought to implement and operate an appropriate instrumentation and field testing program to support management of the VGCS through construction and on into its service life. This program augments the traditional visual inspection program to provide objective, quantitative data for use by ODOT in assessing the status of the structure.

References

1. D. Nims, A. Helmicki, V. Hunt, **"**Instrumentation of the Maumee River Crossing, Phase I: Modeling, Design of Instrumentation Suite and Installation of Embedded Sensors**,"** Proposal to ODOT, District 2, by University of Toledo and University of Cincinnati, 2002.
2. A. Helmicki, V. Hunt, D. Nims, **"**Instrumentation of the Maumee River Crossing," RFP: # PS-04-14**,"** Proposal to ODOT and FHWA, by University of Cincinnati and University of Toledo, 2003.

Chapter 2 Proposed and Implementation Plans

2.1 Proposed Design of the Monitor and Test Program

As you may recall, this research project was conducted in two phases. The first phase, regarding the design of the monitor and test program, was contracted through the District. The services to be provided under this phase of the research project cover the initial activities leading up to the installation of the monitor instrumentation and the installation of the embedded sensors. They can logically be broken down into the following tasks:

Task 0: Bridge Plans Addendum and Construction Contract Bid Documents

This task encompasses all pre-planning activities necessary to develop Addenda for the bridge plans and documentation to be inserted into the construction bid package so that all contractors are aware of the research and instrumentation aspects at the MRC and so that all necessary equipment and access requirements are met in order for the research to proceed in conjunction with construction. The researchers are and will continue to work closely with ODOT and the bridge designers to provide the necessary language for bid documents and engineering change orders so that all preparatory work for instrumentation and testing are properly addressed with the construction contractor. In addition, these documents will outline the equipment necessary for instrumentation and the requirements for access during construction and testing. In this way, the contractor, as part of the construction contract, will absorb all the costs for the equipment and access.

Task 1: Bridge Modeling and Analysis

This task encompasses FE modeling and structural analysis (static and dynamic) of the bridge both during construction phases and in its final, in-service state. An FE model of the superstructure system will be developed using the information provided in the drawings. The model will reflect the characteristics of the sectional properties and will be adjusted to reflect any reported changes to the plans during construction. This model will be used to simulate the structural response of the bridge due to dead load, the expected forces in the stay cables, unexpected cable loss, the intended scenario for cable replacement, wind loads, thermal loads, time dependent effects, construction sequence, and the specified vehicle and lane loadings for both capacity and fatigue as per the construction drawings and AASHTO Specifications. The

results will be analyzed to determine critical load carrying paths and to bound expected response levels and characteristics. These findings will, in turn, be used as one of the inputs to the sensor suite design and controlled test design described below.

In addition, the model will be adjusted to compensate for possibly undetected anomalies or for previously unexplored conditions at cable stay locations and supports (e.g., varying degrees of fixity, axial forces upon the exterior girders, etc.). Again, the above loading simulations will be run to consider the effects of these hypothetical or worst-case scenarios. These modified simulations will be used to maximize the effectiveness of the instrumentation.

Model validation will occur in two phases: (1) initially, the model will be validated against the independent design calculations provided by the designer to ODOT, and (2) once sensors are in place and data is obtained from actual field measurements, these measurements will be compared against theoretically expected model output and used to tune the model.

Task 2: Instrumentation Suite Design and Installation

This task encompasses the use of modeling results from Task 1 as a basis to select exact types, numbers, and locations for all sensor and data acquisition placements. In addition, ordering of all components and communications with component vendors will be initiated.

In this task, researchers will make an initial indication as to which locations and cables are to be instrumented as well as what the particular instrument configurations (e.g., numbers and types of sensors) are likely to be. The inputs that will drive this selection process include the following:

- Modeling analysis results from Task 1,
- Critical members, connections, cable details specified within the design plans and construction manuals
- Members, connections, details indicated by consultation with the design engineers, the contractor, other noted designers, specialists in the field of cable stay assessment, and
- Members, connections, details indicated by ODOT as regions of concern.

Based on our past field testing experiences, the sensor suite is likely to consist of vibrating wire strain/temperature gages (used to obtain reliable long-term environmental response

characteristics) and resistive-based, high speed strain gages (used to obtain low noise, dynamic load response characteristics). Additional gaging (i.e., accelerometers) will be used for ambient vibration studies. A weather station will be erected to monitor wind speeds in three dimensions, rainfall, temperature, and humidity.

It is assumed that all instrumentation will be operated by an automated, computer controlled, digital data acquisition system located on-site and accessible either manually or tele-remotely (e.g., via either direct modem/telephone connection). Where possible, the researchers will employ proven, off-the-shelf, turn-key components to assemble the pieces of the proposed monitor. This will serve to minimize monitor development time and maximize reliability.

Also, where possible, all gaging will be placed embedded in (i.e., attached to rebar, etc.) or affixed on (i.e. tack-welded or epoxied to steel surfaces, etc.) the structure during fabrication. When precast elements are employed, researchers will travel to the precasting site to embed gages during fabrication. During this phase of the project, sensors, typically vibrating wire and electrical resistance strain gages, will be cast into the mainspan segments as segment production permits. As part of this task, the operation of the cast-in-place instruments will be verified for proper functioning.

Task 3: Data Collection, Archival, and Interpretation

Based on the construction schedule, erection of the main span was nearly half complete by the end of Phase I of the research project, i.e., October 2003. Therefore, collection of the initial construction data necessarily began.

Task 4: Preparation of a Research Proposal for Phase 2

A research proposal for Phase II of this research, including monitoring of the balance of construction and initial service, will be prepared and submitted to the Ohio Department of Transportation. Phase II includes gathering, storing and interpreting all remaining data from construction, traveling to site to periodically collect in-service monitoring data during the first year of service, and subsequent interpretation of construction and in-service data.

2.2 Proposed Execution of the Monitor and Test Program

The second phase, regarding the execution of the monitor and test program, was contracted through Central Office. This phase of the research will follow on the heels of the Phase I activity wherein structural analysis, preliminary modeling, and instrumentation suite design have been completed. In addition to continuing effort on the above Phase 1 tasks, the work of Phase 2 can logically be broken down into the following tasks:

Task 5: Establish test schedule

Design activities will be conducted to develop a regimen of bridge tests and strategies:

§ **Construction event monitoring:** The research team will work with the designer and contractor to identify key/critical construction events such as movement of construction equipment on the structure, installation of specific segments, tensioning of tendons and stays, etc. Researchers will use these as opportunities to collect data for use in subsequent analysis, verification, and calibration studies.

§ **Truck-load testing:** Both static and crawl speed tests will be considered. Truck-load configurations and transit paths will be developed. Several loaded and weighed tandem or larger trucks will be required to force a measurable response from the structure and the installed sensors.

§ **Ambient vibration monitoring:** An ambient modal test will be designed to evaluate vibrational characteristics in the selected locations. The results of this testing will serve to further clarify the loading environment by wind, traffic, and other forces, vibrational patterns of the cable response, member and connection responses, and possible fatigue-prone regions within the system.

§ **Long-term environmental monitoring:** An automated data acquisition system will be designed to interface with that portion of the sensor suite developed to track the long-term environmental response of the bridge. This system will be configured to run continuously in the standalone mode to sample and record measurements at fixed intervals (e.g., every 15-30 minutes) without human intervention. Periodically, the data will be downloaded for analysis and to clear the data acquisition system memory for more measurements. The download operation will be handled initially by manually plugging a laptop into the data acquisition system at the

site. Upon completion of construction, the system will be upgraded so that data can be obtained remotely through the use of a fiber optic internet connection.

Task 6: Conduct construction event and ambient monitoring

In order to validate the design steps for both the structure and its monitoring system above, the researchers will immediately begin the regular and automated data acquisition with a permanent data system for the first and successively installed sensors in each of the instrumented segments. In addition, a high-speed data system would be used temporarily to collect dynamic ambient (e.g., wind, construction) measurements from the appropriate sensors by the research team on day trips to the construction site once segments are installed on the main span. The data obtained from this monitoring would be used for several purposes:

§ validate (by comparison of theoretical estimates from modeling and actual field measurements) the results obtained from the analytical modeling studies upon which the sensor suite and testing plan designs were based,

§ obtain preliminary data on some of the critical locations to initiate the procedures for data post-processing and analysis for member capacity, etc., and

§ debug field operations specific to the site, installation methods, access issues, provide information for data system calibration, etc.

Task 7: Field testing for baseline and service condition assessment

Truck-load testing will consist of an initial baseline test to track any changes in bridge state in response to live loadings. The truck-load test will take several days to complete and require several loaded, pre-weighed tandem or larger trucks of a known axle configuration. When appropriate, lane or bridge closure, traffic control, and the loaded trucks will be provided by ODOT. Full bridge closure will be necessary during portions of the test. Ambient vibration monitoring will also take several days to establish the vibrational levels and characteristics of the structure, including cable stays. Accelerometers would be temporarily bonded to a select subset of stay cable conduits at certain intervals along their length in order to record their response profiles to ambient loading. Bridge traffic will provide input excitation for the structure and so the bridge will remain open to traffic for most of the test. However, identification of the bridge response to wind loading will require full closure of the bridge and should be conducted just

before the bridge goes into service. Scaffolding, rigging, snooper or bucket truck, or other means of access may be required to install and remove the accelerometers from the stay cables.

Task 8: Data analysis/reporting phase

All test data would be post-processed and findings delivered to ODOT. Intermediate results and findings will be reviewed with ODOT on a continuing basis as they become available. Findings would include: breakdown of construction, truckload and ambient bridge member responses, comparative analysis of bridge member response both temporally and spatially, verification of design calculations, and capacity rating of instrumented members. In order to reduce life-cycle costs, recommendations will be made for actions to take during the service inspection, maintenance and management activities for the MRC in particular and for cable stay bridges in general. A detailed description of the analysis to be performed includes:

§ Evaluate segment/cable/connection performances using long-term environmental monitoring to determine: dead load stress at the instrumented locations, peak and cumulative stress from all construction at instrumented locations, thermal induced stress/cycles, and thermal effects on instrumented locations

§ Evaluate member/cable/connection performances using baseline and service field tests to determine: load-carrying/transfer capability for controlled loading, maximum measured stresses within members/connections and where such measured stresses occur, maximum vibration amplitude (g's) at instrumented locations, natural frequencies, and vibration (mode) shapes, and HS25-44 load, Michigan grain train, and fatigue rating of instrumented members

Task 9: Reporting Activities

In addition to the normal communication of findings as described above, the research team shall formally submit quarterly progress reports to ODOT in the required format. Six months prior to the completion of the contract, the research team shall submit a draft of the project final report complete with executive summary for ODOT's review. This report will fully describe the activities undertaken on the project, incorporate all results and findings obtained, as well as any recommendations for actions to take during the service inspection, maintenance and management activities for the MRC in particular and for cable stay bridges in general. After

review of the report, ODOT comments and suggestions will be incorporated in a final version of the project report and be officially submitted to ODOT.

Task 10: Training Activities

A primary goal of this research is the formation of a team (including government, industry, and university personnel) with the knowledge to support ODOT's efforts to effectively manage the MRC and other cable-stayed bridges in the state. An important component of this goal will be to provide training to ODOT employees to allow for future periodic data acquisition for the purpose of MRC health monitoring.

2.3 Proposed Implementation Plan for ODOT

Any proposal submitted to the ODOT Research Office has a requirement for a proposed plan on the implementation of the research by the department. We recommended that a number of deliverables as discussed above could form the basis of items which could be immediately implemented to enhance and improve ODOT's understanding of this unique structure and its operations, maintenance, etc. Others form the basis for more long term strategies which involve either this particular structure or the class of cable stayed bridges in general. In the section, the researchers try to present a breakdown of some of these issues. The goal will be to identify specific ODOT design, construction, operation, and maintenance codes/practices/activities which could and should be modified for structures of this type in order to maximize performance and reduce total life cycle costs. Thus, in this sense, the implementation plan for this research is a work-in-progress.

Short Term Implementation Issues: The main goal of this research is the development of a database of objective information on the structural behavior of the MRC obtained through the analysis of measurements taken by an instrumented monitoring system designed and installed concurrently with the bridge's fabrication and erection. The process of designing this monitor and its sensor suite as well as the process of collecting and analyzing the preliminary data present several natural and immediate opportunities for implementing the research.

The design and construction of a bridge such as the MRC is a highly complex and iterative process. Not all the details are worked out ahead of time. Many are finalized as the process proceeds. Moreover, many of the structural characteristics of the final bridge depend as

much on how the erection is sequenced as on the design details found on the plan sheets. At each step as the fabrication of bridge components proceeds, designers and ODOT engineers are working through a myriad of finalizing, low-level decisions. At certain points in this process, problems arise, new ideas come to mind, etc. At a number of these points, instrumented monitoring and the associated scientific, quantitative data obtained provide a useful tool in the decision making process.

Where the data is already in hand as part of the ongoing research operations, it will be freely shared to aid in decision making. One such instance that has recently occurred might serve as an example of this type of implementation: The instrumentation design process ongoing under Phase I has identified certain critical bridge main span segments for instrumentation. In order to maximize reliability and life expectancy of the instrumentation package, sensors are being embedded as these segments are formed and poured. A natural by product of this sequence of events is that for selected segments data (temperature, strain, etc.) can be obtained during casting, curing, post-tensioning, and storage. This data will be reported to ODOT. It can be used by ODOT and the fabricators for comparison against expected profiles and may shed light on how the fabrication process is proceeding. In fact, recent temperature measurements taken from the practice instrumentation of a segment have revealed rather large internal thermal gradients which may contribute to segment micro-cracking during fabrication. While this micro-craking is in a compression region, it may provide a pathway for moisture to penetrate the segment and initiate subsequent deterioration mechanisms. The measurements have identified specific regions where localized heating of the casting form could be implemented in order to equilibriate these gradients during curing operations immediately after a pour.

Similarly, readings taken during segment transport and storage at the casting yard may prove insightful and useful. This is especially true as winter approaches and the environment in the casting yard is likely to see significant fluctuations.

On occasion, questions about various bridge components have and will arise that are outside the main scope of the research described herein, but for which quantitative measurements would prove valuable. At these points, researchers will augment their instrumentation efforts to obtain the needed measurements at minimum additional cost for ODOT. One such example is the recent instrumentation of a main span delta frame to measure stresses induced during fabrication.

As the fabrication of delta frames drew near, final design calculations revealed possible overstressing at certain locations as the delta frames were lifted out of the form and placed into storage and again when the delta frame is erected. Certain changes in the re-steel and member dimensions were implemented to address these issues. However, in addition, the research team was asked to place strain gages in one delta frame during fabrication in order to obtain measurements for verification of the predicted fabrication/erection-induced stresses. This additional monitoring effort has been implemented, monitoring efforts are currently under way, and the data is being delivered to ODOT, Figg, and Fru-Con.

Once erection of the main span begins, the monitoring system architecture has been configured so that data can be continuously obtained from the segments instrumented during fabrication. This data will be used for comparison against the erection and construction loads predicted by the design and erection analyses, particularly during construction events deemed "critical" by the designer and contractor. On one hand this data will provide validation of sensor installation and operation. On the other hand, this data will be available to document the erection state of stress and dead loads. The capacity ratings of a structure as massive as the MRC are mainly a function of the dead load distribution, which, for the class of cable-stay bridges, is heavily dependent on the erection sequencing. For this particular design, this is even more critical due to the unique features of the continuous cable stays and cradle arrangement at the plyon. In addition, the designers will be trying to conduct the erection using a one-time only stay tensioning operation. The data obtained during erection will therefore serve implement the feedback of very important information on the erection behavior of certain unique features of this structure.

Near the end of erection, but before the bridge is opened to service, a series of baseline tests will be conducted as part of the research project. These will include truck-load tests and ambient vibration monitoring studies. The results of this testing will serve to further clarify: the live loading environment due to wind, traffic, and other forces; vibrational patterns of the cable and superstructure response; and possible fatigue-prone regions within the system. These baselines, together with the archive of dead loads from above will serve to completely characterize the bridge performance at the instrumented locations. This database will have a number of ready implementations: The data will provide a check of the loading behavior predicted by design and erection engineers. A regular regime of readings taken during the

bridge's service life can be incorporated into the bridge's maintenance and inspection process (particularly in regions where high stress amplitude and/or stress cycles are observed). These can be compared against the baseline readings in order to track and/or trend changes on structural performance. Once the bridge is opened to service, the embedded sensors will serve to monitor both the structure's responses to environmental events (wind, temperature. etc.) as well as its responses to traffic. Data will be collected and archived in an automated fashion. This database of ongoing, long term measurements will serve to augment visual inspections and track structural performance. Identifying exactly which sensor readings will provide the most useful information and what post-processing of the readings is needed for interpretation is a major part of the proposed research project.

At the end of the research project, a calibrated analytical FE model of the MRC main span system will be available. This model can be used as a tool of ODOT structural engineers to perform simulation studies for various purposes. In the near term, such a model could be used much like BARS to provide information necessary for overload permit issuance and load rating. In the long term, the model will be available for simulation-based studies in case of damage occurs or repairs or retrofits are needed. Also, the model will be available in the unlikely event that one or more aspects of the performance of the bridge does not turn out as anticipated by the designers (e.g., vibration levels, etc.).

The examples above give the flavor of some of the short term implementations that are likely to accrue from the proposed research on and installation of an instrumented monitor system on the MRC. As with many of UCII's previous projects, still other implementations, as yet un-thought-of, will reveal themselves as the research proceeds and information on structural behavior is collected and analyzed. The researchers intend that such circumstances will be reviewed with ODOT personnel and further investigated on a case-by-case basis as a byproduct of the proposed research project.

At the end of the project, all such findings, together with a full set of recommendations for a routine MRC health monitoring program will be developed and coordinated into any maintenance manual prepared for the bridge. This activity will be perhaps the most direct implementation of the research and will be conducted jointly with the researchers and ODOT personnel. This will include full documentation of the monitor system hardware and software

together with a comprehensive listing of the data to be collected, the frequency of collection, any data post-processing steps necessary, and a standardized set algorithms/methods/strategies for data interpretation.

Medium-to-Long Term Implementation Issues: The discussion above focuses on several potential implementations relating directly to the research project objectives and the immediate findings of the monitoring conducted during the research project. Follow-on developments and/or enhancements to this research could include a number of items such as the following:

The detailed, final written report of all activities and findings obtained by researchers in the course of conducting this project will be delivered to ODOT. It will include an explanation of how "lessons learned" from this structure can be applied to other cable stay bridges.

The members of the research team will be available to ODOT throughout the period of the contract to discuss findings of the project and their interpretation for cable stay bridges. After the contract has expired, the members of the research team will be available to serve ODOT as part of a pool of expertise.

After the period of this contract, continued operation of the monitor could either be handled by ODOT personnel or contracted back to the researchers. Along similar lines, it would be ideal to revisit the full diagnostic schedule of tests after one year of service life for the bridge and then again at regular intervals. A series of truckload, modal/vibration, and ambient monitoring tests would be conducted for comparison against baseline tests run prior to placing the bridge in service. These would serve to track changes in bridge behavior. In order to minimize the effect upon bridge traffic, the test configuration could be designed for either intermittent bridge closure, intermittent lane closure, or "rolling" lane closure. Otherwise the bridge would be fully open to traffic during testing.

Based upon and incorporating the above physical and learned results for this specific bridge, a full scale and dynamic bridge health monitor could be designed in the future by the research team. This monitor would incorporate the hardware and software on the bridge at the completion of this project. In addition, the monitor would incorporate additional cutting-edge infrastructure technologies such as, but not limited to:

a) weigh-in-motion scales or pavement loops for real-time monitoring and statistical documentation of every vehicle/axle weights, speeds, and classification;

b) real-time, on-line capacity assessment of the instrumented members/locations;

c) real-time, instantaneous control actions including electronic paging/email, variable message signs (VMS), video camera surveillance, etc.;

d) Internet connectivity for a user-friendly and graphical presentation of the collected database and current bridge condition to any ODOT engineer's desktop; and

e) a dedicated website for community access to the bridge history, general description, selected bridge and traffic conditions, future plans, email feedback, etc.

Here, the authors would like to note that we actually did implement the latter two bullets in the list above as part of our deliverable to provide documentation and training to ODOT for continued use of the bridge monitoring system.

The intended audience or market for these research products would be any current or prospective owner of a cable stay bridge, in general. However, the Ohio Department of Transportation is the specific client that is expected to benefit primarily from this research. The team, which includes key personnel in the Structures Office, will be immediately available to implement these proven strategies on other cable stay bridges in Ohio. Inspection and maintenance concerns will be addressed directly within the plans for future bridges as either new standards or comments on the General Notes pages, key events or action items during construction on the Bridge Staging pages, or additional comments or specifications on the individual pages of each section and/or member of the bridge. There are few impediments to this implementation and the additional costs to ODOT would be quite minimal.

At the discretion of each bridge owner, additional research studies may be implemented on other existing or future bridges of this type. Although it is hard to estimate here the costs for such efforts, it is clear that such research could build on the knowledge obtained from this project or could simply apply a subset of the proven field methods to check the critical results discovered in this undertaking.

2.4 Research Results and Conclusions

Based on the discussion above, this project sought to implement and operate an appropriate instrumentation and field testing program to support management of the MRC through construction and on into its service life. This program augments the traditional visual inspection program to provide objective, quantitative data for use by ODOT in assessing the status of the structure.

References

1. D. Nims, A. Helmicki, V. Hunt, **"**Instrumentation of the Maumee River Crossing, Phase I: Modeling, Design of Instrumentation Suite and Installation of Embedded Sensors**,"** Proposal to ODOT, District 2, by University of Toledo and University of Cincinnati, 2002.
2. A. Helmicki, V. Hunt, D. Nims, **"**Instrumentation of the Maumee River Crossing," RFP: # PS-04-14**,"** Proposal to ODOT and FHWA, by University of Cincinnati and University of Toledo, 2003.

Chapter 3 Preliminary Design

3.1 Design of Instrumentation Plan

The selection of segments to be instrumented was done in phase I of the research project. The primary criteria for selecting the segments to be instrumented was predicted stresses and rating factors using the analytical data provided by the designer (Figure 3.1). Four segments were selected (Figure 3.2), two controlled by positive moment and two by negative moment. A practice segment was located in Span 26. Within each segment, the gage locations were selected to capture the desired response and permit ease in installation. Special care was taken to make sure that the gages in the segments were placed away from areas of high strain concentration. These typically occur in delta frame segments associated with stay anchorages and deviator segments with arrangements for longitudinal (along the length of the bridge) tendon deviators.

Approximate gage locations for a typical NB and SB segments are shown in Figure 3.3. The gage locations for SB segments are symmetric to NB segment locations. There are sixteen gages in each instrumented segment, eight vibrating wire gages and eight embedment foil gages, for a total of 128 strain gages. It should also be noted that each vibrating wire gage includes a thermistor to account for thermal affects. Hence, the total number of sensors would be 192. Sampling rate for vibrating wire gages has a lower bound of 1 per second, whereas for foil gages the sampling rate can be set much faster in order to measure events in near real time (e.g. 200 per second). The more stable vibrating wire gages are used for long-term measurements and, in the case of truck load tests, for static load positions. The embedment foil gages are used for dynamic load cases like the pseudo static load case, as in low speed moving truck load tests or for construction live loads. Construction live loads considered included response to loads such as continuous segment hauler movement and the crane roll-off loading.

At each of the sensor locations shown in Figure 3.3, there are two gages, vibrating wire gage and an embedment foil gage. The first character in the nomenclature is “V” or “F” for vibrating wire gages and foil embedment gages, respectively. The second character can be “T”, “W” or “B” representing the top flange, the web or the bottom flange of the segment. The third character indicates transverse location starting from the outside end (outside parapet of the bridge) going towards the median end (inside parapet close to center line of the bridge) and is

represented by characters from “A” to “K”. And the last character in the nomenclature designates the orientation of the gages where, “L” stands for longitudinal direction of the bridge and “T” stands for transverse. At all the locations, the embedment foil gage and the vibrating wire gages were placed close to each other and their locations were recorded when the gages were installed.

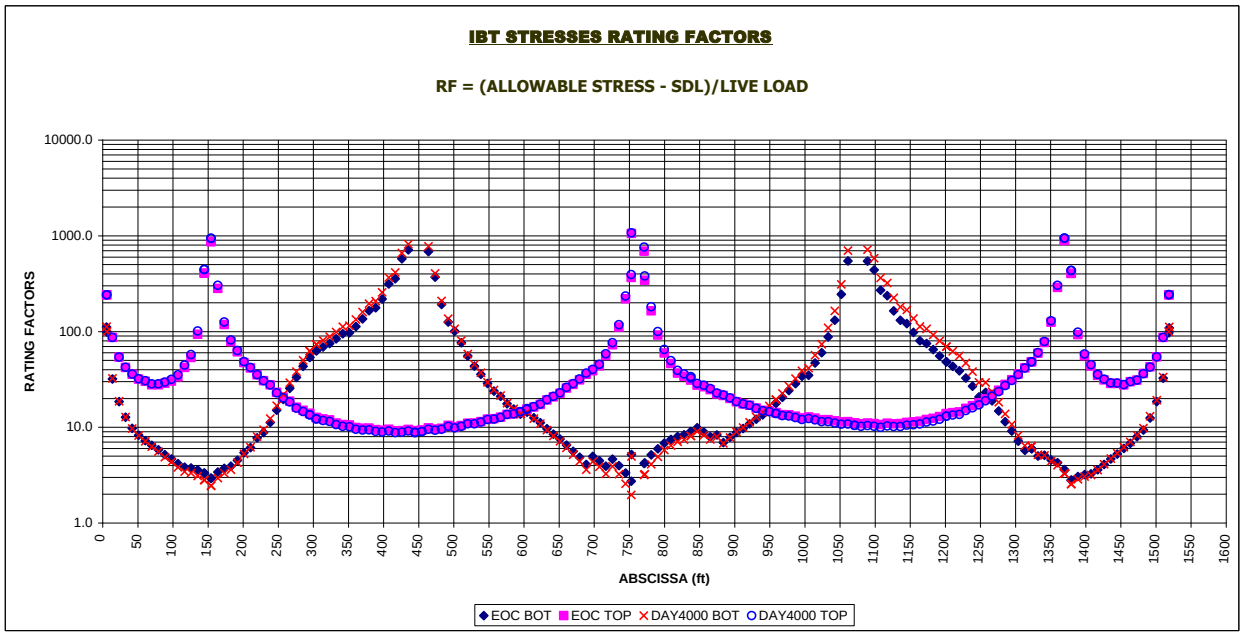

Figure 3.1 Inventory Allowable Stress Ratings of Superstructure (Figg, 2001 and IBT, 2003)

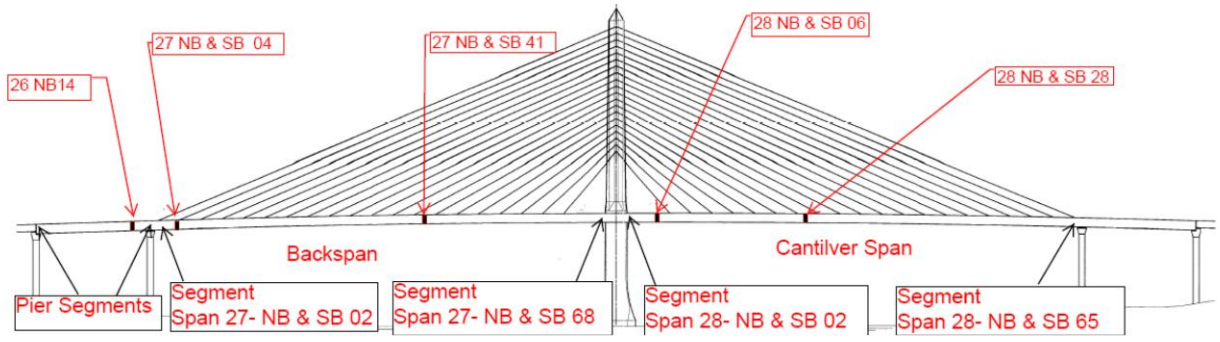

Figure 3.2 Instrumented Segments of MRC/VGCS (darkened segments are the instrumented segments. E.G. 27 NB & SB 04) (Nimse, 2007)

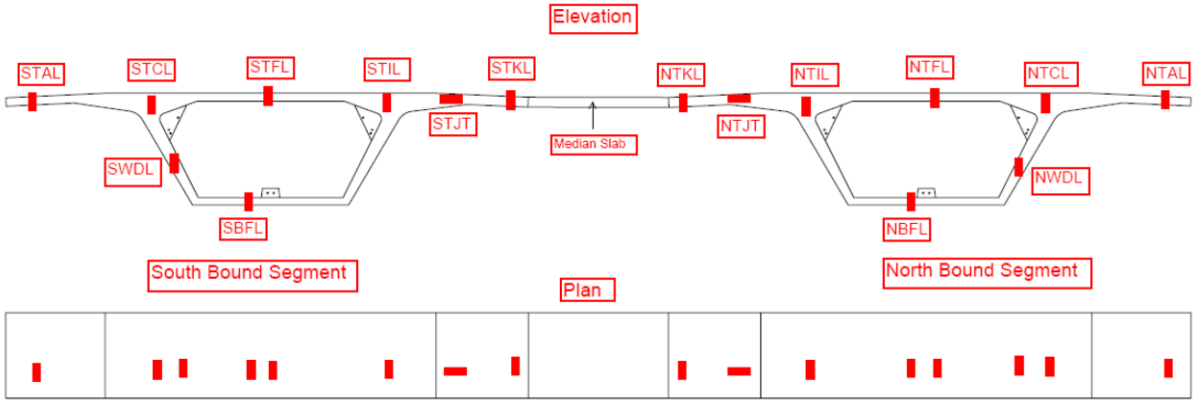

Figure 3.3 Section Diagram of Segment Instrumentation (Nimse, 2007)

3.2 Incorporation within the Bridge Construction Plans

An addendum to the plans was prepared in order to facilitate the research project (University Research Team, 2001). This documented the items to be installed by the contractor (e.g., conduit, junction boxes, main data cabinet, phone service, power outlets, etc.), the general plan for instrumentation and testing (see also Chapter 2), the required access to the site and casting yard by the university research team (URT), the requirements for notification during construction, and the protection of instrumentation, wiring, and data acquisition equipment. The Contractor was to coordinate the construction of the permanent conduit runs to along the parapet and through the pylon as shown on the Preliminary Schematic Instrumentation Permanent Wiring Plan (Figure 3.4). This plan sheet was later revised to include more details (Figure 3.5).

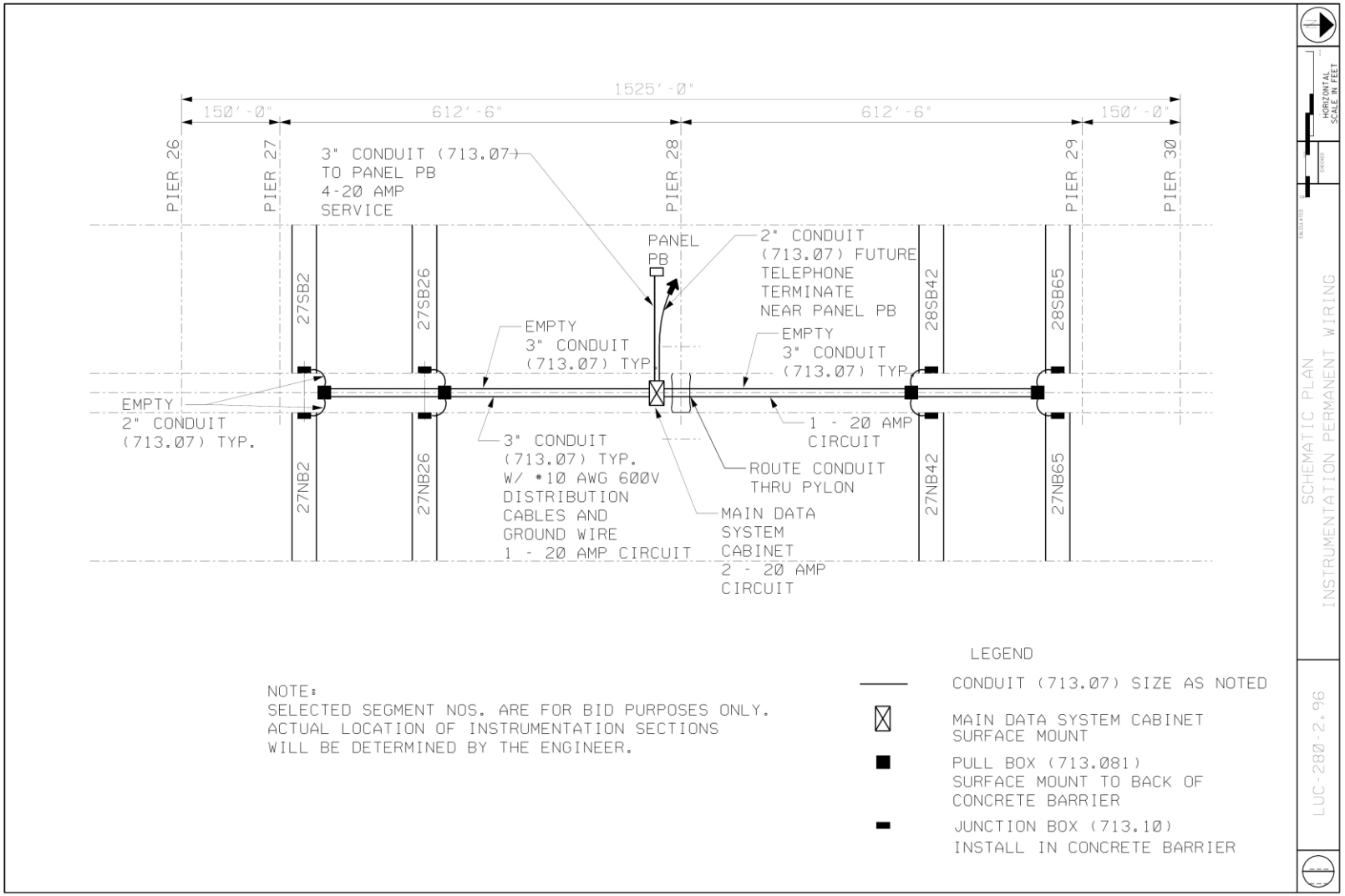

Figure 3.4 Preliminary Schematic Instrumentation Permanent Wiring Plan (URT, 2001)

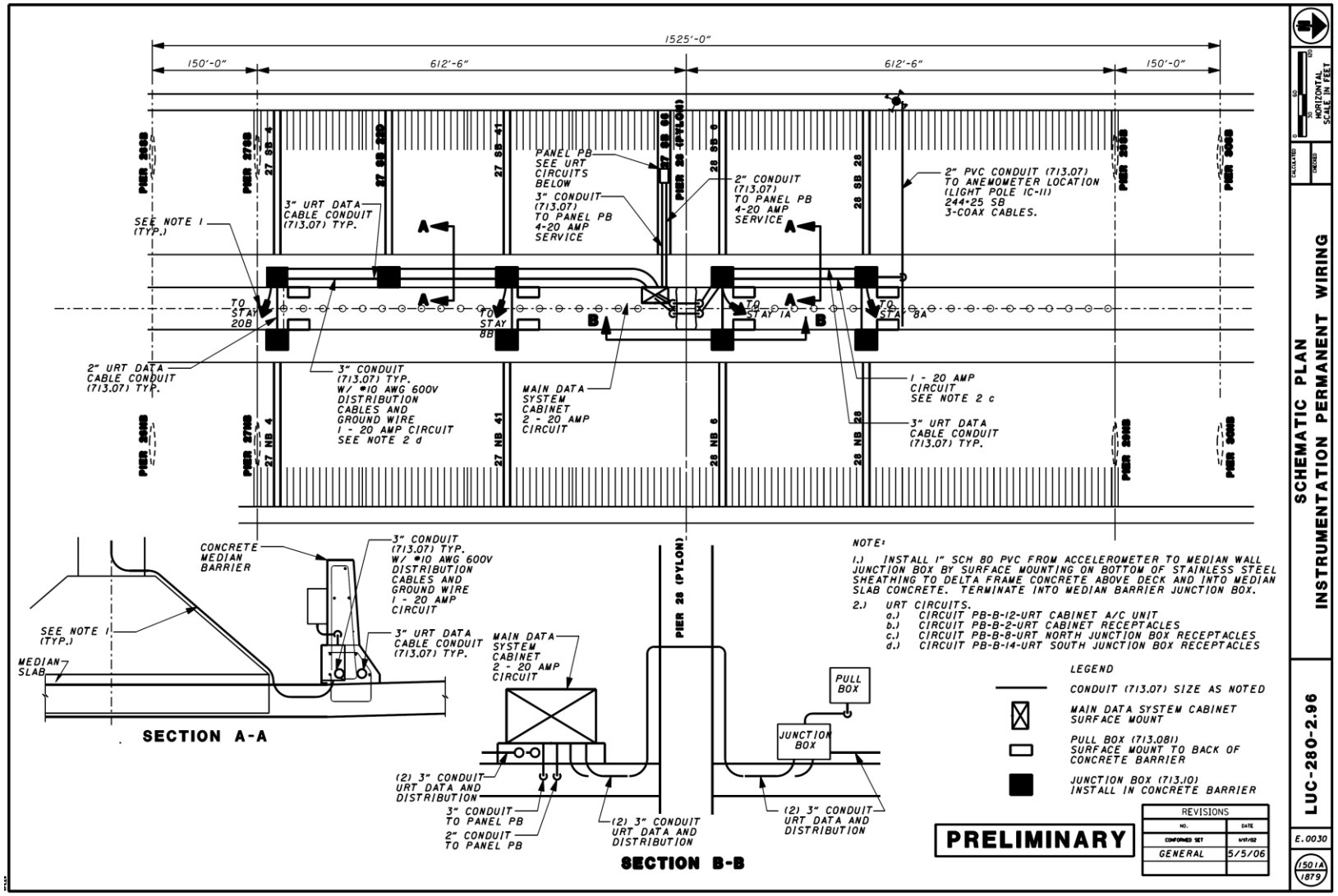

Figure 3.5 Final Schematic Instrumentation Permanent Wiring Plan, Revised (Final VGCS Plans, Drawing 1501A)

3.3 Initial Data Collection during Construction

Once these gages were installed on the rebar cage of the segment before it was cast, the lead wires were routed to the inside parapet end. The wires and electronics were protected from the elements by using trash bags and a white NEMA 4 box (Figure 3.6) in order to limit the humidity and potential for damage prior to and during shipment. Each box was tied to the segments through scupper holes on the wings using steel tie cables to ensure it would not fall during shipment and installation. The vibrating wire gage wires were passed through a multiplexer (MUX) to allow the inputs from all gages to be switched through a single output to a vibrating wire interface and recorded by a Campbell Scientific CR10X datalogger. Initially, each segment was handled independently (e.g., in the casting yard), but ultimately both northbound and southbound segments were combined at one MUX after their installation on the bridge. The CR10X used calibration factors provided by Geokon Inc. to translate voltage measurements into strain and temperature values which were stored onboard until a site visit was made to download the data and change batteries. Data collection began before the segment was cast and in many cases has been continuous throughout storage and construction. The embedment foil gage lead wires were left in a protected environment until needed, when they were attached to a portable Optim Megadac data acquisition system (DAS) for truckload tests.

Figure 3.6 Data Collection during Construction (Wright, 2007)

3.4 Final Data Collection and Archival System

As per the plans, the contractor installed conduit along the length of the parapet, mounted the white boxes to the side of the parapet, installed the main data cabinet near the pylon, and connected all these together to enable one common architecture for the health monitoring system. In addition, specified cable was pulled through the conduit such that all the electronics could be interconnected and controlled from the loggers, now relocated to the main cabinet. The main cabinet was provided with 120VAC power, air conditioning, shelving, and a high speed internet connection from the local fiber optic network for the roadway weather information system (RWIS) installed by ODOT. With an IP address as specified by ODOT, the loggers may be polled remotely by the computers at the university labs, archived in various database formats, and provided in a user-friendly manner by a dedicated website service.

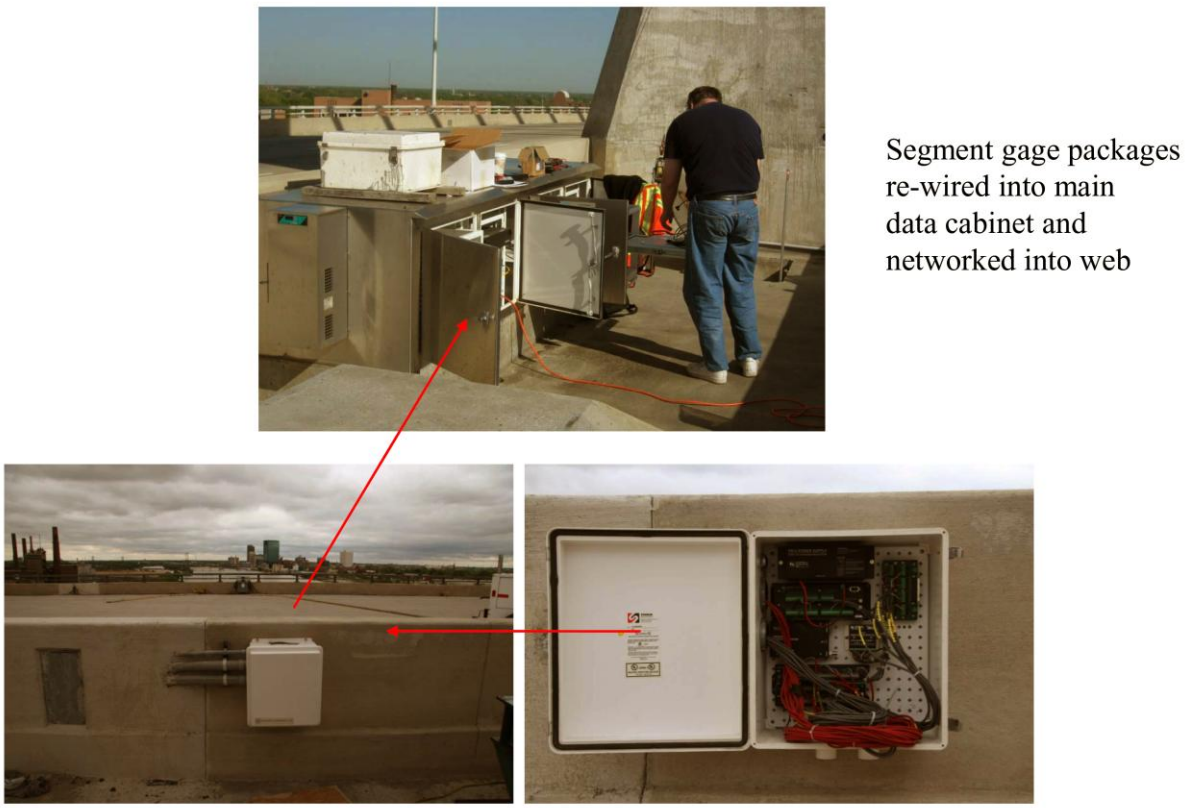

Figure 3.7 Data Collection after Construction (Helmicki, 2010)

As part of the VGCS Ice Prevention and Removal Project, information from the RWIS and strain are posted on the VGCS website. This compactly presents icing conditions and strain information on one website. Thus, the website is a "one-stop-shop" for all archived and ongoing VGCS information. The diagram in Figure 3.8 shows the relationship of the two instrumentation backbones and how the data would be collected, archived, processed and made available for analysis. This would involve making the RWIS sensor and video camera data available for on-demand retrieval, as we have done already with the bridge sensors.

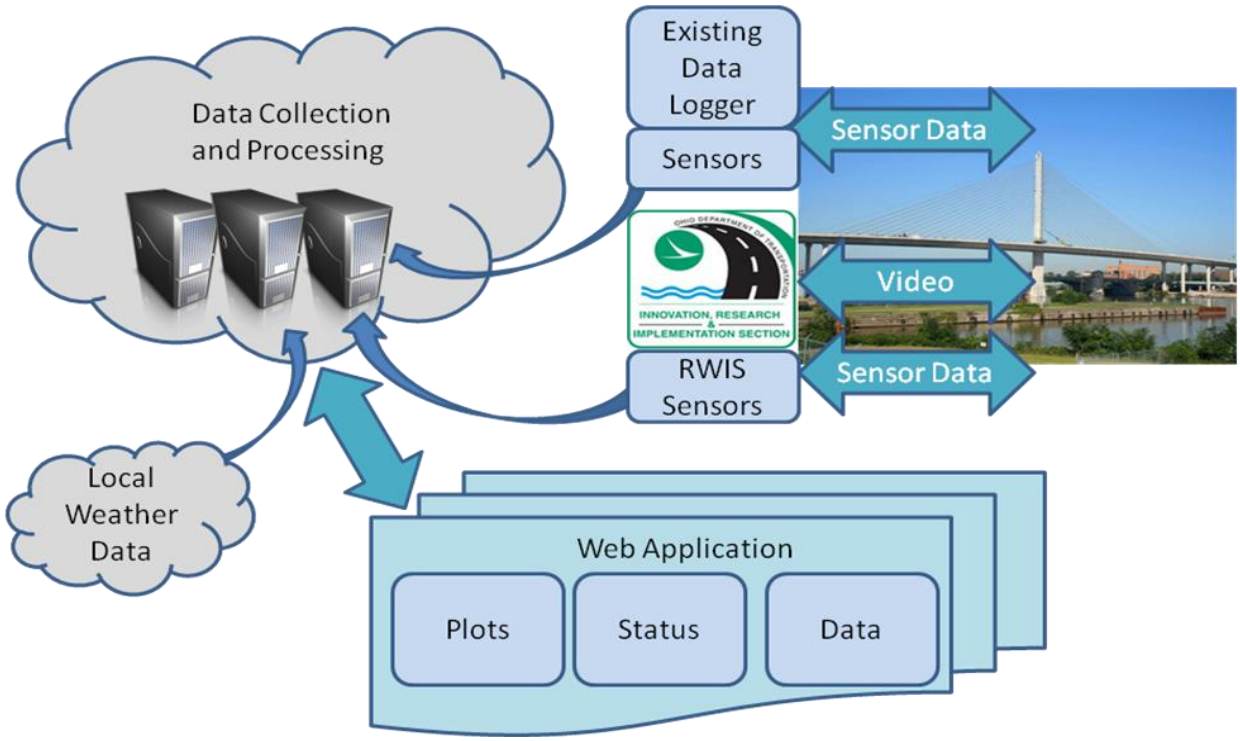

Figure 3.8 Dual Purpose Website Implementation (Nims, 2010)

The coordination of this with any additional data available already on the Internet (e.g. national weather service, conditions at the local airport, etc.) can be collected and used for local weather condition analysis in order to address the icing issue for the bridge stays. Available information to monitor icing is on the VGCS website. As additional metrological instruments are added or other aspects of VGCS are addressed, the information will be posted on the website. When the system begins operation it will be necessary to review the data closely and ascertain the system is functioning properly. This will be facilitated by the web application which will provide the ability to check the status of, plot and access all sensor data and archived video from both the RWIS and the research instrumentation backbones. This will also provide the research group the information needed to assess the equipment and system performance and validate any research findings or conclusions.

3.5 Research Results and Conclusions

A health monitoring system for the bridge was designed, planned, and implemented for the Veteran's Glass City Skyway bridge, with data collection and archival throughout its construction and ultimately an automated, user-friendly interface on a dedicated website. The primary criteria for selecting the segments to be instrumented was predicted stresses and rating factors using the analytical data provided by the designer. An addendum to the plans was prepared to document the items to be installed by the contractor (e.g., conduit, junction boxes, main data cabinet, phone service, power outlets, etc.), the general plan for instrumentation and testing, the required access to the site and casting yard by the university research team (URT), the requirements for notification during construction, and the protection of instrumentation, wiring, and data acquisition equipment. Once gages were installed on the rebar cage of the segments, the lead wires were routed to the inside parapet and protected from the elements by using trash bags and a white NEMA 4 box. Initially, each segment was handled independently (e.g., in the casting yard), but ultimately both northbound and southbound segments were combined at one multiplexer after their installation on the bridge. As per the plans, the contractor installed conduit along the length of the parapet, mounted the white boxes to the side of the parapet, installed the main data cabinet near the pylon, and connected all these together to enable one common architecture for the health monitoring system. This will be facilitated by the web application which will provide the ability to check the status, plot and access all sensor data from the instrumentation backbones. This will also provide the research group the information needed to assess the equipment and system performance and validate any research findings or conclusions.

References

1. A. Helmicki, V. Hunt, D. Nims, "Instrumentation of the Maumee River Crossing/Veterans' City Glass Skyway Phase II ," Annual Project Review Meeting, University Research Team, University of Cincinnati, University of Toledo, Columbus, OH, 2010.

2. Nims, D., Helmicki, A., Hunt, V., "Ice Prevention or Removal on the Veteran's Glass City Skyway Cables ," Annual Project Review Meeting, University Research Team, University of Cincinnati, University of Toledo, Columbus, OH, 2010.

3. C. Qiao, "Analytical and Experimental Stress During Construction of the Veteran's Glass City Skyway," Thesis, University of Toledo, 2009.

4. P. Nimse, "Calibrated Baseline Model of a Large Cable Stay Bridge," Dissertation, University of Toledo, 2007.

5. R. Ward, "Short-term Construction Load Monitoring & Transverse Bending of the Bottom Slab on the I-280 Veteran's Glass City Skyway," Thesis, University of Toledo, 2007.

6. K. Bosworth, "Health Monitoring of the Veterans' Glass City Skyway: Vibrating Wire Strain Gage Testing, Study of Temperature Gradients and a Baseline Truck Test," Thesis, University of Toledo, 2007.

7. B. Wright, "Experimental and Analytical Analysis of Concrete Strain Concentrations on the I-280 Veterans Glass City Skyway Cable Stayed Bridge," Thesis, University of Toledo, 2007.

8. International Bridge Technologies (IBT), Bridge Designer II-D (BD2) Model of Maumee River Mainspan, Ohio Department of Transportation, Columbus, OH, 2003.

9. University Research Team (URT), Addendum 10, Support of Instrumentation and Testing of Superstructure, Maumee River Crossing Plans (LUC-280-2.96), PID 20208, Project No. 010493, Ohio Department of Transportation, Columbus, OH, 2001.

10. Figg Engineering, Maumee River Crossing Plans (LUC-280-2.96), PID 20208, Project No. 010493, Ohio Department of Transportation, Columbus, OH, 2001.

Chapter 4 Bridge Modeling and Analysis

4.1 Introduction

With the recent increase in the cable stayed bridge inventory in the US, a better understanding of cable stayed bridge characteristics and the development of accurate 2D and 3D models of these structures have been realized. Collecting strain data through monitoring of bridges is a useful tool for obtaining baseline structural behavior and maintenance planning. Moreover, development of an as-built calibrated finite element model is another efficient tool that may serve as a baseline for future reference.

Development of a finite element model and its subsequent calibration is the ultimate goal of this work. For calibration in general, the steps are 1) Selection of model type, two dimensional or three dimensional and preliminary development of the model, 2) conduct load tests and monitor the response, 3) simulate the load test on the model and compare the model output against the measured response, and 4) make changes in the model so that the model output correlates with the measured response. This chapter is focused on the preliminary development of the model and the rest of the steps are included in the following chapters.

Cable-Stayed Bridges in general are highly nonlinear and undergo large deformations under loading. For such structures, it is essential to account for the deformed configuration in analysis. But the VGCS is a short span bridge and for its span the arrangement of box girders and delta frames make it very stiff. It is therefore expected to undergo small deformations only. Considering this, the design [IBT, 2005] models had assumed linear behavior. The linearity assumption allows superposition of responses to all the loads. This assumption of linearity can be verified by doing visual inspection of data. Apart from this, the assumption of linearity can be verified by performing linear analysis and comparing it with the measured response. The only nonlinearity considered in the design models was that of material nonlinearity. The other important assumption, as far as model development is concerned, is that the arrangement of delta frames and segments means there is no contribution to longitudinal stiffness from the delta frame. The available design models are two dimensional and were used for self weight and construction dead load analysis as well as live load analysis. Separate models were also available for critical load combination analysis.

It would have not been possible to simulate the test load configurations with a two dimensional model and get an output that correlates well with the measured response. Thus, a three dimensional model was necessary to represent truck load in 3D. Also, since the design models are not necessarily required to be very accurate, and as long as they satisfy the code requirements, the level of detail is not sufficient for maintenance. Whereas, a baseline calibrated model essentially is a very important maintenance tool. Therefore, a three dimensional model able to represent the real three dimensional bridge geometry accurately, as well as having the ability to simulate symmetrical and unsymmetrical loading, was needed.

4.2 Model Description

The delta frame model, described in chapter four of Nimse (2007) dissertation, was used to simulate the component stiffness of the delta frames in the full bridge model. This was done with confidence since the delta frame model correlation which showed a close match with the measured data and verified that the elements used to represent the delta frames accurately simulated the stiffness under varying loading and boundary conditions. The delta frame does not provide longitudinal stiffness.

Larsa 4D [Larsa 4D, 2007] was used to develop a three dimensional finite element model of the bridge simulating as-built geometry, stiffness and boundary conditions. A few assumptions were made for developing the model and are based on the design assumptions [IBT, 2005]

1) Bridge response is linear (small deformation theory). Small deformations can be expected and the progressive calibration and final calibration support this assumption, as were discussed in chapters 6 and 7 of Nimse (2007) dissertation.
2) The elastomeric bearings at the permanent piers offer minimal stiffness in longitudinal, transverse and all the rotational directions and so their stiffness contribution in those directions was neglected. The assumption of neglecting bearings stiffness was validated by calibrating the model to field results. The combination of bearing stiffness and permanent concrete pier stiffness is simulated by providing a vertical spring with compressive stiffness of 87,971 kips/ft. The
3) The stays for the VGCS are continuous through the cradle, but in the model they are represented by two separate stays stressed at the same time. Instead of strand by strand

stressing the sum of the forces in all the strands of a particular stay are applied as a single pretension force.

The values for spring stiffness are physically reasonable and provide reasonable results, which were shown in chapters 6 and 7 of Nimse (2007) dissertation. The breaking down of single stays into two separate stays and stressing them simultaneously is supported by the results of the tests done on the cradle [Public Roads, 2002]

The bridge will experience maximum deformation during construction of the cantilever span under self weight and during stay stressing. This work calibrated the model for two stages. The first one is very close to end of construction except for the boundary conditions and two stays unstressed (chapter six of Nimse 2007 dissertation). The second corresponds to end of construction before the bridge is opened to traffic (chapter seven of Nimse 2007 dissertation). For both the stages it is expected that the deformations under self weight are higher than due to live loads. For developing the model, one of the elements used is the cable element which is a nonlinear element with stress stiffening properties and requires nonlinear analysis. However, since the self weight is so high it is expected that the cables will always be in tension and none of the expected live loads would reverse the cable stresses. Therefore, the stress stiffening properties were not utilized. These arguments were verified since the linear and nonlinear analysis responses were found to be similar, and were explained in chapter six and seven of Nimse 2007 dissertation.

4.3 Elements

Three types of elements are used, the Larsa 3D beam element, the Larsa cable element and the Larsa grounded spring element.

The beam element [Larsa 4D, 2007] has six degrees of freedom at each end joint: translational displacements in X, Y and Z directions and rotational displacements about X, Y and Z directions. This element includes axial and shear deformations, twisting about its x-axis, bending in two perpendicular planes, and associated shears. The beam element is capable of exactly representing constant axial deformation along the beam with constant torsional shear deformation and linear bending deformations within the element. This is accurate for analyzing structures with loads applied at joint points. However, modeling these deformations requires a

higher order representation due to axial loads, torsional loads, lateral loads, and moments along the elements.

The cable element is identical to the truss element except a cable element cannot resist compressive force. The cable element can only be used in a nonlinear analysis. If the axial force in a cable element becomes compressive during the analysis, then the cable element is assumed to have no axial stiffness and cannot carry any load. It is kept in the model as an inactive element with no contributing stiffness. During the loading process of a nonlinear analysis, if the element can become tensile again, it is included in the model with contributing stiffness to the system. This element has geometric nonlinearity and stress-stiffening in all nonlinear analysis types. But, for VGCS the basic assumption of linear behavior was made. Therefore, linear analysis was run and Larsa converted the nonlinear cable element into linear truss elements for linear analysis. The truss element has only translational displacements in X, Y and Z directions at each end and it has no rotational stiffness. These elements can carry axial force only. The cross-sectional area determines the axial stiffness of the element, and it is the only stiffness required to be entered for sections assigned to truss element members. The values for Ix, Iy, Iz and shear areas are ignored for truss and cable elements.

The grounded spring element is defined using a single joint and there is no length associated with the element. The element represents a spring connecting a joint in the structure to the ground. The nonlinear grounded spring element is a general foundation element. Since the pier segments for VGCS are placed on elastomeric bearings attached to the top of the concrete piers and there is no structural element connecting the pier segment to the bearing, the compression stiffness provided by the bearings is very high compared to the tension stiffness provided by the bearing. However, completely neglecting the tension stiffness will lead to use of a nonlinear spring requiring nonlinear analysis. Because no gaps due to uplift were observed during construction between the pier segment and the elastomeric bearing, a tension stiffness equal in magnitude to the compression stiffness was assigned for the bearing spring.

4.4 Arrangement of beam elements

The delta frame model is shown in Fig. 4.10 and Fig. 4.11 of Nimse 2007 dissertation.

Fig. 4.1 shows the use of the delta frame model in the arrangement of beam elements at the cross-sections of VGCS where stays are anchored. The delta frames are connected to the nodes of the main span beam elements (representing the box girders) using rigid members.

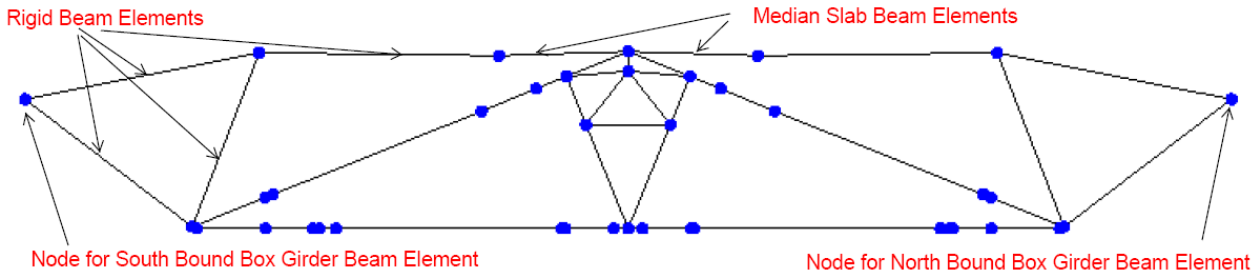

Figure 4.1 Arrangement of beam elements at stay anchor cross-section (Nimse 2007, Fig. 5.1)

A partly isotropic elevation of the bridge, which shows the point where the stays are connected to the delta frame can be seen in Fig. 5.2 and Fig. 5.3 of Nimse 2007 dissertation. They also show the details of the stay and pylon connection. It can be seen that the stay is connected to rigid members, which are connected to the pylon. The node where the stay connects to the pylon corresponds to the point in the physical structure where the cradle begins for that individual stay. Fig. 4.2 shows the full isotropic elevation with pylon support and span 26 and span 29 with their spring supports.

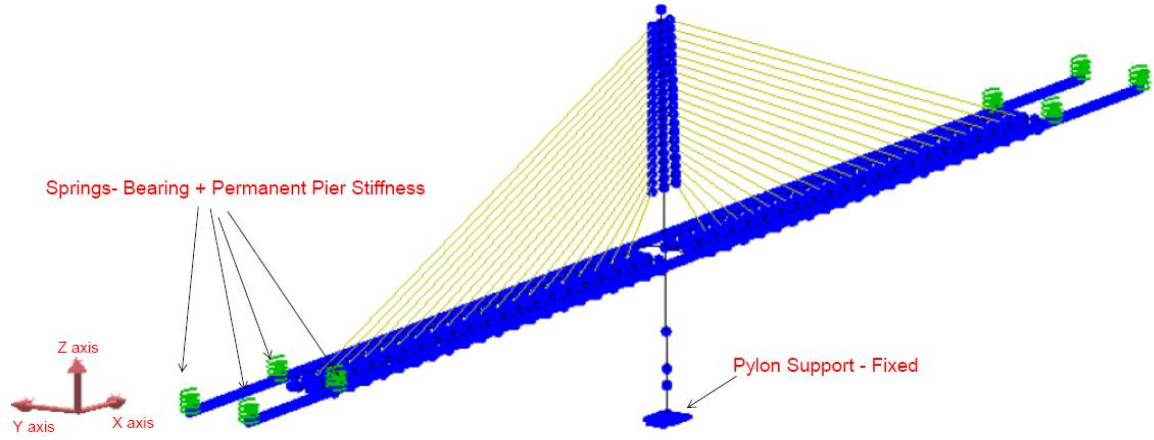

Figure 4.2 Full elevation (Nimse 2007, Fig. 5.5)

4.5 Conclusion

Since a cable stayed bridge may exhibit a complex nonlinear behavior, it necessitates that all the assumptions made during the design stage be verified. Above all, if the cable stayed bridge is made of concrete segments whose behavior is inherently time dependent, it adds to the

problem of predicting a response. It was concluded from the literature references that assumptions and choices affect the analytical precision required are: 1) the 2D or 3D analysis, 2) the use of particular type of finite element for elements like segments and cables, 3) the material property representation in the model, and 4) the assumption regarding the way the bridge is going to behave at the connections. These all help in determining the validity of the model. These assumptions might speed up the analysis and may be acceptable at the design stage but they need to be verified before they could be used to generate quantitative data to be used for maintenance. For the proposed study, reviewing previous literature research efforts have yielded significant information that will used to develop initial models in such a way that they will require minimum changes afterwards to calibrate them. Also keeping in mind that the instrumentation suite employed for VGCS is a sparse one, it was decided to progressively calibrate the model, that is, make changes to the model parameters such as stiffness and support conditions so that the model output correlates well with the measured data even for intermediate stages of construction. This was done to instill confidence in the use of the model that give a baseline dead and live loads for the bridge. Future changes in stress indicate a change in bridge condition. Therefore, a calibrated model is an essential maintenance tool.

References

1. Nimse, P.S., 2007, "Calibrated Baseline Model of a Large Cable-Stayed Bridge." Ph. D. Dissertation, The University of Toledo.

Chapter 5 Analytical and Experimental Stress during Construction of the Veteran's Glass City Skyway (VGCS)

5.1 Introduction

Previous short-term studies on the VGCS have been performed by Dr. Parag Nimse (2008) and Mr. Robert Ward (2008). This study was the first review of the long-term performance of the bridge. The bridge segments were instrumented when they were cast and data has been collected from the casting through the present in order to compare experimental and actual stresses, and verify the long-term performance of the health monitoring system (Chong Qiao, 2009; Yi, 2010; Gupta 2011).

The fundamental problem is to compare the experimental stresses derived from the health monitoring strain gages during the life of the I-280 Veteran's Glass City Skyway to the calculated stresses that were anticipated during design. The work performed herein focuses on stress comparison for construction events since the largest change in strain occurred during the main span construction, which represents the initial in-depth review of the strain gage and analytical data. Therefore, the focus is on reasonableness and behavior rather than an exact procedure. This comprehensive overview will be used to define the future data reduction tasks that will be completed.

The measured strain time histories at selected locations were converted to stress time histories and compared to the construction stress time histories calculated by International Bridge Technologies for the contractor, Fru-Con. Data without corrections for time and temperature effects were reviewed to get a basic understanding of the data and the necessary resources to perform the required comparison. The strains at all gage locations were reviewed to establish the validity of the approach and identify areas for refinement. Based on this initial review, data reduction were recommended.

Previous works done by Nimse (2008) and Ward (2008) present the strain gage installment method. 128 health monitoring strain gages were installed at four sections (32 gages for each section) to measure the actual effects of construction or load effects. Selected segments and gage locations are shown as figure 3.2 and figure 3.3. Each location has 2 gages. One strain gage is a vibrating wire. The vibrating wire gage has a built in thermister to measure temperature. The other strain gage is a foil resistive gage. This present study addresses long term effects, so only the vibrating wire gages are considered.

For each gage, the strain and temperature are reported. The strain data are recorded in micro strain ($\mu\varepsilon$), while the temperature data are recorded in degree Celsius. For each section, the files of collected data were formed and transferred to a simple matrix for each gage's information utilizing Matlab software. Of the eight segments which have strain gages installed, northbound and southbound span 28 segment 28 (28BB28) would be significantly influenced by construction procedures since it is located at middle span of span 28 which was a cantilever in construction. Data from 28BB28 was recorded in main span construction procedure which made 28BB28 a good trial section to see if the data set holds up. A command program was written (Chong 2009, Appendix) to combine data and to illustrate the strain time line history for a certain gage.

By comparing the entire strain time history line of northbound and southbound spans, a difference was found for span 27 directions due to a difference in construction methods. Southbound spans were constructed using an under-slung truss that carried the segments at the lower surface, while the northbound side of the backspan was constructed using the AG-1 gantry that supported the segments from the upper flange. At the end of the construction, the temporary supports were released and then these north and south bounds performed identically thereafter. From the same trend during construction, the assumption of identical performance in both spans has been confirmed.

Fru-Con's model is a 2 dimensional model. Therefore, the stresses reported by the model depend only on the longitudinal position and gage elevation. The calculated stresses are independent of transverse position. Strain from gages at the same elevation within one segment and on the northbound and southbound have been compared and found similar. In general, this means only one gage or an average at each elevation needs to be examined at each section. For each cross section's load condition, one top longitudinal gage and one bottom longitudinal gage were studied.

5.2 Obtaining Stress from the Analytical Model

The construction company Fru-con developed a construction simulation finite element model by using BRIDGE DESIGNER II (BD2) to simulate construction events in different phases. It uses basic matrix structural analysis formulation combined with time-dependent material properties, to carry out a time simulation of the bridge design during construction. During this process, all stress conditions are checked at every construction step as well as in

service. Every construction stage was simulated in the model. Additionally, stresses and deformations are calculated at specific times. Fru-Con adopted the FIP-CEB model to estimate the time dependent behavior of modulus of elasticity of concrete. However, for data reduction, an approximate equivalent constant E was used.

5.3 Comparing the Stress Time History Data from Measurement and Analysis

Experimental strain data was extracted from the collected strain data file, and plotted as a strain time history line for checking with construction events. The initial strain was obtained from the time history information at the casting date. Then the strain time history line was normalized by subtracting the initial strain. The experimental stress can be obtained by multiplying the strain by an estimated modulus of elasticity E. The stress information for each cross section was picked from the stress output file. The stresses for representative events were picked out and arranged in the stress time history line to check the consistency between the analytical and experimental result.

Experimental data from span 28 strain gages matched analytical data during construction. For gages at bottom of segment such as 28NB28BFL and 28NB06BFL, the analytical stresses and the experimental stresses have almost perfect fit in both trend and value. For gages at top of segment such as 28NB28TFL and 28NB06TIL, since they are located near the neutral axis which is about one third of the segment's height from the upper surface, the stresses amplitudes are not as large as bottom gages, but they also show good matches between analytical stresses and experimental stresses.

The stay cable stressing processes generated the most obvious signatures of strain, and it was the most convenient set of events for checking because the change in strain amplitude was big and the exact time information was available in the cable stressing log. Figure 5.1 shows the 28NB28BFL comparison between analytical and experimental stresses in stay cable stressing construction events. The analytical stresses are from segment #330 in Fru-Con's model.

Data from span 27 strain gages did not fit as well as span 28 during construction. Because span 27 was erected span-by-span and supported by temporary piers there are not the large changes in stress as seen in span 28. The reasons for these differences may come from the complex load conditions in span 27. The analytical stresses and the experimental stresses in span 27 have a basic match.

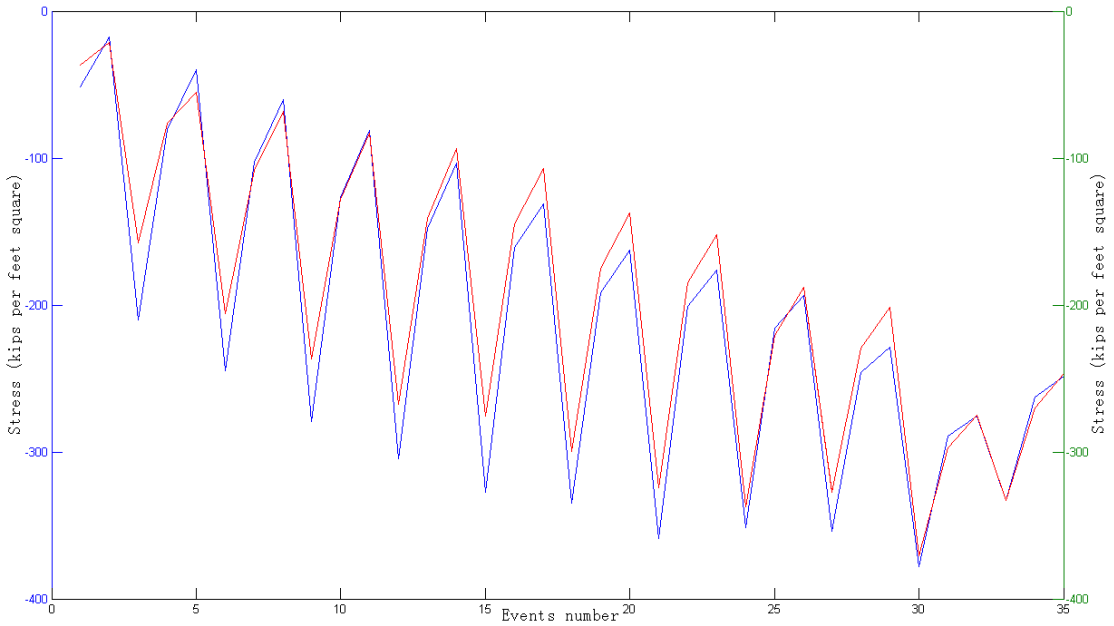

Fig. 5.1 Events comparison between experimental and analytical stresses in 28NB28BFL (Chong 2007, figure 4.4 and 5.5)

The day 2000 match for each gage is not a good fit. This discrepancy reflects the assumption of the constant modulus of elasticity. A time varying modulus is necessary to simulate long term behavior.

5.4 Conclusions and Future Studies

A total of 128 vibrating wire strain gages were installed in eight segments at four cross sections to monitor the long-term behavior of this bridge. Data from these gages has been collected since the casting date of each segment. During Chong (2009) work, a method of assembling the time line was developed, a Matlab program was written to combine the strain time history line for the data of one strain gage, and the experimental stresses were compared to analytical stresses calculated by the contractor.

From the sample study of the time history line from 28NB28BFL, a good match between construction events from the construction log and health monitoring strain gage data was observed. Other gages' data also showed a good fit to construction events. These good matches

indicated that the gages worked properly during construction, and the data from these gages is an accurate reflection of the actual strains in the bridge.

By checking the gages at the same elevation located in the same longitudinal position, the assumption of a two dimensional model, where there is little bending about the vertical axis was verified. Based on this verification, information from one top and bottom gage in each cross section is concluded to be representative for the local load condition.

The next step was using the strain gage data to derive experimental stress time histories to compare them to the construction finite element analyses. To calculate converted stress time histories, the initial strain and modulus of elasticity are required. The initial strain for each gage can be obtained from the strain time history on the casting date. It is a reasonable first approximation to consider the modulus of elasticity to be a constant because the construction procedure took a few months and the segments were typically several hundred days old. Thus, looking at Fig 12.2 the modulus was nearly constant.

By following this research procedure, the comparisons between analytical stress and experimental stress for selected gages were done.

Above all, this work supplied a convincing confirmation of both the accuracy of the gage monitoring process and the finite element analysis used in the design and construction of the VGCS.

The following actions are recommended for further data review:

- The modulus of elasticity as a time dependent coefficient should be used in the future to generate a more accurate experimental stress time history line for a long time comparison and prediction.
- The continuous database of collected strain should be updated in the future. Based on this database, the long-term monitoring, the future load condition prediction, and load rating can be correlated with the contractor’s or another model.
- The zero strain estimate for each strain gage is inherently uncertain. The method of determining the zero strain should be more fully developed to minimize the uncertainty
- Other factors, such as temperature and geometry, which could influence the reduction of the strain gage data needs to be studied in the future to get a more accurate result.

Based on future truck testing and improving the accuracy of the long term strain data reduction, improved estimates of the short term and long term stresses can be made. These estimates of live load and dead load stresses can be used to establish an experimental load rating.

References

1. Nimse, P.S., 2007, "Calibrated Baseline Model of a Large Cable-Stayed Bridge." Ph. D. Dissertation, The University of Toledo.
2. Qiao C., 2009, "Analytical and Experimental Stress During Construction of the Veteran's Glass City Skyway" Master Thesis, The University of Toledo.

Chapter 6 Monitoring of the Veterans' Glass City Skyway Vibrating Wire Strain Gage Testing

6.1 Introduction

Vibrating wire strain gage technology has been around for quite some time and has become a well-established and trustworthy system of instrumentation. Vibrating wire strain gages have been used on a variety of infrastructure projects including dams, tunnels, foundations, bridges and buildings (Coutts, 2001). The ability of these gages to accurately track long-term stresses can lead to a better understanding of the behavior of construction materials which can lead to less over-designing and a higher quality product.

These gages have shown throughout the years that they are robust, easy to install, and accurate. In comparison to other gages, vibrating wire strain gages are more rugged, and can be used for long term monitoring for 20 to 30 years without worry of glue debonding from the specimen, or drift, which plagues bonded electrical resistance strain gages. For example, many vibrating wire gages can be attached externally by welding or epoxy, and can even be embedded into the specimen, (Bosworth 2007, figures 2.1, 2.2, and 2.3 respectively).

Vibrating wire strain gages measure strain by use of a frequency-sensitive sensor, which determines the frequency of the wire contained within the metal sheath. The gage is capable of determining the strain in a specimen by determining the fundamental frequency of the wire, which depends on the length and tension of the wire, which in turn depends on the strain in the specimen.

While vibrating wire strain gages are resilient and accurate, they have their drawbacks. One drawback is the small number of readings they are capable of in a period of time. The process of determining the fundamental frequency of the wire is accurate yet slow, as typically vibrating wire strain gages can at most take one reading per minute. This speed means that it is not capable of measuring rapidly changing conditions, The second drawback is the effect of temperature on the gage. The second drawback stems from the difference between the coefficients of thermal expansion of the gage and the specimen, which causes the gage and specimen to expand or contract at different rates. However, since the gage is permanently affixed to the specimen, the gage is forced to expand or contract with the specimen; thus introducing thermal strains and/or stresses into the gage readings which was accounted for by installing a thermistor within the vibrating wire strain gage housing, which records the

temperature along with the strain. With the temperature of the gage and specimen known (assuming the gage and specimen are at the same temperature), it is theoretically possible to determine the strain associated with the loading separately from the strain due to temperature by adding the change in temperature multiplied by the difference in thermal coefficients for the gage and the material which is being monitored.

6.2 VIBRATING WIRE STRAIN GAGE LAB TESTING

During construction there was concern about stress concentrations in the bridge. The stresses predicted by the model were high enough to warrant an elaborate finite element analysis and a field study. Therefore, external vibrating wire strain gages were installed in segments 28SB25 and 28SB15 where the high strains were expected. These gages were mounted on the bottom slab of the concrete box segments to measure the strains due to self-weight as shown in (Bosworth 2007, Figures 1.1 and 1.2). Initial data retrieved from the gages showed very small strains in comparison to what the model predicted, on the order of 25 times smaller. Due to this discrepancy, the URT is investigating the gages and the whole chain of data collection equipment, including the CR-10X system, ribbon cables and the laptops used to download the data from the CR-10X. This investigation confirmed the data obtained was accurate that no problem existed in any piece of the data collection equipment.

6.3 Lab Testing Setup

In order to check the proper functioning of the installed strain gages and data collection equipment, a test setup was designed and manufactured, as seen in Figure 6.1. This setup will be similar in design to the setup that Geokon uses to calibrate their strain gages, seen in Figure 6.2. The gages tested were Geokon Model 4000 Vibrating Wire Strain Gages. The main components of the test setup as described in section 2.2.2 and Figure 2.6 of Bosworth 2007 thesis.

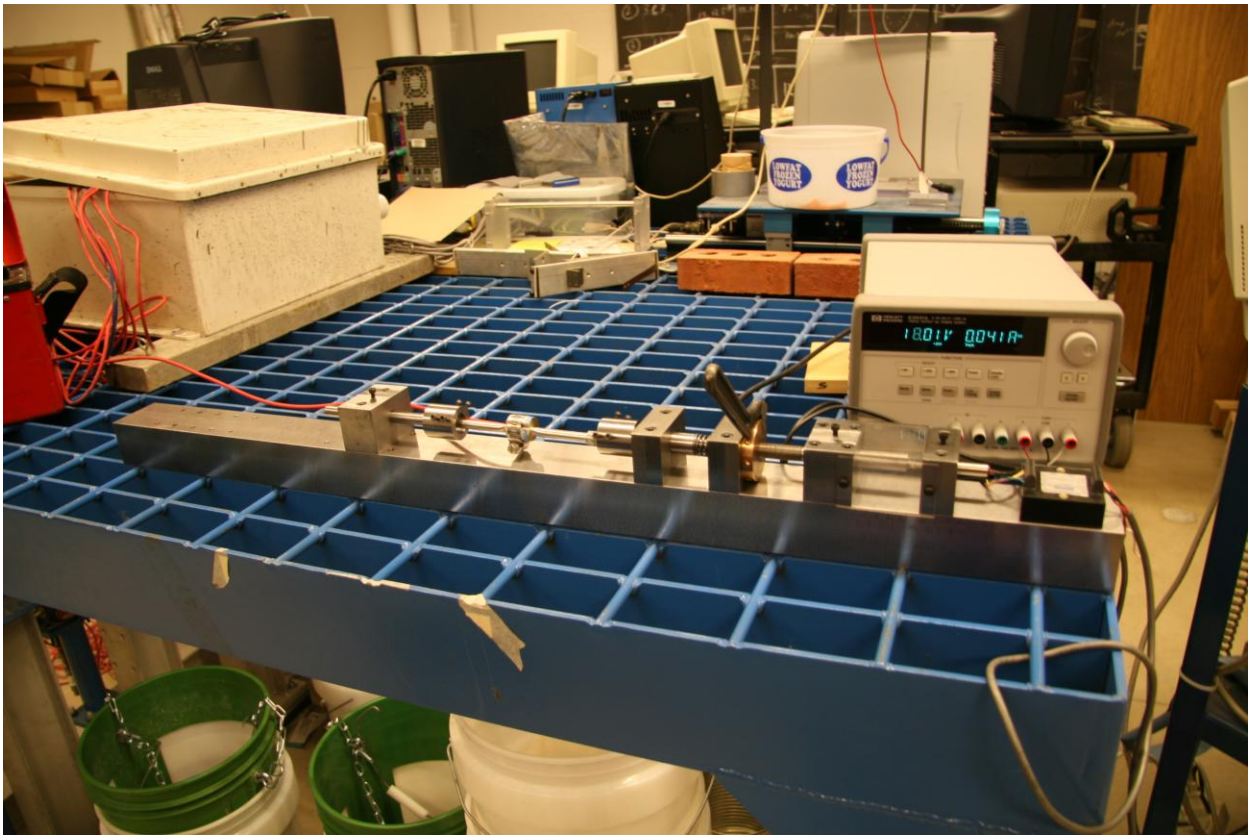

Figure 6.1. URT's Vibrating Wire Strain Gage Test Setup (Bosworth 2007, Fig. 2.4)

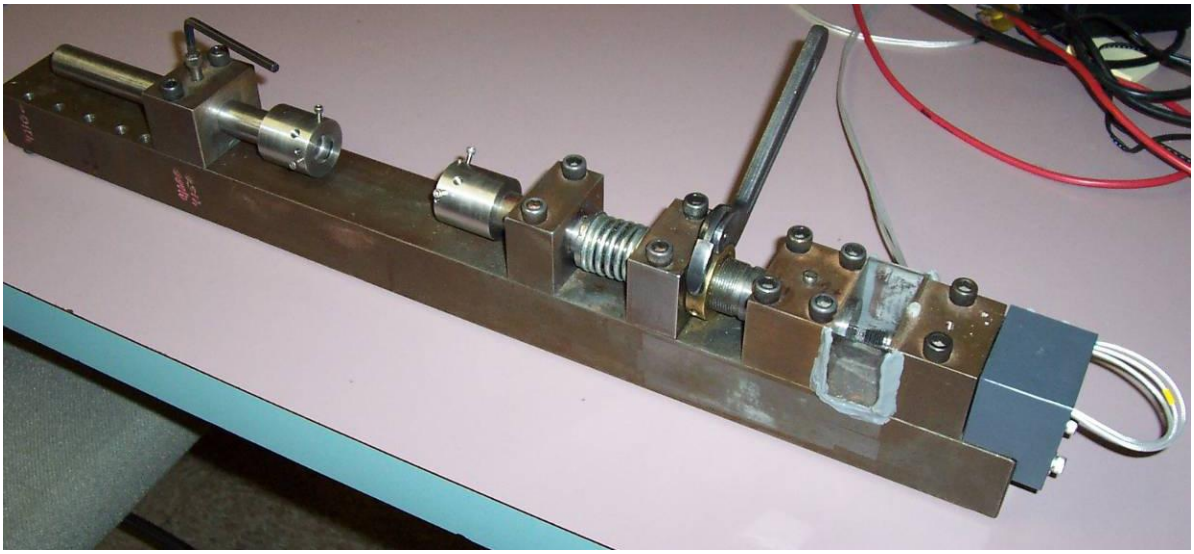

Figure 6.2. Geokon's Vibrating Wire Strain Gage Test Setup (Bosworth 2007, Fig. 2.5)

6.4 Data Collection and Processing

In order to confirm the proper functioning of the gages installed in 28SB15 and then 28SB25 as well as the whole chain of data collection equipment, several tasks were accomplished. See Appendix "A" of Bosworth (2007) thesis for a complete step-by-step description of how to perform the calibration. First, the gages were removed as carefully as possible from the segment and brought back to the lab, identifying which gage was in which location in case anomalies required further investigation. Figure 6.3 shows the gages as they were installed in the bottom slab. It should be noted that several of the gages had become partially embedded in grout during the construction process, as seen circled in Figure 6.3, and as such, removal of the gages involved hammers, screw drivers, fine chisels and a powered rotary tool. The removal methods used by the URT team members were crude with respect to the level of sophistication and accuracy of the vibrating wire strain gages; however, it certainly confirmed the robustness of the gages after all the gages were tested and found to work properly. Back inside the lab, testing was performed in a room with a fairly constant temperature, as this avoids the use of temperature correction equations and the use of a reference gage. Next, the LVDT was calibrated (Bosworth 2007, section 2.2.3). Then, each gage was tested in the test setup using the GK-403 Readout Box. Finally, each gage was tested using the CR-10X system, which allowed the URT to check the performance of the CR-10X system and the laptop used to download the data from the CR-10X.

After the data was collected, the data was processed and analyzed to extract the information required to check the proper functioning of the URT data collection equipment. One goal of using the test setup was to compare the strain readings of vibrating wire strain gages to the known displacements of the LVDT, which was used to calculate the strain in the gage based on the LVDT.

The strain readings from the vibrating wire strain gages were manipulated into an easy to use format: the strain readings were zeroed based on the average strain readings at zero displacements of the LVDT and then multiplied by the batch factor, a calibration factor used to correct the readings obtained from the vibrating wire strain gages.

Figure 6.3. Vibrating Wire Strain Gages in Segment 28SB25, Partially Embedded (Bosworth 2007, Fig. 2.8)

In order to obtain the strain reading based on the displacements of the LVDT, several steps were taken. First, the final output of the LVDT and Oscillator/Demodulator was DC voltage, which was converted into distances based on the calibration done with a micrometer. Once the strain based on the LVDT was determined, it was directly compared to the experimental strain as output by the strain gage and plotted on graph of Strain vs. Displacement so as to determine if the gages installed in the concrete box segments were functioning properly. Lastly, an experimentally determined batch factor was calculated by minimizing the percent error when comparing the strain readings from the GK-403 Readout Box to the strains based on the LVDT displacements.

6.5 Results and Conclusions

The main task concerning the topic of vibrating wire strain gages was to perform a chain calibration on the data collection equipment used by the URT when data was being collected and monitored in a segment.

Results for the seven Model 4000 Vibrating Wire Strain Gages that were installed in 28SB25 were plotted and analyzed, and can be seen in Appendix B of Bosworth 2007. Based on these results it can be said with certainty that there was nothing inherently wrong with these

gages, except Gage 6, which may have been damaged during removal, as they were tested in the same test fixture with two different methods of data collection. It is also highly unlikely that all seven gages were somehow installed improperly and yet yielded readings that seemed reasonable, both during construction and in the lab. When a basic installation procedure was violated, such as placing a wire in the wrong connector, crossing wires or improperly tightening set screws, it was obvious in the results, as the data for a gage might read -55°C or +or-9999με. After checking the data from the CR-10X and laptop used to download the data with the data obtained from the GK-403 Readout Box, the URT is confident that the CR-10X and laptop worked properly when data was being collected. Not only did this test fixture confirm the functioning of the whole string of data collection equipment, it can be used in the future to calibrate Geokon gage Models 4000 (End Block Gage), 4200 (Embedment Gage) and 4220 (Crackmeter), all of which are in use or have been used on the VGCS to monitor its health.

References

1. Coutts, D.R., Wang, J., and J.G.Cai. "Monitoring and Analysis of Results for Two Strutted Deep Excavations Using Vibrating Wire Strain Gauges." Tunneling and Underground Space Technology, V. 16, 2001.
2. Bosworth, K. J. 2007. "Health monitoring of the veterans' glass city skyway: vibrating wire strain gage testing, study of temperature gradients and a baseline truck test." Master's thesis, The University of Toledo.
3. Nimse, P.S., 2007, "Calibrated Baseline Model of a Large Cable-Stayed Bridge." Ph. D. Dissertation, The University of Toledo.

Chapter 7 Study of Temperature Gradients

7.1 Introduction

The effects of temperature on concrete bridges must be accounted for in design, as changes in temperature can lead to expansion, shrinkage and thermal-induced stresses and/or strains. There are two main types of temperature effects to be considered for bridges: effective bridge temperature and temperature gradients. Designing for effective bridge temperature assumes the whole cross section of the bridge changes temperature uniformly and the bridge attempts to expand or contract. Depending on the fixity of supports, this temperature change could cause an expansion or contraction if the bridge is permitted to do so; or if the bridge has fixed supports, the temperature change may cause thermal stresses since the bridge tends to expand but cannot. Another temperature effect is a differential temperature effect, also known as a temperature gradient, where the temperature varies across the depth of the cross section. There are two types of gradients observed and defined: positive and negative. The positive temperature gradient is defined as occurring when the top of the cross section is warmer than the middle and bottom. Conversely, the negative temperature is defined as occurring when the top of the cross section is colder than the middle. The temperature gradient effect in bridges is typically of more concern than the effective bridge temperature. Negative temperature gradients in particular can cause unacceptable levels of tension in the top slab, which can cause the concrete to crack unless sufficient reinforcing or pre/post tensioning is provided. These small cracks pose a large potential problem for prestressed concrete bridges, as cracking can allow water to seep into the cross section and corrode the prestressing strands, which is typically undetectable.

The research work in this chapter involves studying temperature gradients within the concrete box girders. The purpose of studying the temperature gradient, with special attention given to the negative temperature gradient, was to preliminarily assess if the VGCS response is consistent with the AASHTO design code; and to lay the foundation for future temperature gradient studies.

To accomplish this task, a large amount of data must be collected over several years spanning several seasonal temperature cycles in order to draw firm conclusions about how a bridge behaves in response to temperature. At the time of this study, a relatively small data set had been collected from the bridge segment studied, only 8 full months of data. Therefore, the

results from this study were only used as a preliminary assessment and to set a basis for future work.

Data was collected from the bridge by use of a temperature gun for surface temperatures, which was used to confirm the reliability of the thermistors embedded in the segments with the vibrating wire strain gages. Once confirmed, the temperature readings from the thermistors were used for the remainder of the study. This collected data was compared to the temperature gradients as specified by codes, as shown in Figure 7.1 for both positive and negative temperature gradients. From such figures it can easily be seen whenever the temperature gradient exceeds the AASHTO Code. Lastly, a conclusion was made based on the results.

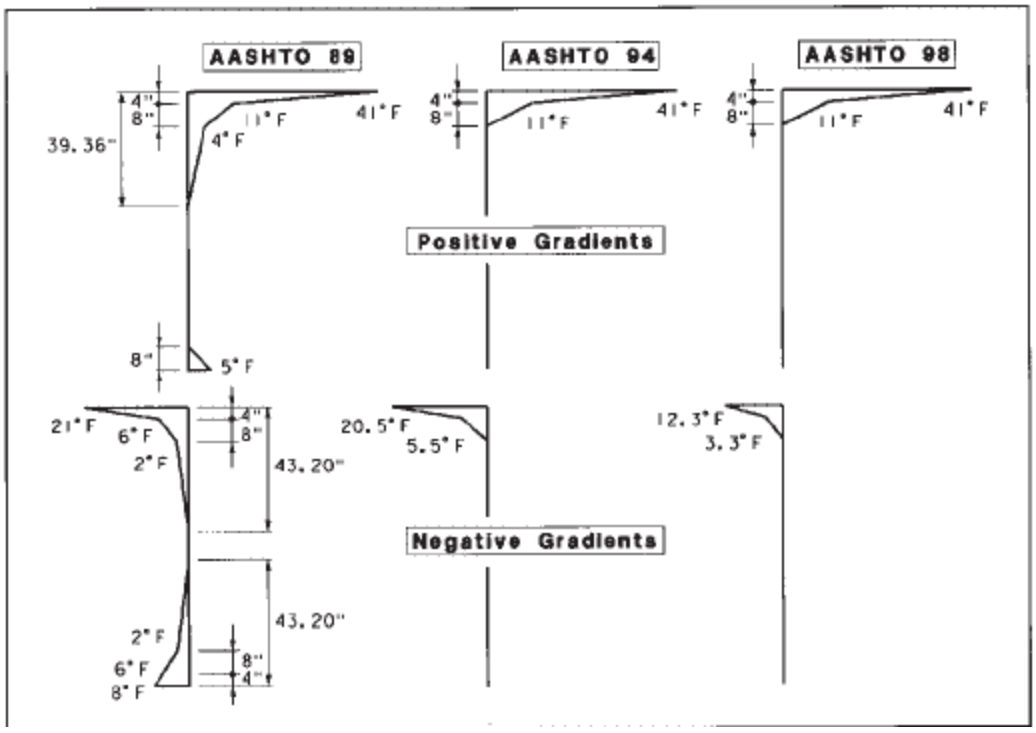

Figure 7.1 AASHTO Design Gradients (Bosworth, 2007)

To ensure that the thermistors function properly, a comparison of the measured temperature difference to the maximum based on AASHTO was performed to determine if the thermistors produce reliable data. All thermistors were found to have reasonable agreement with the nearest surface temperature data when compared to the Code, therefore, the thermistors were further confirmed by use of Priestly curve, that is, a temperature gradient that varied as a fifth-order

curve across the height of the section according to New Zealand specification. Priestly curve was used to predict surface temperatures based on the temperature readings of the thermistors at the depth of the gage. Only the gages in the top slabs of segments 28BB28 were used for predicting the surface temperature, since the Priestly curve does not always accurately predict temperature below the top-most foot or two of the section.

7.2 Comparison of Code To Collected Data

With the confidence that the thermistors were reliable, the temperature data for each gage was plotted against time and the calculated maximum positive or negative temperature gradient from October 2005 to September 2006 for Segment 26NB14 (Bosworth, 2007). In order to compare each gage with the positive or negative temperature gradients, the location of each gage was used so that the design temperature gradient at the height of each gage could be determined (see Figure 7.2).

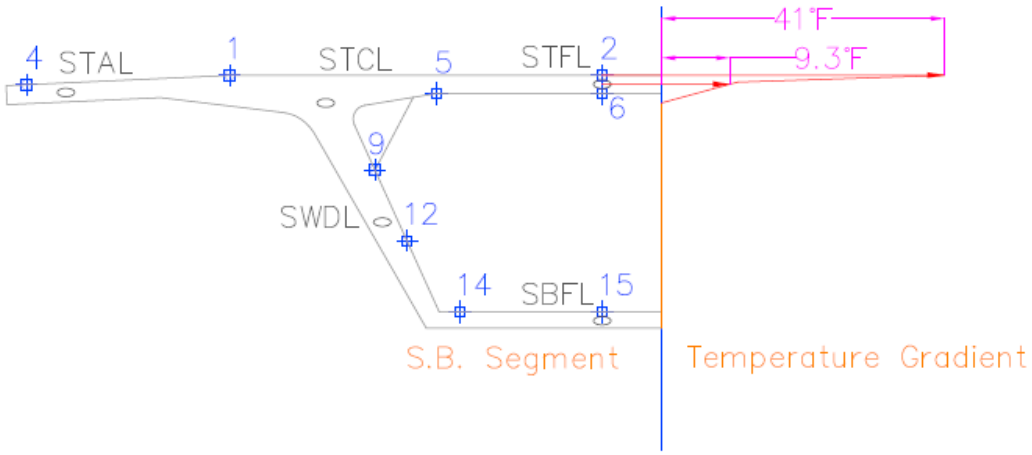

Figure 7.2. Height of Section and Temperature Gradient (Bosworth, 2007)

Another important assumption that was used for processing the data was that the bottom slab gage, VBEL, was the coldest temperature in the segment for the positive temperature gradients, and the warmest temperature in the segment for the negative temperature gradients. This assumption was based on the design temperature gradients, where there is a zero temperature gradient throughout the mid height to the bottom of the cross section.

A Matlab program was written to determine the highest positive and negative temperature gradient in each month and plotted out the two temperature profiles for further analysis (Nimse, 2007). For the positive temperature gradient, the Matlab program took the maximum

temperature from the five top slab gages and compared that to the temperature of the bottom slab gage VBEL for all points in time for each month. Then, for each month the time at which the maximum difference between the top gage and gage VBEL occurred was used to plot the temperatures in all the gages over the height of the section, or temperature profile, as this was considered to be the maximum positive temperature gradient for that month. Similarly, the negative temperature profile for each month was plotted, except the minimum temperature from the top gages was subtracted from VBEL, and the maximum difference was used to then find the time that it occurred, and then the temperature profile was plotted. These plots were then overlaid with the design temperature gradients, placing the zero portion of the gradient in line with gage VBEL, similar to what is shown in Figure 7.3. As mentioned earlier, it should be noted that the VGCS was not outfitted with gages to specifically track the temperature gradient across the height of the section. Consequently, these plots may not allow as much information to be gathered and inferred as a cross section that was specifically instrumented to monitor the temperature gradient. However, these plots will still be helpful in determining how the bridge responds to temperature changes and if the bridge performed within AASHTO guidelines.

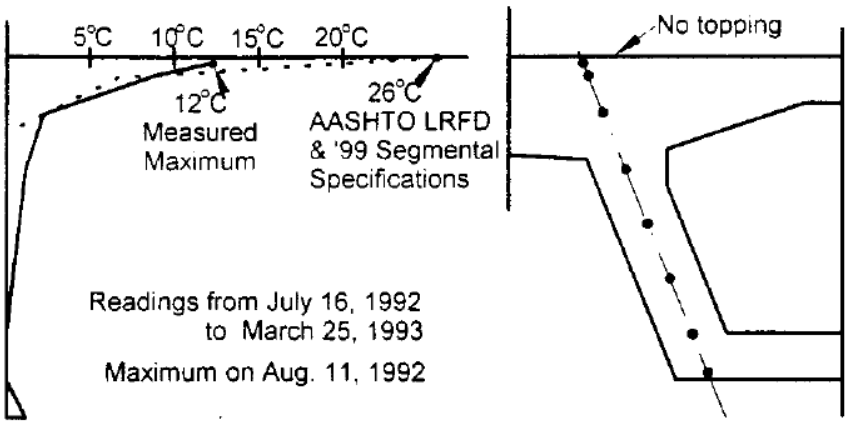

Figure 7.3 Temperature Gradient Over the Height of the Section (Bosworth, 2007)

7.3 Results and Conclusion

Temperature gradients in the VGCS were studied with two main goals: to preliminarily assess if the bridge behaves as the AASHTO Code predicts, and to lay the foundation for future studies of temperature gradients.

Results of the maximum and minimum temperature gradients in Segment 26NB14 were plotted for October, November, December of 2005 and January, February, March, April and

September of 2006. It should be noted that the accuracy of the thermistors is +/- 0.5ºC, or +/- 0.9ºF. This amount of error could have a significant effect on the shape of the temperature gradients, as will be seen in the following figures, as often the range of temperatures for a temperature gradient was at most 8ºF. Depending on which way the individual thermistors err, the range of 8ºF could easily decrease to almost 6ºF or increase to nearly 10ºF.

Plots of the Positive Temperature Gradients were fairly consistent for most of the eight months of collected data. This consistency was in the shape of the gradient, while the actual temperatures varied.

Consistency, however, was not the only attribute to observe from the temperature gradients; comparison of the actual gradients to the design gradient was done as well. It was found by inspecting the plots that the actual gradients follow and typically fall within the design gradient. One interesting similarity in the positive temperature gradient plots is that one or two of the upper gages, Gage VTHL and VTHT, was consistently colder than the bottom slab gage VBEL. This anomaly could be explained by the gage being located in a spot where it is surrounded by more concrete than other gages and that at the time of the maximum positive temperature gradient occurring the concrete immediately surrounding the gage did not have sufficient time to warm up as did gage VBEL. Lastly, the upper-most gages all fell within the design code, reaching upwards of 8ºF warmer than gage VBEL, while the design code temperature difference is 11ºF for the cross section at the height of those gages.

Plots of the negative temperature gradients were not as consistent as the positive temperature gradients, however, they were still insightful. Plots for two of the eight months of negative temperature gradients followed the general idea of the top slab being colder than the bottom slab, while the other six months actually were positive temperature gradients, indicating that negative temperature gradients never occurred during those months. Looking at the temperature difference in December between the coldest top slab gage and gage VBEL, it was found that this value was within the specified code value of 3.3ºF. However, in November, the gradient was not a maximum between the top-most gage and gage VBEL, it was between the one upper gage and the top-most gage. This could be explained in a similar way as in the positive temperature gradients when the gage takes longer to be affected by temperature changes since it is embedded deeper in concrete than other gages.

Based on the results from the small set of data used, it can be said that the VGCS behaves within reason to the AASHTO Design Code. Sometimes the gradient didn't follow the code well, as seen with the variability in even the well-behaved positive temperature gradients, or the two negative temperature gradients that occurred. However, taking into consideration the error of the thermistors, the variability of temperature cycles, the fast-changing weather patterns of northwest Ohio and the small data set available, the results were reasonable enough to indicate that the bridge performed within the code. Based on the confirmation of the thermistors and the preliminary results from eight months of temperature data, it is recommended that temperature gradients in the instrumented bridge segments are studied for long periods of time, on the order of years, using the framework from this thesis and the Ph.D dissertation by Nimse (Nimse, 2007) as a basis.

The fact that only two of the eight months produced negative temperature gradients demonstrates that negative temperature gradients do not occur very often, and underlines the importance of studying temperature gradients and analyzing several years' worth of data versus several months.

References

1. Bosworth, K. J. 2007. "Health monitoring of the veterans' glass city skyway: vibrating wire strain gage testing, study of temperature gradients and a baseline truck test." Master's thesis, The University of Toledo.
2. Nimse, P.S., 2007, "Calibrated Baseline Model of a Large Cable-Stayed Bridge." Ph. D. Dissertation, The University of Toledo.

Chapter 8 A Baseline Truck Test to Calibrate a Baseline Model

8.1 Introduction

There are several purposes for carrying out the truck test on the VGCS that occurred on June 17th, 2007. The main purpose of the truck test, which employed both static and dynamic loading, is to gather strain information that will be the baseline for the long-term monitoring of the bridge. This baseline has set the stage for future truck tests to be run, and by integrating the baseline with other information, researchers will be able to monitor the health of the bridge.

A second purpose of the truck test is to further confirm the Larsa model, a finite element model created by Nimse (Nimse, 2007), by checking if the strains predicted by the model match with the strain data collected during the truck test.

Two types of strain gages are installed on the VGCS, Geokon vibrating wire strain gages and bonded electrical-resistance (foil) strain gages. In the main span segments of the bridge, vibrating wire and foil gages are paired together embedded in the concrete (see fig. 8.1 for instrumented segments). While the electrical-resistance strain gages are well-suited for rapidly changing loading conditions, the vibrating wire strain gages excel in long-term monitoring. For the dynamic truck tests, in which the trucks traveled at speeds of about 10mph, only data from the electrical-resistance strain gages will be used. However, for the static truck tests, readings from both vibrating wire gages and electrical resistance strain gages will be reviewed. Due to the limitation of vibrating wire strain gages only taking readings at most once per minute, the trucks will be required to remain in the appropriate loading location for a minimum of 5 minutes to obtain several readings.

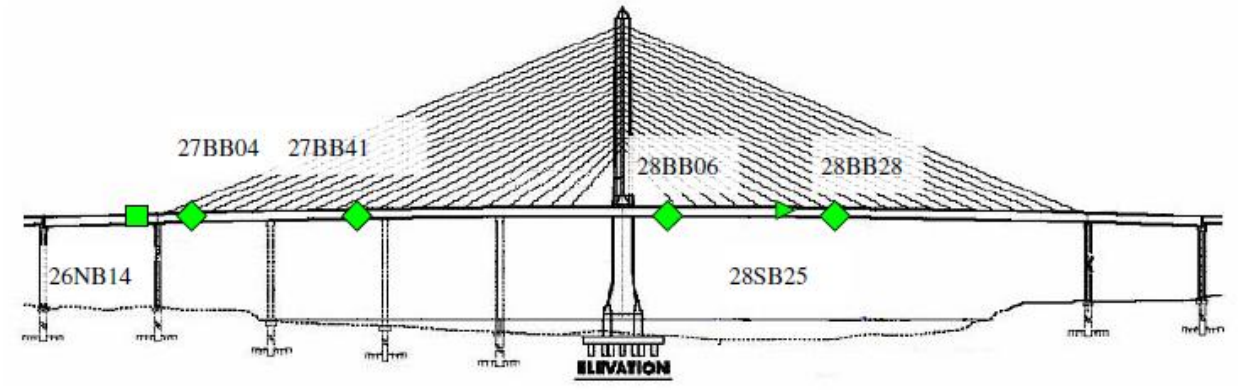

Fig. 8.1 Instrumented Sections

8.2 Truck Test

In order to obtain the best results and an acceptable response of the bridge, from the truck test, previous tests, such as Crane Withdrawal and Mini Truck tests (Bosworth, 2007) performed during construction and subsequent analyses have been investigated, along with model output. Influence lines for each instrumented segment were analyzed to find the locations of the maximum and minimum strains outputted by the Larsa model, which clearly shows the locations of maximum positive and negative moments. These locations were then used to place the trucks in the static load cases in order to obtain the maximum response of the gages.

A total of 25 configurations were planned and carried out for the Truck Test. These configurations fell into two main categories: static and dynamic. The static tests focused on maximizing the response from the gages, with typical loadings as well as worst-case scenario loadings. Dynamic tests focused on obtaining influence lines for the main span, which tracks the gage response as the loads moved across the bridge. Both static and dynamic tests were further categorized depending on the positions of the trucks, including symmetrical and asymmetrical cases about the longitudinal axis of the bridge. Some of the asymmetrical cases were aimed specifically at tracking the effect of placing loads at differing lateral positions. Figure 8.2 shows the main span of the bridge labeling specific piers, spans between piers and instrumented segments.

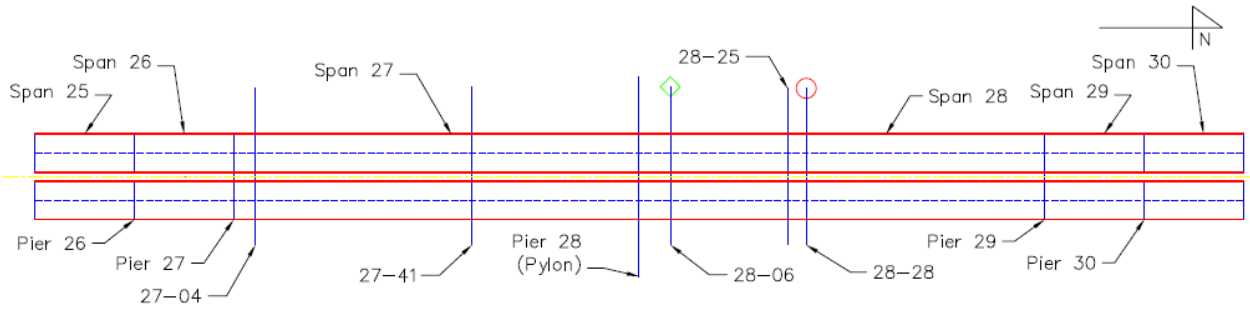

Fig. 8.2 Mainspan of Bridge, Plus Span 25 and Span 30

The goal of performing static load tests was to maximize the strain response from the gages by placing trucks in varying configurations. For most static cases, the trucks started at a location that was off the main-span of the bridge, south of Pier 26 in order to provide zero readings in the vibrating wire and foil strain gages. Then, the trucks moved into their appropriate positions according to previously planned configuration, recording the time that the trucks reached the position. Once in position, the lateral position of the trucks was determined by

measurements from the interior barrier or exterior parapet. The lateral positions were very important to obtain so that the trucks could be placed in the computer model at the correct position and then the results from the computer model could be compared to the field results with confidence. After recording the lateral positions of the trucks, the trucks remained in position until they had been there for a minimum of 5 minutes so that the vibrating wire strain gages, which collect strain data at a rate of one data point per minute, could record a sufficient amount of data.

The main goal of the dynamic load tests was to obtain influence lines for various configurations of trucks. Similar to the static load test, dynamic tests simulated typical loadings such as two trucks driving side by side on the bridge, as well as heavier loadings where three trucks drove side by side down one side of the bridge, maintaining in line positions with each other while driving side by side, and a relatively slow speed of 10mph was used to keep the trucks moving together. For all dynamic tests, the trucks started from rest at the center of Span 25, the span just south of the mainspan of the bridge. Trucks in this test moved across the bridge and as soon as they crossed the expansion joint, time was recorded and two data acquisition systems recorded data. When possible, the team data recorder noted the times when the trucks passed landmarks on the bridge, such as the center of the pylon, or a particular stay anchor, which was useful in determining the speed of the trucks as well as being able to match strain data with locations of the trucks at particular times.

8.3 Load Cases

Symmetrical load cases were used to check symmetry on the bridge. Checking the symmetry of the bridge is a valuable use of time since the bridge was designed and was anticipated to act symmetrically. In order to check symmetry, load cases were run in pairs; for example, one test would entail two trucks driving down the Northbound side of the bridge, followed by a test with two trucks driven down the Southbound side of the bridge. Then, according to symmetry, the results of the trucks driving down the Northbound lanes should be theoretically equal to the results from the test where trucks drove down the Southbound lanes.

Another type of load case used for the Truck Test was created to be able to check the superposition of loads on the bridge. Using the principle of superposition is a fairly common task in structural engineering, as most loadings are not high enough to cause non-linear effects.

While common, it is still highly valuable to confirm that the principle of superposition can be used for the Truck Test since it is a basic assumption in the model.

8.4 Results

While 25 load cases were run on the day of the Truck Test, Bosworth work (Bosworth, 2007) discussed a small subset of load cases, covering the ideas of influence lines, symmetry and superposition of loads.

One important step in analyzing the results of the Truck Test was to filter the noise from the foil gage data. In order to do so, an ideal fft-ifft (Fast Fourier Transform-Inverse Fast Fourier Transform) filter was created in Matlab. By removing the high frequency portion of the signal considered to be noise, the remaining data was the desired strain signal. It was important to filter the data to clearly obtain the values of the maximum and minimum strains and where they occurred.

After processing and reviewing the data from the truck test it was found that good data was collected from about 95% of the gages installed on the VGCS. Fortunately, all gages that had no valuable data are located in the top slab of the segments, where there are five other gage pairs. This is a much better situation than losing the one gage pair in the web, WDL, or the one bottom slab gage, BFL, as these gages are the only ones in their respective height of section.

For analyzing the results of the Truck Test, influence lines from the model were compared to the influence lines obtained from the dynamic truck load cases. In order to compare the Larsa influence line to the influence line obtained from the foil gages, bottom slab gage BFL was selected since positive moment in the segment leads to tension in the bottom, or positive strain . When analyzing the two figures, two ideas were kept in mind to account for dimensional irregularities, even though the general shape of both figures was the same. The model output plotted the influence line as Moment vs. Load Position; however, data from the foil gages was outputted initially as Strain vs. Time. These irregularities were overcome by understanding that on the y-axis, moment is a function of strain, so while the dimensions don't match, moment and strain are related to each other in a linear fashion. Similarly for the x-axis, since the trucks maintained a constant speed while driving across the bridge, the values of time were used to determine the load position with the simple velocity equation with no acceleration. Therefore, with those two ideas in mind, simply comparing the shape of the influence lines was sufficient

for confirming the Larsa model. To further confirm the model, the locations of maximum response were compared. In the model, the maximum positive moment is predicted at a position of 1020 ft, while the maximum positive strain obtained from the load test occurred at 1005 ft. When looking at the entire mainspan of the bridge, which is 1525 ft, a difference of 15 ft was certainly within acceptable error ranges.

Symmetry of the VGCS was checked with the results of the Truck Test, which was important because knowing that the bridge behaves symmetrically confirms that the bridge was built as according to the plans and that the bridge was in fact designed with the Northbound side of the bridge the same as the Southbound side of the bridge. In order to check symmetry, three dynamic load cases were analyzed: Load Cases 6.2, 7.2 and 9.2. Plots of Microstrain vs. Time was generated and showed, as expected, that the results for Northbound gages when the trucks were on the Northbound side of the bridge matched quite well with the results for Southbound gages when the trucks were on the Southbound side of the bridge.

The principle of superposition was also checked with the results of the Truck Test. In order to check superposition, the same load cases as used for checking symmetry were used. Based on the principle of superposition, adding the strain response for gage SBFL when the Southbound side of the bridge was loaded ($SBFL_{SB}$) to the strain readings for gage SBFL when the Northbound side of the bridge was loaded ($SBFL_{NB}$) was equal to the strain for gage SBFL when both sides of the bridge were loaded (SBFLBB). Similarly, gages STFL, NBFL and NTFL were analyzed, adding the maximum positive strain response for BFL gages and the maximum negative strain response for TFL gages: the difference between the sum of the individual responses and the response from both sides being loaded was 3με for NBFL. This error is small and confirms that the principle of superposition holds for the bridge under the loads during the truck test.

8.5 Model Calibration

The objective was to utilize a sparse, relatively inexpensive instrumentation array to measure response for plan truck load test, and use this measured response to verify design assumptions and to complete the baseline progressive calibration of the finite element model.

From the available pseudo static tests, Nimse used the bridge measured response for model calibration (Nimse, 2007). All the gage responses were studied and compared with the strains calculated from the model (model output).

The design model, as well as, the model that was proposed by Nimse (Nimse, 2007), were based on the assumption of linear behavior. The measured response returned back to zero once the load has passed off the bridge. the response was continuous and without any discontinuity. Hence, this confirms that the proposed model (Nimse, 2007) was a linear model and the model analysis was linear analysis which confirms that the bridge behaves linearly in the load range it was exposed. In addition the Design assumption of symmetrical response was also confirmed.

It was also concluded that the non-structural component such as the ODOT traffic barrier do not contribute to the cross-sectional stiffness as assumed.

Another feature of the VGCS bridge design is that it has redundancy built into it. It was confirmed in both the measured response and model results that the bridge can operate with a missing stay.

With close correlation between the model output and the measured response it can be concluded that the VGCS finite element model has been progressively calibrated and the load ratings generated using this model are baseline ratings. The model, which captured baseline information and was progressively calibrated, is very robust, can handle a variety of loading and boundary conditions and, hence, can serve as a reliable maintenance tool.

8.6 Conclusion

The Truck Test was planned and run with two main goals in mind. One goal was to obtain baseline readings of the bridge so that future load tests could be run and the two sets of data could be compared. Comparing the data sets will be useful when assessing the health of the bridge, as increased levels of strain could indicate a loss of structural integrity such as excessive concrete cracking, or post-tensioning strand deterioration. The other main goal of the Truck Test was to confirm the Larsa model. By comparing the influence lines with the dynamic loading data, the model was confirmed. This confirmed model can be used in the future to predict stresses, strains or moments for any load configurations for future truck tests. The model could also be calibrated in the future to account for structural deficiencies found during future truck

tests. With a model calibrated for structural deficiencies, it would be possible to look at any point in the bridge and determine if there were any sections which were overstressed, or could potentially become overstressed if further deterioration occurred. Thus, the health of the bridge could be monitored over time and structural repairs could be suggested based on any deterioration found either through visual inspection or by increases in strains from a truck load test (Nimse, 2007).

References

1. Bosworth, K. J. 2007. "Health monitoring of the veterans' glass city skyway: vibrating wire strain gage testing, study of temperature gradients and a baseline truck test." Master's thesis, The University of Toledo.
2. Nimse, P.S., 2007, "Calibrated Baseline Model of a Large Cable-Stayed Bridge." Ph. D. Dissertation, The University of Toledo.

Chapter 9 Delta Frame Monitoring and Calibration

9.1 Introduction

Delta frames are critical elements in the structure of the VGCS cable stayed bridge. They are triangular elements which carry live and dead loads from the twin box segments (Fig. 9.2) to the stay cables. The VGCS delta frames were difficult to model because of their geometry, changing boundary conditions associated with various construction stages and also since they were subjected to heavy post tensioning. This led to two basic problems: development of an accurate finite element model and potential cracking during post-tensioning, handling and erection. Also, because the delta frame model was to be used in a larger model of the entire bridge, an accurate model was essential. On the other hand, development of cracks may have resulted in maintenance problems and would have shortened the service life of the delta frames. These problems were resolved using a sparse instrument array.

This chapter will address four important sections associated with the delta frame: 1) basic delta frame instrumentation and data collection, 2) comparative analysis of measured data against design calculations, 3) monitoring of the delta frame and develop a calibrated finite element model of the delta frame, and 4) measuring the changes in strain in the delta frame lower chord due to two events: the tensioning of the DF-4 tendon and the stressing of the stay.

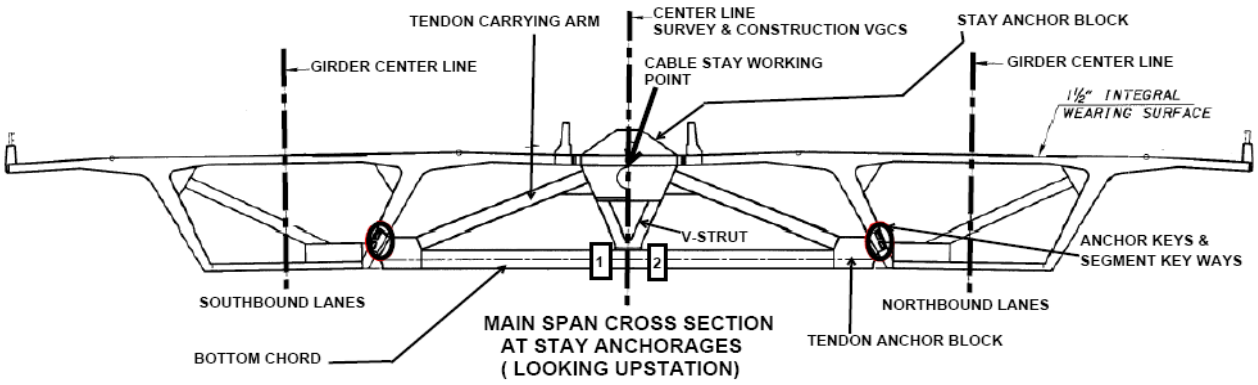

Figure 9.1 Bridge cross-section at stay anchorage point. Delta frame and two box segments

9.2 Basic Delta Frame Instrumentation and Data Collection

Delta frame no.18B (the eighteenth delta frame on the back span) was selected for instrumentation since it was among the first to be cast (Fig. 9.2). The gages used were vibrating wire gages model 4200 (embedment) and 4911 (sister bar) manufactured by Geokon (Geokon, 1997). Both the models came equipped with built-in thermistors for temperature monitoring and thermal correction. The gages were located in regions of expected high tensile strains in the bottom chord based on a centroidal deflected shape generated by a two dimensional model simulating tendons DF1 through DF3 post-tensioning effects.

The gage output includes the effects of axial and bending forces. Because the crucial piece of information to be acquired was the tensile strain and cracking was a possibility, one gage of each type was put at the same vertical elevation at each section.

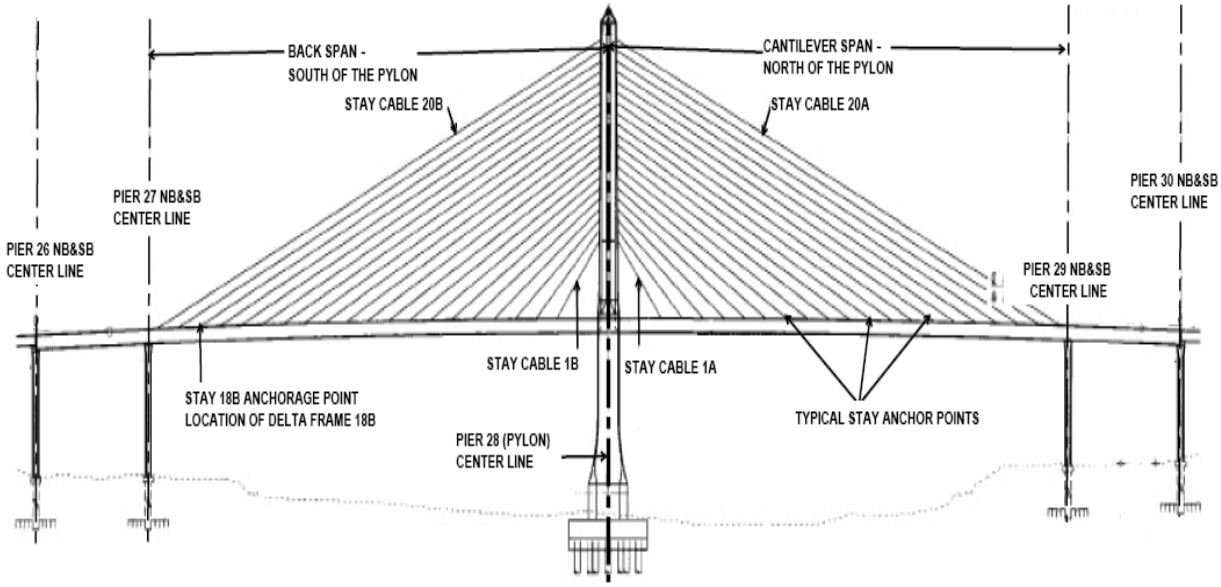

Figure 9.2 Main span of VGCS with location of delta frame 18B (looking west)

To minimize cost, only two gages were placed at each instrumented section. Since both gages were at the same elevation, their readings were not independent. This meant the gages can not independently capture the axial and bending force at a section. Therefore, the finite element model must capture the internal forces and overall behavior. Thus, the gage configuration selected is a sparse economic array that captured the desired strains, had sufficient redundancy, and had the potential to be used to verify the finite element model.

Data was continuously collected beginning the day when the delta frame was cast. This data was collected at 15 minute intervals. The strain data was also collected at 15-minute intervals during the initial post-tensioning and at one-minute intervals during for the final post-tensioning. The collected data was transferred to a laptop computer which was hooked to the data logger on visits to the casting yard, mostly coinciding with battery changes.

9.3 Monitor the delta frame and develop a calibrated finite element model of the delta frame

Nimse (2007) utilized Larsa 4D [Larsa, 2007] to simulate the staged post-tensioning DF1 to DF3 and the construction sequence and subsequent final post-tensioning. Only beam elements were used to develop these models since Larsa can incorporate tendons only with beam elements. The structural information, including geometry, section properties, material properties for both concrete, non-prestressed and post-tensioning steel, and tendon geometry was derived from the as-built construction drawings. The construction event timings came from the post-tensioning logs and information provided by the contractor. The global torsional degree of freedom, rotation about the x axis, was released.

Since the short-term elastic strains used for calibration reflect only the change in response of the delta frame for individual post-tensioning events, only member stiffnesses were involved in the analysis. Member mass and long term effects had no influence.

Fig. 9.3 shows the model developed for the initial post-tensioning phase. The supports were provided at the three locations, two on the bottom chord beam elements (Y, Z translation constrained) and one at the top most point (x translation constrained). Each of the post-tensioning stages DF1 to DF3 was set as a construction stage and Larsa stage construction analysis was carried out.

Effects of parameters, such as the stiffness of the members, used to simulate the stay anchor block and the tendon anchor block were observed. These particular elements of the delta frame were critical to simulate observed response since the load from post tensioning goes to the bottom chord through these elements. It was found that rigid beam elements with dimensions summing up to that of the 3D block geometry, (Fig. 9.3) were able to simulate the behavior matching the measured response. A short study on how different combinations of support

constraints simulated in the model affected the comparison between the analytical data and the measured response was done before arriving at the final support conditions.

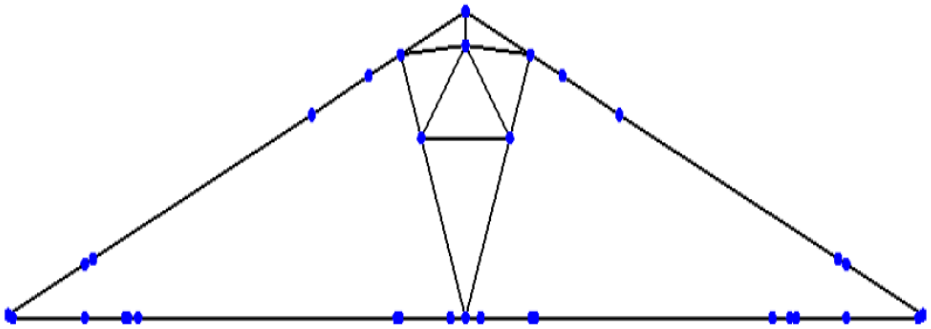

Figure 9.3 Delta frame model for initial post tensioning

9.4 Comparative Analysis of Measured Data against Design Calculations

In correlating the analytical output from the models with the recorded data, the following assumptions were made:

1) The strains were recorded at the gage location which was measured at the center of the gage. Though the sister and vibrating wire gages integrate the strain over their lengths the assumption is only strictly valid as long as the bending moment diagram is linear over the length of the gage and acceptable linearity was verified by the finite element model.
2) The contribution of time dependent effects in concrete like creep, shrinkage and relaxation are negligible over few hours duration of post-tensioning of tendons DF2-DF3-DF1and DF4.
3) Plane sections remain plane before and after post-tensioning.
4) Concrete is homogenous.

The stresses obtained from the Larsa model were converted to strains and were compared with the measured data. As explained in the data reduction section, the short term effects, the initial and final post-tensioning were considered separately. For initial post-tensioning, the datum was selected as a strain level just before the DF2 post-tensioning was started and the final reading corresponded to a strain level when DF1 stressing was completed. Therefore, the isolated strain values have the cumulative effect of DF2 to DF1 stressing. Then changes (parametric changes such as member stiffness and support conditions) were made in the model so as to get a better fit between the actual and analytical strains. Once an acceptable match was obtained this

model was made a part of the second phase model with other bridge elements and a similar procedure was followed.

The comparison between measured strains and model output (analytical strains) showed a good correlation. Once the model was calibrated, the centroidal forces were used to calculate the surface strains for both stages of post tensioning.

Since total strain levels were required to be checked against cracking, corresponding dead load strains were added to both ends of initial post-tensioning and final post-tensioning strains. Samples of concrete were taken while the delta frame was being cast. The average compressive strength was found to be 7813 psi and modulus of rupture as 802 psi when tested at the University of Toledo. The compressive strength was used to calculate modulus of elasticity for the initial post tensioning whereas for final post tensioning the modulus was calculated based on CEB-FIP90 [Comité euro-international du béton, 1993] code equations. The results showed the strain level verification for initial and final post tensioning events. They also showed surface strains from the calibrated model for locations other than the gage location. These additional locations are shown in Fig. 9.1. The delta frame was also inspected [Nims, D.K., 2006] in the field after the initial post-tensioning and after the second post tensioning for cracks. No cracks were found.

9.5 Measuring the changes in strain in the delta frame lower chord due to two events: the tensioning of the DF-4 tendon and the stressing of the stay

Nimse (2007) studies the response of delta frame post tensioning after reducing the data to isolate response of each of the post tensioning stages. DF2, which lies in the same vertical plane as gages 18BSNTO, 18BVSTO and 18BSSBI, was tensioned; these gages went in compression due to the moment about the vertical axis (M_{yy}). Whereas, the gages on the positive z-axis were in tension due to moment M_{yy}. DF2 is in the arm on the south bound side of the delta frame, but similar effects were seen in the north bound arm. The difference was that the change in strain was smaller on the north bound side. Thus, DF2 tensioning created an asymmetric stress field. When DF3, which runs through both the north and south bound arms and lies on the positive side of the z-axis (Fig. 9.5), was tensioned it had similar effects. Even after DF3 was tensioned, the delta frame was still asymmetrically post tensioned. Since DF3 goes from one tendon anchor block to the other, it also pushed the stay anchor block (Fig. 9.4) down and the

load was transferred through the V-strut to the central part of the bottom chord bending it downwards.

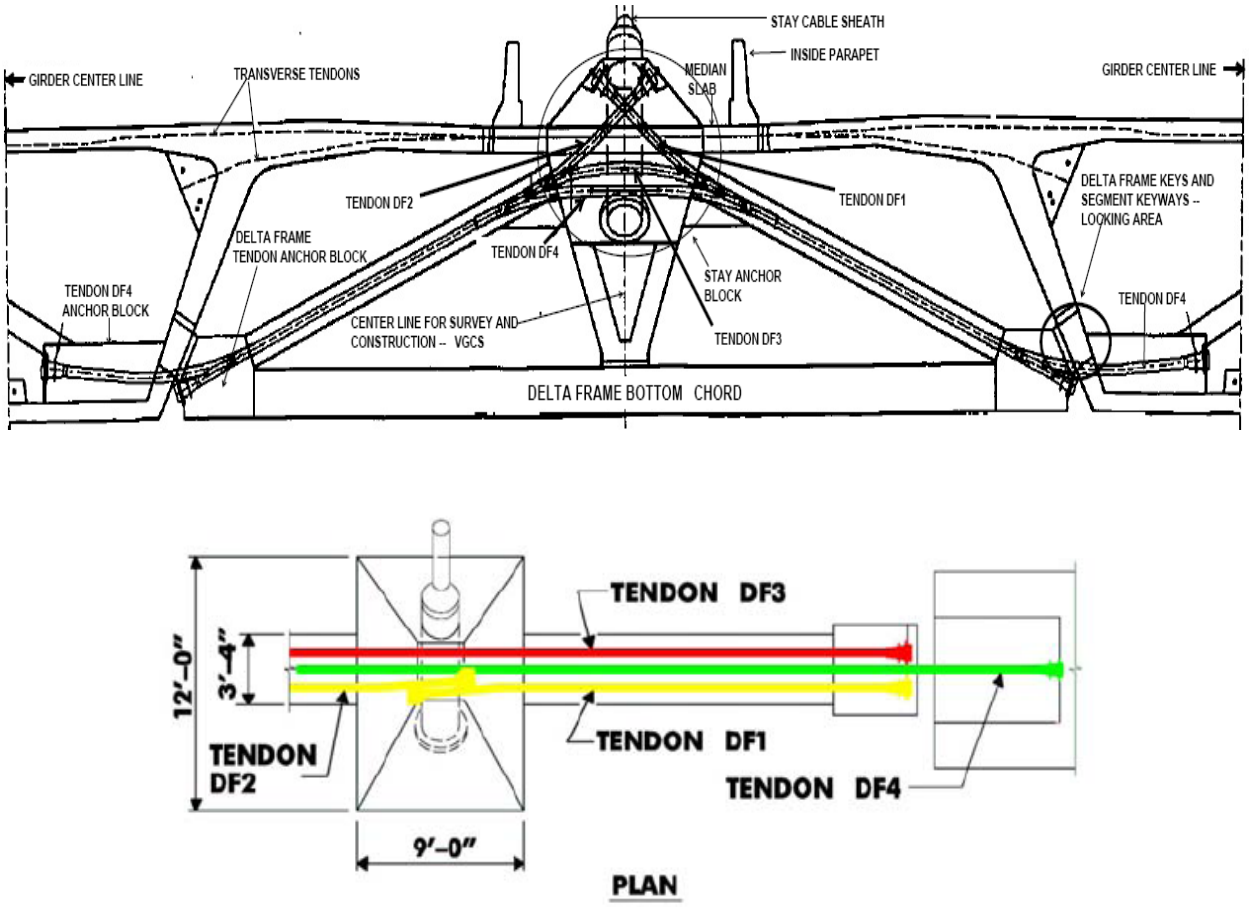

Figure 9.4 Delta frame with tendons. Plan view [Carballo et. el. 2006]

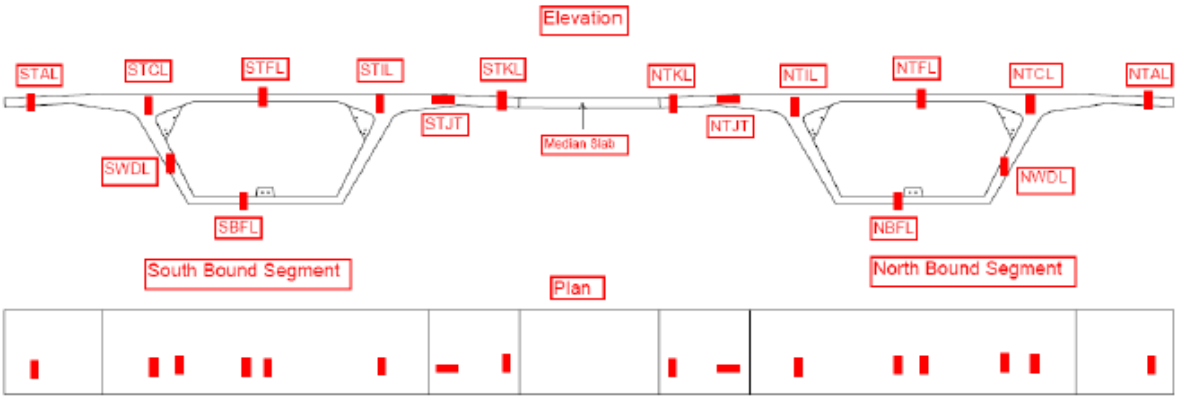

Figure 9.5 A typical pair of instrumented segments with approximate gage locations (cross-section, facing north)

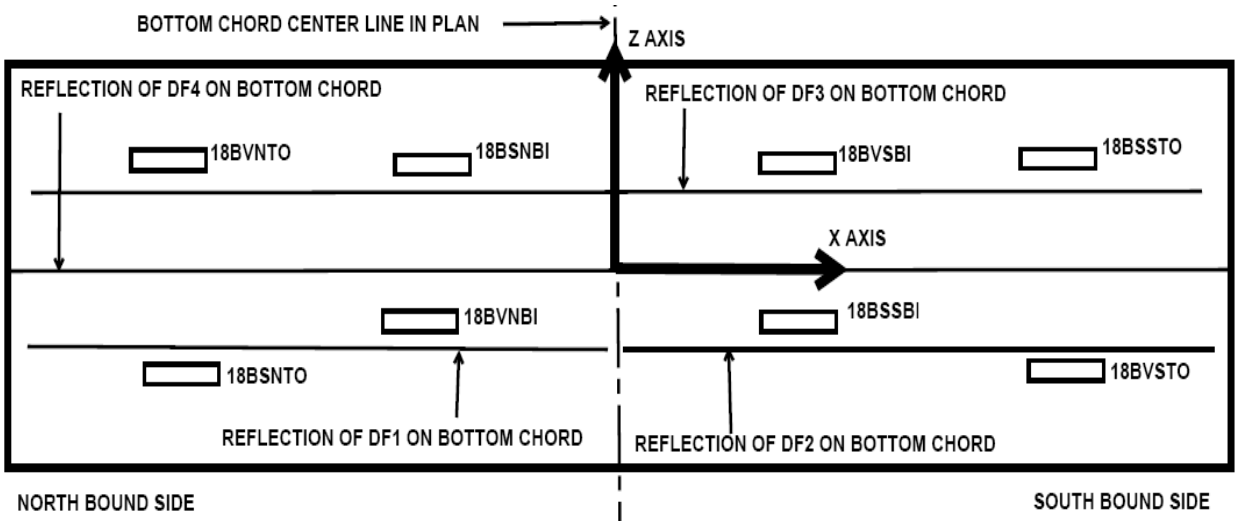

Figure 9.6 Plan view of delta frame bottom chord

As a result, the four gages near the V-strut showed tension and the gages at the tendon anchor blocks showed compression. The tensioning of DF1 led to symmetry in stress field due to post-tensioning. All four gages at the anchor blocks were in compression and all four gages in the center were in tension. This agreed with the shape predicted before tensioning. After DF-1, 2 and 3 were tensioned the delta frame was laid on its side in the casting yard for eighteen months.

At the end of the storage period, DF-18B was then shipped to the site and moved into final position where DF-4 was tightened. DF4 (Fig. 9.4) lies on the centerline in the XZ plane so tensioning of DF4 had an effect similar to tensioning DF-3. DF-4 compressed the tendon carrying arms, moving the stay anchor block down relative to the tendon anchor blocks and induced additional tension in the critical regions of the bottom chord.

The deformation of DF-18B when DF-4 was stressed was constrained because of the construction supports. At the deck level, the stay anchor block was prevented from moving freely because of the median slab in place and also since the transverse tendons were stressed (Fig. 9.4). At the bottom of the delta frame, tendon anchor blocks were locked into the segments on both sides by pouring concrete into the gaps in the keyways making them part of the segment webs on both sides. Thus, the stiffness of the entire cross-section came into play and the movement of the delta frame was restricted. Despite these constraints, as expected, the tension in all the gages increased which was incorporated in the model calibration and the strain verification process.

9.6 Delta frame – Conclusion

During Nimse (2007) work, a sparse array of instrumentation concentrated in areas of high strain was used to resolve uncertainties in modeling of a complex element of a cable stayed bridge. After calibration, the element model was used to verify that there was no cracking before service. Finally, the calibrated model of the element can be placed confidently in a model of the overall bridge. Also, the VGCS delta frames were heavily post tensioned during construction, inducing tension in the bottom chord. This could have potentially lead to development of cracks. Therefore, the bottom chord of VGCS delta frame 18B was instrumented in a few critical locations with the highest expected tensile strains to verify strain levels corresponding to critical post tensioning events. A relatively inexpensive sparse instrument array was installed and the measured response against the post tensioning events was used to develop a calibrated component model of the delta frame. First the model was calibrated against initial post tensioning and then used to generate surface strains for the initial post tensioning plus self weight. These strains were then checked against the cracking strain. Then this calibrated model was fit into a complex model of the cross section and the calibration was verified at this stage against measured response from final post tensioning. Surface strain levels at this stage were also checked against cracking. It was found that at both stages of post tensioning the surface strains were well below the cracking level. Since the final loading of the delta frame is stay stressing which induces compression in the delta frame bottom chord, it can be concluded that the bottom chord of the delta frame did not crack due to construction loads. This conclusion was also supported by the visual inspection of the delta frame done during construction.

Since the VGCS Bridge is instrumented for long term monitoring, the calibrated model of the delta frame which showed good correlation to measured response during the second post-tensioning was now ready to be used as a component of the full bridge model. Therefore, this work also contributes towards developing long term maintenance planning of VGCS. Though the efforts were directed towards expected problems at the VGCS, the verification of delta frame behavior under various construction arrangements will, provide more support for their use in this future.

References

1. Nimse, P.S., 2007, “Calibrated Baseline Model of a Large Cable-Stayed Bridge.” Ph. D. Dissertation, The University of Toledo.

Chapter 10 Use Intermediate Construction Live Loads for Progressive Calibration

10.1 Introduction

Progressive calibration is calibrating the finite element model developed for intermediate construction stages against construction loads when the structure geometry is incomplete and the boundary conditions are changing. Progressive calibration instills more confidence in the use of the model, as the model is checked for varying structural geometries and loading conditions and, therefore, is more robust. The model calibration procedure provides an opportunity to capture as-built procedures and is tuned against a variety of loading and boundary conditions**.** Generally, the model is calibrated using the measured response from truck load tests conducted just before the bridge is opened to traffic.

The process of calibrating the VGCS Bridge began with determining if the data collected was acceptable. Therefore, the first objective was to study the quality of the data collection mechanism used for live load tests; and to check the performance of the instrument suite. After the data quality was confirmed, the test data was used to calibrate the model for construction live loads. This objective is very important in the context of the ultimate goal of developing a calibrated finite element model, which is also calibrated "progressively" through construction. The second sub-objective was to use data collected during these tests to plan the final truck load tests.

VGCS bridge segments were instrumented during casting and data was acquired continuously since casting. Therefore, it was a unique opportunity to monitor the measured response from casting, through storage, then erection and on into service. It was decided to calibrate the model progressively through construction since the VGCS had a sparse instrumentation array and only four sections in the bridge are instrumented. There are advantages to developing a calibrated model progressively. First, calibration during construction provides useful measurements and analytical results that assist in generating plans for the final truck load test. It provides a better understanding of quality of the measured response, the effectiveness of the instrumentation suite, the bridge behavior and it confirms the design assumptions for the construction loads. This is especially important because the bridge is subjected to some of the heaviest loads and largest deformations in its life during construction while the bridge stiffness is reduced and geometry is changing. Finally, the range and variety of construction loads enhance

the calibration of the model by making it more robust. This increases the confidence that the model can sensitively and accurately reflect future changes. This is very significant since the final baseline model developed as part of the VGCS monitoring program will be used to monitor long term changes.

For the VGCS, the first opportunity to progressively calibrate the model against construction live loads was presented when the segment hauler transported the segments across the bridge to the tip of the cantilever span as the cantilever advanced. A second opportunity was available when the Demag AC400 cranes used to hoist and install the segments and the delta frames onto the cantilever span, were driven off the bridge. This crane withdrawal occurred close to end of construction, but before closure. This chapter describes these construction live load tests, the instrumentation response study and development of a calibrated model using these construction live loads. In the coming sections a study of the response to understand the quality of measured data and bridge behavior is presented. This is followed by a description of finite element model calibration.

10.2 Construction Live Load Bridge Model

Fig. 10.1 is a typical isometric elevation of the bridge model developed to simulate the crane roll-off and segment hauler movement events.

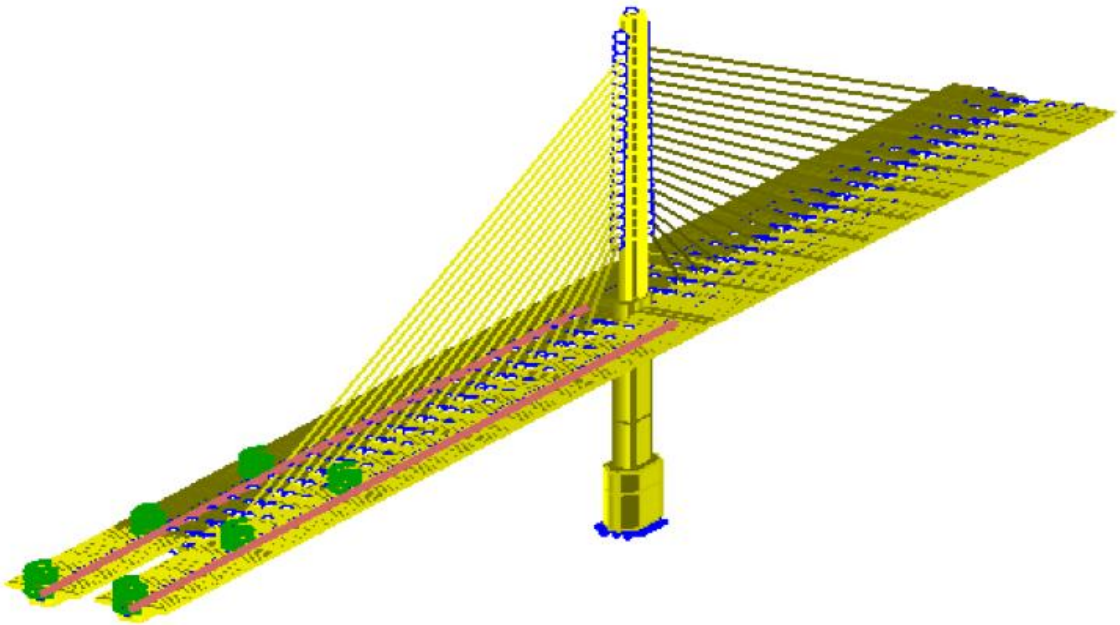

Figure 10.1 Isometric view of the model for segment hauler tests. For crane roll off one stay and four segments are added and the rest remain the same.

The segment hauler model has 3486 beam elements and 36 cable elements. There were six spring elements used, two for pier 26 (North Bound (NB) and South Bound (SB)), two for pier 27 (NB&SB) and two for pier 27A (NB&SB). The stiffnesses assigned were combined effects of the supporting piers and bearings [IBT, 2005]. In the case of pier 26 and 27, it was a combination of the concrete permanent pier and the bearing placed on top of it. For pier 27A, it was a combination of the temporary steel pier and the bearing placed on top of it. For progressive calibration, it served as an excellent check to insure the structural framework developed to simulate the stiffness of the bridge and flow of forces matches the actual bridge response to the construction live loads.

The dynamic load (segment hauler) path was determined by construction arrangements. Per the construction specification, as far as possible, the loaded segment haulers were supposed to move along the center of each of the twin box girders. The bridge lane which carries the dynamic loads was assumed as the width along the center line of the segments.

The static load positions were governed by the location of the instrumented segments. The only construction live load used for static loads is that of the Demag crane. When the crane rolled-off the bridge these static tests were conducted. The crane was stopped at instrumented segments for three to four minutes and data was collected by the vibrating wire gages.

10.3 Test Description

The process of calibration began with determining if the data collected was acceptable. Therefore, the first objective was to study the quality of the data collected and to check the performance of the instrument suite. The criteria for data quality checking were 1) the reproducibility under repeated loadings and 2) any drift during individual tests. The second objective was to gain some insight into the basic bridge behavior during construction based on the design assumptions. The assumptions verified were symmetric response and elastic behavior, which allowed linear superposition. The final objective was that of progressive model calibration done against test records corresponding to the construction stages.

There were twenty-two test records [Ward, 2007] available related to segment hauler movement. These corresponded to loaded segment hauler movement from pier 26 to the tip of the cantilever, as well as for the return trip of the empty segment hauler as the construction progressed. The test record for the crane roll off was broken down into eight subsets. All of these

tests were studied and it was found that the response was consistent and as expected. Pairs of tests were selected for reproducibility and symmetry.

To perform the reproducibility check on the data quality, a pair of tests was selected in which the data was collected when the segment hauler was on the return path after delivering the segment to the tip of the cantilever span. Data collection started in both the cases when the segment hauler left the pylon and stopped when the segment hauler drove off the bridge on the back-span side (north bound or south bound back-span side). It was found that the measured response of two representative gages, a top flange gage and bottom flange gage, was repeatable.
To verify the symmetric response of the bridge, two tests were performed to confirm that gages located at comparable locations respond and behave similarly. In the first test, date was collected when the empty segment hauler moved southward over the southbound back-span from pylon to the south end. Similarly, the second test monitored the movement of the empty segment hauler on the northbound span as it moved southward over the back-span. After comparison, it was concluded that the gage response at comparable locations compared well.

In order to confirm the elastic response of the bridge, as well as check drift of the embedment electrical resistance strain gages (foil gages), a third test was selected. This test was performed using the dynamic DAS connected to segment 27NB41. The beginning and ending values of strain were equal to the noise level as the segment hauler passed from the south end of the main span to the pylon carrying segment 28NB61. It was concluded that the bridge response is elastic and there is no drift in the strain gages. Similar tests for drift were done throughout the testing before and after closure.

Once it was established with reproducibility, symmetry and drift testing that the gage response was reliable and that the bridge response to these loads is linear, the measured values were used to fine tune the finite element model.

10.4 Model Calibration

The crane roll-off static and crawl speed loadings are especially important for calibration since it was possible to script the Terex-Demag AC400 crane roll-off movements and because the roll-off happened at night when the least amount of construction equipment movement occurred on the bridge. At predetermined locations, these cranes (one each on NB & SB lanes) were made to pause for three to five minutes to simulate static loading conditions. On the other

hand, the segment hauler tests were used to obtain continuous measured response to compare with model output. Segment hauler and crane axle loadings were simulated in the bridge model. First, crane static positions at 28NB28 & 28SB28 and 27NB41 & 27SB41 were used for comparing measured and analytical results. It was found that the suggested arrangement of beam elements and rigid elements (Fig. 10.2) works well to simulate the bridge stiffness. Effect of support conditions was also studied. Since the approach spans to the south of pier 26 were already constructed, translational restraint in the longitudinal direction (along the X-axis in the

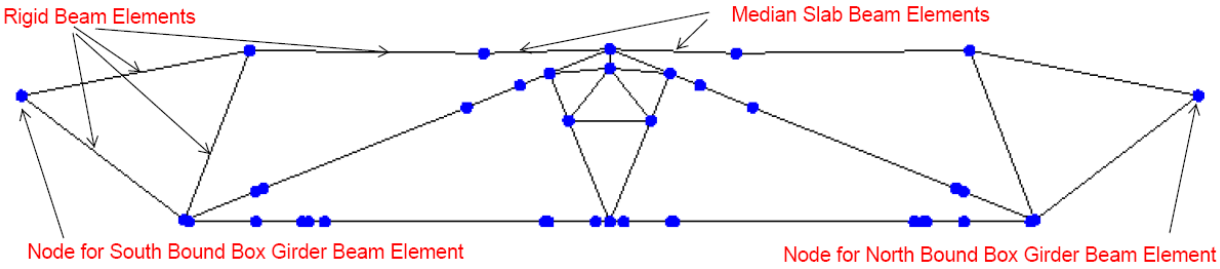

Figure 10.2 Arrangement of beam elements at stay anchor cross-section (Nimse, 2007)

model) gave good results. To begin with, the restrained conditions used to simulate supports, temporary pier 27A and permanent pier 26 and 27, were such that they had only compressive stiffnesses and their magnitudes were as suggested in the reports submitted by IBT (IBT, 2005). But results obtained using these restrains did not compare well with the measured values. After a few iterative studies and updating the in-situ support condition details, changes were made to the model. The spring supports at pier 27A (SB & NB) were provided with constraint in vertical direction (Z axis), since in-situ, these pier segments were connected to the temporary steel pier using four PT bars to prevent uplift. Since the permanent piers 26 and 27 had elastomeric bearings with no provision for uplift, only compressive stiffnesses were used. For the temporary piers, as well as the permanent piers, the stiffnessess provided by IBT, (IBT, 2005) were found to give comparable results.

Ward compared the measured data to the analytical data and the model output (Ward 2007). The foil gage response of the instrumented segments for cranes for cranes positioned at the pylon was used as the datum to calculate the response for cranes at segments 28NB28 & 28SB28. For the cranes positioned at 28NB28 & 28SB28, it can be seen that analytical strains compared well with measured strain for all the instrumented segments. At 27NB04, the

measured response is well within the range of noise and because of that these readings were not taken into account while making changes to the model. Similarly, for cranes positioned at 27NB41 & 27SB41 only the response at 27NB41 was used for calibration as the rest of the gage response was in the noise range. Once again the analytical strains compared well with the measured response for static load crane load positions, the model output was also verified against segment hauler moving loads.

10.5 Conclusion

In the initial phase of this work, the foundation for performing progressive calibration was laid. It assured the quality of the data collected. It verified the design assumptions of linearity and symmetry. Since the project employed a sparse array of instrumentation, achieving these objectives was important to prove that the instrumentation array was sufficient for carrying out model calibration.

The uniqueness was in the progressively calibrated model of the bridge. The design models available for bridges were underlain by design assumptions, predicted responses to construction procedures and loads. Such design efforts satisfied the code requirements and had been found to be sufficient enough to ensure the service life and safety of the structure. But they lack the sophistication and accuracy required to be useful for maintenance purposes. Whereas a model developed and calibrated progressively is more responsive to changes since it is fine tuned with changing geometry, stiffness and against a variety of loading conditions. Satisfactory verification against all monitored construction stages instills confidence in its future use for inspection and maintenance purposes.

References

1. Ward R. J., 2007, “Short-term Construction Load Monitoring & Transverse Bending of the Bottom Slab on the I-280 Veteran’s Glass City Skyway” Master Thesis, The University of Toledo.
2. Nimse, P.S., 2007, “Calibrated Baseline Model of a Large Cable-Stayed Bridge.” Ph. D. Dissertation, The University of Toledo.

Chapter 11 Strains in the Bottom Slab

11.1 Introduction

This chapter focuses on the investigation of the strain concentration in the floor slab behind delta frame anchor block (Wright, 2007); and on the additional strain measurements that were required in the cantilever span in the bottom slab at the strain concentration regions between the bottom slab and the walls at two locations in span 28 (Ward, 2007). Prior to the construction of the VGCS, no research had been done investigating the bottom slab bending behavior of concrete box girders.

The finite element model created by the construction engineer to analyze the transverse bending of the main span, showed that there was potential for the bending moments due to the self-weight of the structure to locally exceed the available strength (see Figure 11.1) before the application of live load. This could lead to future maintenance issues such as cracking. A separate analysis performed by the design engineer did not show a potential of exceeding the available strength.

Testing was elected as a method to resolve the difference in the potential high stress disagreement and reconcile discrepancies between the construction and design engineer as described in the remainder of this chapter. It was found through testing that the measured strain levels were significantly less than yield and no cracking at the bottom of the concrete slab was observed.

A consultant's finite element model (IBT 2006) showed a stress concentration behind the delta frame anchor block occurring in the bottom slab of the delta frame segments. Outputs from the models indicated that the segment weight and the tensioning force of the DF-4 tendon were creating a high tensile stresses in the bottom slab behind the anchor block. The area was instrumented using external vibrating wire strain gages. The strains in the floor slab behind the anchor block were investigated to compare results with the FEM in question. A key element to study this behavior was determining the actual strains through experimental testing to validate an FEM model for the bottom slab and show that the stress pattern behind the delta anchor block from our FEM makes sense.

Additionally, while performing a check of the proposed construction erection sequence, concerns arose from finite element modeling that there was a potential for the capacity of the bottom slab to be exceeded in transverse bending (see Figs 11.2 & 11.3 below). For the transverse bending of the bottom slab, results of the finite element analyses generated by the construction engineer and the designer were compared with data collected at various construction stages to determine whether the predicted levels of stress occurred.

11.2 Strain in Bottom Slab Adjacent to Delta Frame Anchor Block Due to DF-4 Tensioning

Early in 2006, finite element models developed by the consultant retained by the contractor showed areas of high tensile stress in the bottom slabs of delta frame segments behind the DF-4 anchor block. These high tensile stresses were from the tensioning of the DF-4 tendon in combination with the segments self-weight.

Three models of the bridge were developed whose analysis results presented potentially high stress areas. An outside consultant developed the finite element model of the bridge and presented its analysis to ODOT which was the first to indicate that the delta frame anchor block areas are under potential high stress, using the segment dead weight and load from the DF-4 tendon. After receiving the consultant's analysis, FIGG developed their own finite element model of the design to confirm the consultant's model. To better understand the stress path from the tensioning of the DF-4, a simple model was also developed using the program SAP. It was not a full-scale bridge model, but rather a system consisting of the bottom slabs of 3 segments, one being the slab containing the DF-4 anchor block. The boundary conditions placed on the system were made to simulate the actual restraint of the slab. The segment weight was not used in the analysis; only the DF-4 effect was placed on the system. This model was developed to see the stress pattern generated from the tensioning behind the DF-4 anchor block, not to produce a set of comparable analysis results.

The generated model was used to locate the testing instrumentations using external vibrating wire strain gages to monitor the strain concentration behind the delta frame anchor block under the segment weight and the tensioning force of the DF-4 tendon; hence, the area was instrumented. The three gages were installed in a straight line at varying distances behind the DF-4 block, slightly offset from the center of the tendon so as to not interfere with the tensioning

procedure. The crack meter was installed next to the strain gage nearest the delta block. The URT stayed on site monitoring the construction progress while frequently downloading and monitoring readings to ensure the data collector was ready when the tendon was tightened.

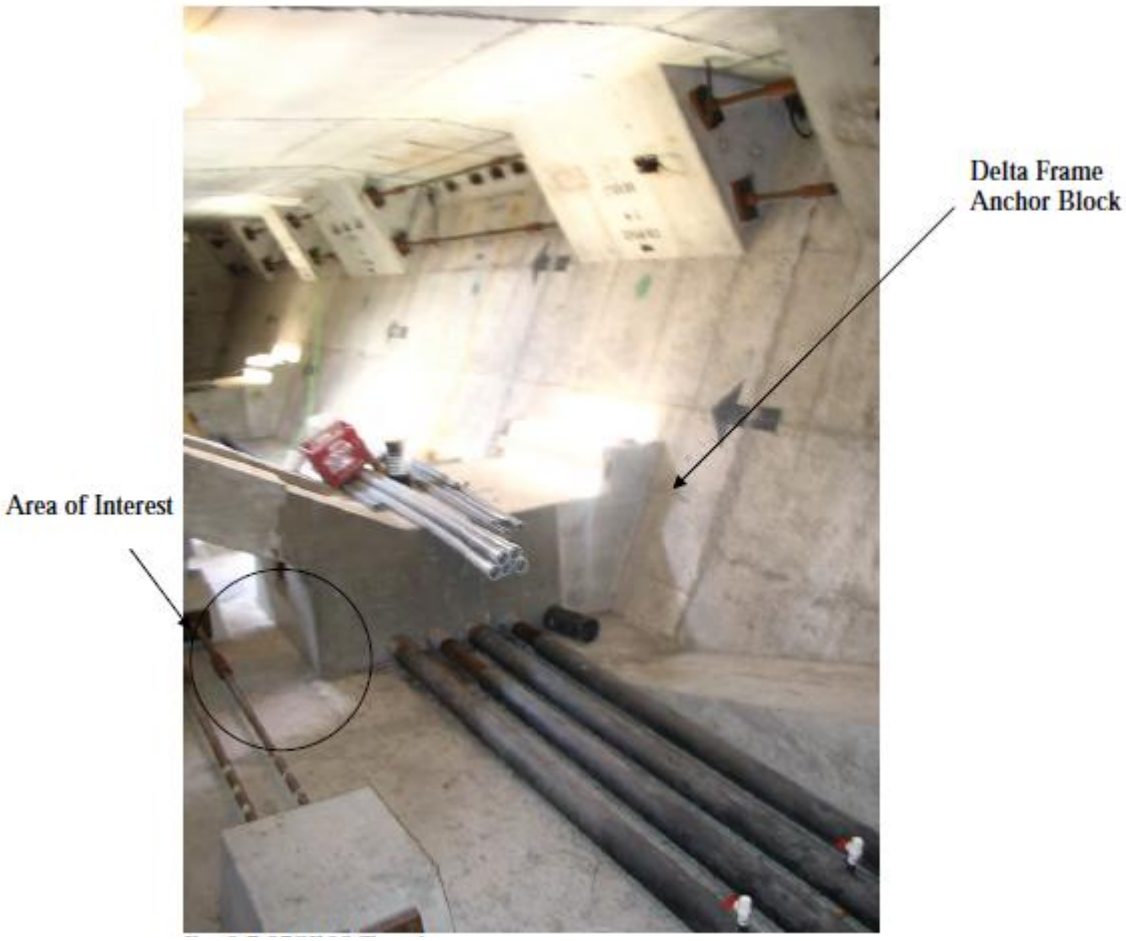

Fig. 11.1 Test Setup (Wright, 2007, Fig. 3.7)

11.3 Strain Due to Transverse Bending

The construction engineer created short, medium, and long span models to check various loading conditions. Short-span model behavior was governed primarily by longitudinal effects such as primary bending; however, in the medium to long span models, the transverse bending behavior of the segments began to surpass the longitudinal effects in some regions. Due to the support conditions of the segment, it was anticipated that the bottom slab could be forced into an "S" bend (see Figure 11.3), which would cause high stresses on the top of the bottom slab near the inside web, and also at the bottom of the bottom slab near the outside web. The transverse bending behavior was caused by the deflection of the outside wall exceeding the deflection of the

inside wall. Since the segments are supported at the delta frame there is a tendency for sag to develop between the supports as shown in Figure 11.3.

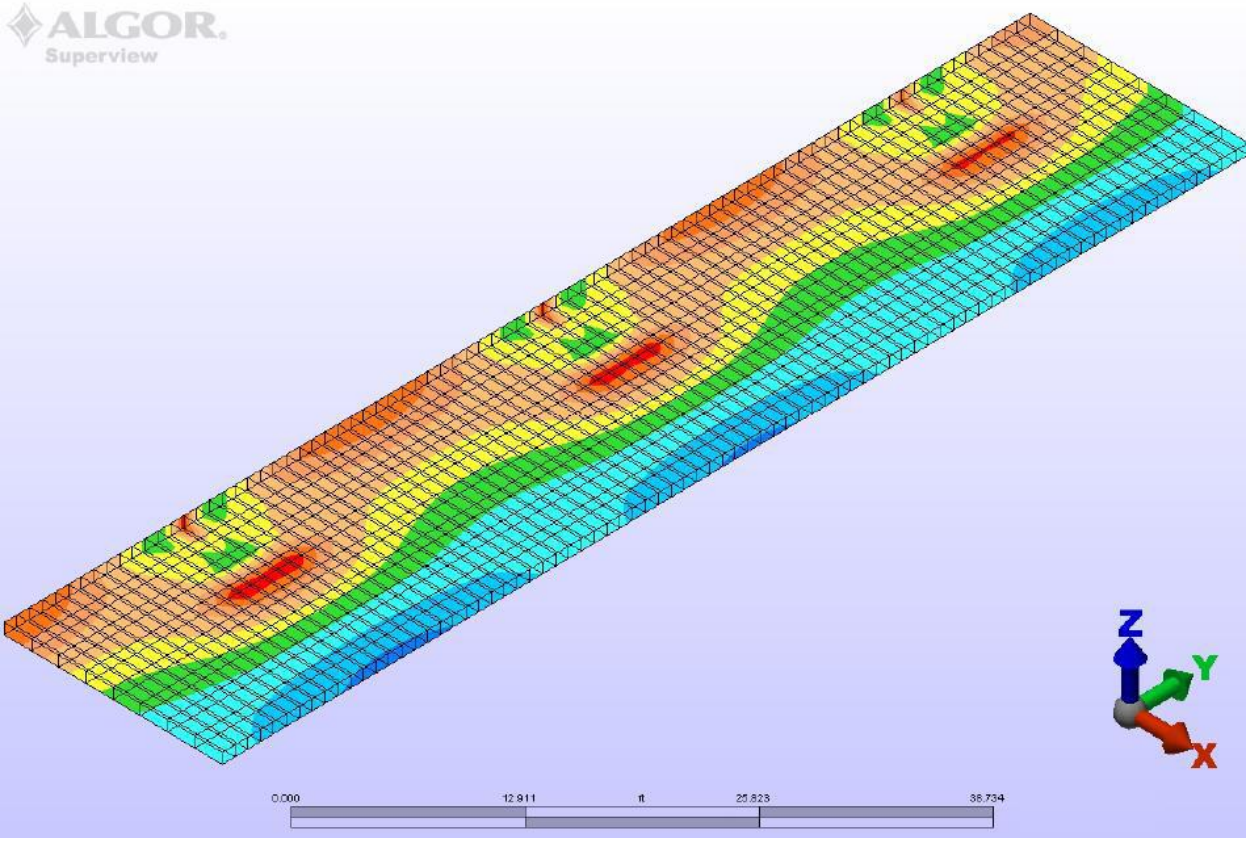

Figure 11.2 Bottom Slab Transverse Bending Moment caused by Unfactored Dead Load (Ward 2007, Fig. 4.1)

Global models were generated for the entire bridge using plate elements and rigid beam elements to model the increased stiffness of corner joints. The global models used by both the construction engineer and the designer were in agreement, but the local models were not. Local models were composed of three dimensional volume elements to locally focus on typical sections of differing lengths ranging from 28-feet to 56-feet long.

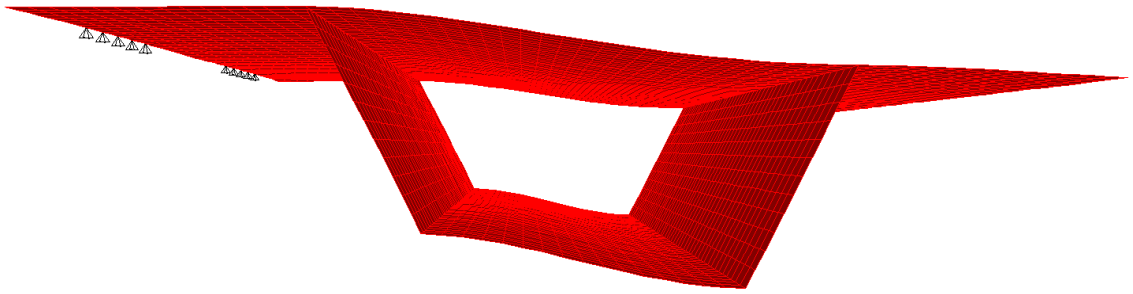

Figure 11.3 Self-weight deflection (Ward 2007, Fig. 4.2)

Boundary conditions for local models were established using the global models. After analyzing the structure as a whole, section cuts could be taken at each end of the local models to be created. From these results, the axial forces, shears, and moments could be applied to the local model to provide accurate representation as well as maintain global equilibrium. The refined local models prepared by the construction engineer did not significantly reduce the local effects of the transverse bending, but did provide for more precise locations where high stress would occur. With these locations, the URT was able to install gages to monitor the transverse bending behavior.

Table 11.1 Algor FEA Legend

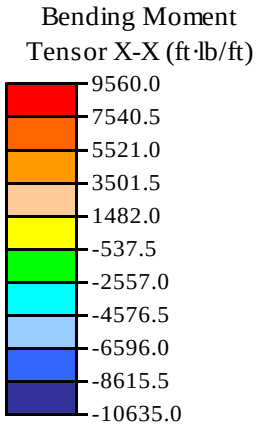

Figure 11.4 Enlarged Transverse Bending Moment

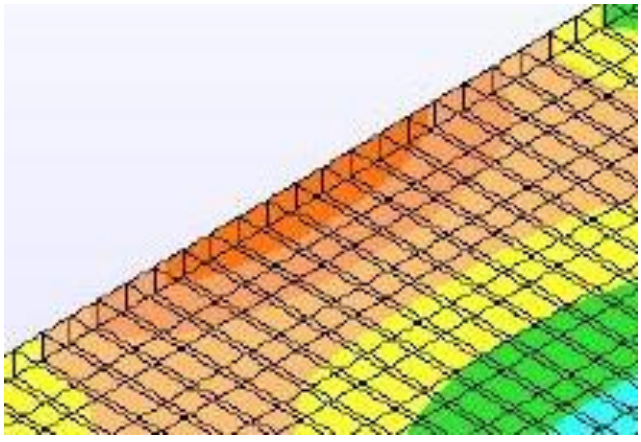

Figure 11.4 shows an enlargement of the region where maximum bending moments where predicted to occur. Although higher values of moment occurred directly behind the delta frame block, the phenomenon has been investigated during prior research by the URT (Wright, 2007) when the effect caused by post-tensioning the segments together was studied.

Table 11.1 is the legend that corresponds to the transverse bending moment contours from the finite element analysis performed by the construction engineer.

The connection between the slab and wall was simulated using approximately very stiff elements. However, the designer noted that the effects of different values for the stiffness of these elements had a significant effect in the local analyses. By using rigid elements that are stiffer, the joints experienced little shear strain and will transmit the entire moment to the bottom slab. Also, the length of the rigid elements in the corner dramatically affected the results of the stresses near the wall. Rigid elements that are short tend to approximate a reentrant corner with theoretically infinite stress. By similar logic, if the corner elements are longer, the stresses near the corner are trend towards a stress with no stress concentration factor. Results from a preliminary investigation of the overall self-weight deflection confirmed the general shape of deflection and moment behavior predicted by the construction engineer.

Analysis results from both the construction and design engineer indicated that the highest transverse bending strains were predicted midway between the delta frame supports where the differential sag of the inner and outer wall was the largest. This location actually occurred at the joint between segments 28SB24 and 28SB25.

Based on the results of the FEA performed by the construction engineer, vibrating wire strain gages were installed on the bottom slab near the intersection of the inside web and bottom slab in segments fifteen and twenty five of span twenty eight on the southbound side (28SB15 and 28SB25). The gages were concentrated in the portion of the slab nearest the predicted strain concentrations. Furthermore, since the largest predicted strains could have exceeded the working range of the normal vibrating wire strain gages (3000με) a vibrating wire crack meter was installed near the junction of the wing and bottom slab. The crack meter had a working range of approximately 3mm. To account for this strain at bottom slab due to self-weight deflection, two simple models were developed. One model consisted of a simply supported slab subject to its own dead weight, while the other had fixed boundary condition. In this manner, the worst case possible between the results was used and the estimation was conservative. Combining the effect of the self weight deflection with the measured results caused by transverse bending behavior of the segment can be summed and compared with the overall model results.

In order to investigate what effect live load contributed to the overall stresses in the bottom slab, the gages installed in segment 28SB25 were set to record data during both the crane withdrawal test and the full scale truck load tests.

11.4 Research Results and Conclusions

Transverse bending of the bottom slab was monitored in order to reconcile discrepancies in finite element analyses performed by the construction and design engineers. Vibrating wire strain gages were installed in the bottom slab of segments to monitor transverse bending. Data was collected during construction, as well as during the truck load test prior to opening the VGCS to traffic.

Two research studies focused on investigating the concentration of strain in the bottom slab of the delta frame by comparing the results of the experimental data to the analysis results provided by the design engineer.

Wright (2007) investigated strain concentrations in the bottom slab of the VGCS caused by the post-tensioning tendons used to hold the delta frames in place. Results of the research monitoring strain levels immediately behind the delta frame tension block following the tensioning of the DF4 tendon indicated that the strain magnitudes attenuated quickly when moving away from the zone of predicted response (Wright, 2007).

Ward (2007) studied the transverse bending behavior of the bottom slab by monitoring the slab prior to installation and after the bridge was completed and opened to traffic. Experimental results at a construction stage prior to stressing stay 8 were compared with analysis provided by the designer. Experimental results were higher than predicted by the design engineer, but less than those predicted by the construction engineer. Strains approaching the yield for reinforcement (approximately 2000με) were not observed at any point during construction. Strain magnitudes did not exceed 300με for any of the gages installed on the bottom slab.

Visual inspection following installation of the instrumented segments, as well as subsequent segments did not reveal any cracking in the bottom slab in the regions where large strains were predicted. Strain magnitudes from the gages installed on the bottom slab of

segments 28SB15 and 28SB25 have been independently verified to be accurate by performing lab calibration of the actual gages used in the field (Bosworth 2007).

In addition, data recorded during live load tests including the crane withdrawal and full scale truckload tests confirms the assertion that dead load bending behavior dominates the transverse bending capacity of the bottom slab.

Dead load effects caused by the self-weight of the segments and delta frames are the predominant factor in determining the capacity of the bottom slab in transverse bending of the bottom slab.

References

1. Ward R. J., 2007, "Short-term Construction Load Monitoring & Transverse Bending of the Bottom Slab on the I-280 Veteran's Glass City Skyway" Master Thesis, The University of Toledo.
2. Wright, B.W., 2007, "Experimental and Analytical Analysis of Concrete Strain Concentrations on the I-280 Veterans Glass City Skyway Cable Stayed Bridge." Master's Thesis, The University of Toledo.
3. Bosworth, K.J., 2007, "Health Monitoring of the Veterans' Glass City Skyway: Vibrating Wire Strain Gage Testing, Study of Temperature Gradients and a Baseline Truck Test." Master's Thesis, The University of Toledo
4. Nimse, P.S., 2007, "Calibrated Baseline Model of a Large Cable-Stayed Bridge." Ph. D. Dissertation, The University of Toledo.

Chapter 12: Bridge Long Term Analytical and Experimental Responses

12.1 Introduction

In this chapter, the analytical and experimental stresses from the time of stay stressing through service life up to the present time are compared. Time history of the analytical stresses in the contractor's as-built finite element model for staged construction (BD2) is compared to the time history of the stresses based on the strain data collected. Representative plots for the comparison are presented.

Stay cable stressing events have a clear signature in the time history line and the exact time of each event is recorded in the stay cable stressing log. Table 12.1 shows a portion of the stay cable stressing log for stay 1.

Table 12.1 Stay 1 Stage 1 Cantilever Stressing Log

Stay 1 Stage 1 Cantilever Stressing Log				
Strand No.	Master Load Cell (kips)	Date	Time	Comments
1	36.5	2006-7-15	9:55 AM	Master Strand
2	35	2006-7-15	10:22 AM	
3	34.3	2006-7-15	10:32 AM	Check teeth pattern at stage 2. Check for full overbite of wedge.
4	34	2006-7-15	11:12 AM	
5	33.9	2006-7-15	11:21 AM	
6	33.6	2006-7-16	11:31 AM	Released sheathing onto the strands.
7	35.4	2006-7-16	11:41 AM	
8	34.8	2006-7-16	11:50 AM	Measured liftoff.

In the log, the master cell force, the date, time and tensioning event are clearly defined. The tensioning events are also phases in the finite element model so matching the measured strains to the analytical stresses for these events is straightforward. Then the measured strains are transformed to measured stresses and the time series of experimental stresses are compared to the time series of the analytical stresses.

12.2 Analytical stresses

Bridge Design II (BD2) (Interactive Design Systems, 2011) is the finite element software used for long term modeling from casting construction through service. It is specifically designed for staged construction of pre- and post-tensioned segmental concrete and cable stayed bridges. The model used here to find the construction and long term stresses due to permanent loads is the as-built model developed by International Bridge Technologies for the VGCS contractor. It has been accepted by Figg and ODOT. During construction the model includes temporary construction loads as well as other static loads such as deadweight and stay and tendon forces. During service, all permanent gravity loads and stay and tendon forces are considered.

BD2 defines every construction stage as a corresponding BD2 Phase. Stresses for all loading conditions can be evaluated at any phase. Stressing, distressing and restressing are specifically addressed as BD2 phases.

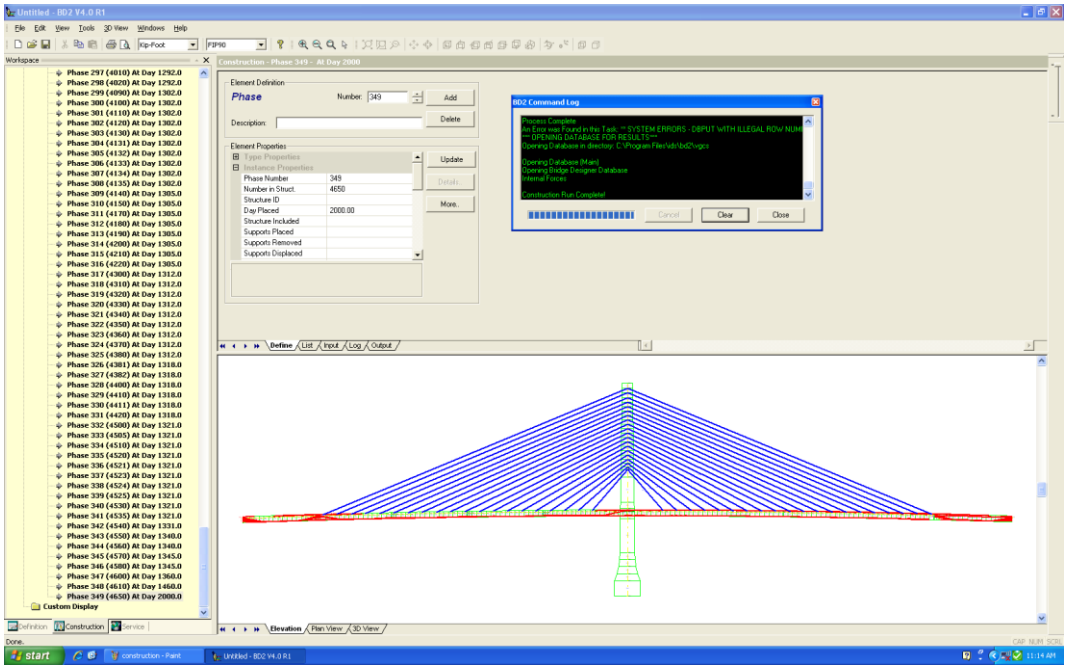

Figure 12.1 Bridge Designer II interface

Figure 12.1 shows the BD2 interface when the database of VGCS was running. The geometry of VGCS can be viewed in elevation or plan.

The principle task of this study is to understand the long-term behavior of VGCS based on the comparison of the analytical stress and experimental stress. Since the steady state condition was of interest, the analytical stress did not consider the temperature gradient. Hence, some deviation from measured can be attributed to temperature effects.

When necessary, a new construction phase corresponding to the time of data collection was defined. No changes in the model or loading were made. The new phases simply calculated the bridge data at required points in time.

Once the new phase is set up, the BD II can evaluate the results of stresses at each segment. Table 12.2 shows the stress results at bottom of Segment 2806 from day 358 to day 2861. I and J represent the south and north end of each segment. Segment 306 of the BDII model represents segments 2806NB and 2806 SB of the bridge. Because the strain gage is near the middle of the segment, the analytical stress used for comparison is the average of the stresses at the I and J ends.

Table 12.2 Analytical Stress in Segments 2806NB and 2806SB (kips/ft^2)

Date	Events	BDII Seg.	bottom		Analytical Stress at Bottom (k/ft^2)
			I	J	
2/6/2007	PHASE 4540 (CLOSE MAIN SPAN AND CAST MEDIAN IN SP29)	306	-147.3	-137.0	-142
2/11/2007	PHASE 4560 (DEACTIVATE PIER 27A)	306	-130.5	-117.6	-124
2/26/2007	PHASE 4580 (REMOVE MISCELLENEOUS LOADS AT PYLON)	306	-123.6	-110.8	-117
6/6/2007	PHASE 4600 (Day1460)	306	-146.9	-131.7	-139
*6/24/2007	PHASE 4640(Day 1478)	306	-154.4	-138.6	-146
12/1/2008	PHASE 4650(Day 2000)	306	-183.9	-165.2	-174
1/21/2010	PHASE 4680 (DAY 2415)	306	-182.3	-164.0	-173
3/20/2011	PHASE 4690 (DAY 2840)	306	-181.6	-163.0	-172

12.3 Experimental Strain to Stress Transformation

The experimental stresses are evaluated from the strain data collected during the long-term monitoring. Based on the elastic relation between stress and strain, experimental stress was calculated from:

$$\sigma_i = E_i \varepsilon_i - E_0 \varepsilon_0 \qquad (12.1)$$

where

σ_i ……Experimental stress at construction phases and today

E_i ……Modulus of elasticity at construction phases and today

ε_i ……Strain data at construction phases and today

E_0 ……Initial modulus of elasticity at an age of 28 days

ε_0 ……Initial strain data at an age of 28 days

In this equation, Young's Modulus varies with time. The values used were calculated by BD2 as shown in Figure 12.2, a model developed by Fru-Con utilizing FIP-CEB model code 1990 to simulate the time dependent behavior. This equation can be written to include many steps in the time history of the segment (Branson, 1977). However, because of the long interval between casting and erection, one step is sufficient in the present analysis. The strain data were collected at each instrumented segment. During the long-term monitoring, there are not enough available strain data at the casting yard. Thus, the initial strain data for each gage needs to be evaluated with the help of BD 2.

$$\sigma_{analytical,i} = E_i \varepsilon_i - E_0 \varepsilon_0 \qquad (12.2)$$

Using equation 12.2, the initial strain, ε_0, can be evaluated after substituting the Young's Moduli, strain ε_i and an analytical stress from BD2.

Figure 12.1 shows the variation of Young's Modulus with time. Since Young's Modulus (E) varies much more slowly after the first of 28 days. E_0 at the age of 28 days 724,000 kips/ft^2 (5,030 ksi) was defined as an initial value for the strain to stress transformation.

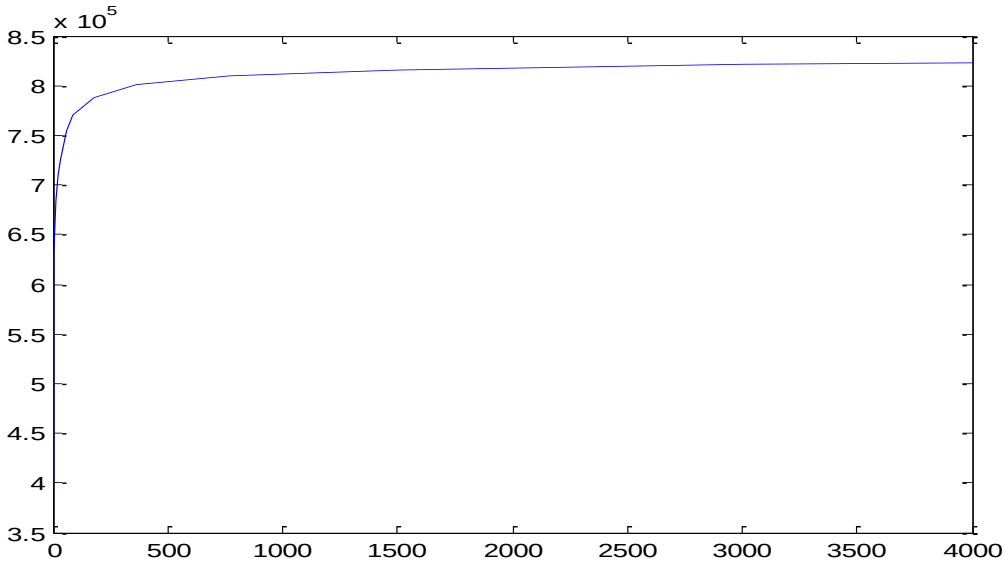

Figure 12.2 Young's Modulus (kips/ft^2) vs. time (days) from BD2 model

The strain data can be obtained at each construction phase (BD2) by comparing the model stages to the construction log.

Table 12.3 Experimental Stress of Segment 2806NB (kips/ft^2)

Date	Events	Experi-mental Strain (bottom)	Initial Strain (28 Days after casting)	E Modulus From BD2	Initial E Modulus	Exper-imental stress	Analytical stress
8/18/ 2006	PHASE 125 (STRESS STAY 4A&B - STAGE 1 DAY1186)	1948	2150	734112	723948	-126	-142
6/6/ 2007	PHASE 4600 (Day1460)	1857.6	2150	769841	723948	-126	-139
12/1/ 2008	PHASE 4650 (Day 2000)	1704.6	2150	800481	723948	-175	-174
1/21/ 2010	PHASE 4680 (DAY 2415)	1681	2150	825456	723948	-169	-173
3/20/ 2011	PHASE 4690 (DAY 2840)	1621	2150	825456	723948	-219	-172

12.3 Representative Analytical vs. Experimental Stress Comparisons

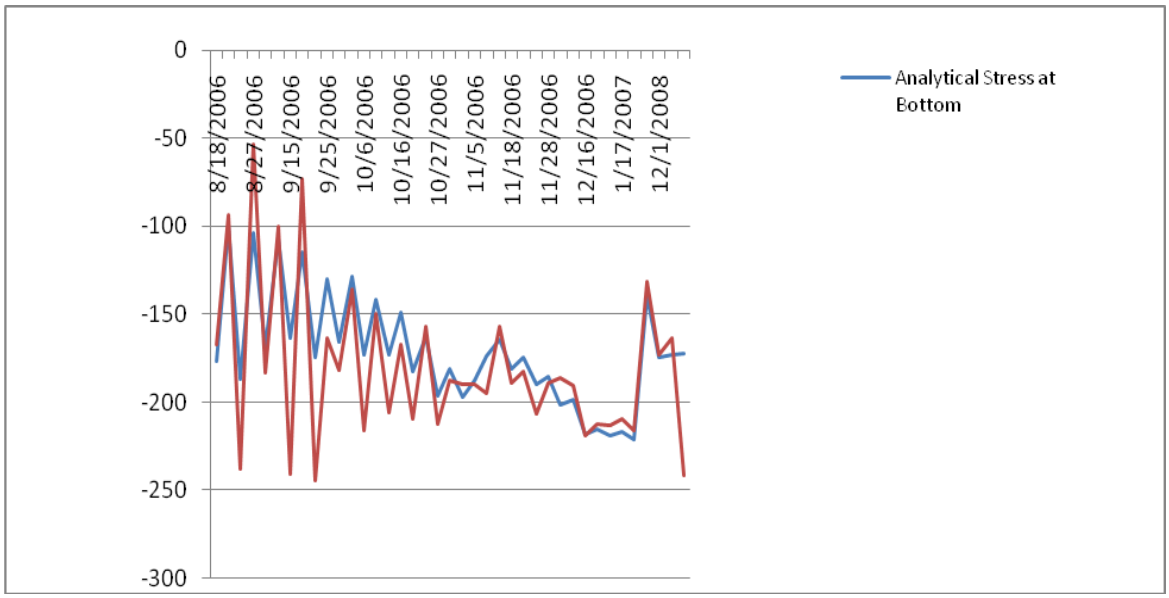

Fig 12.3 Experimental stress and analytical stress (kips /ft^2) at the bottom of segment 2806SB (Feng 2010)

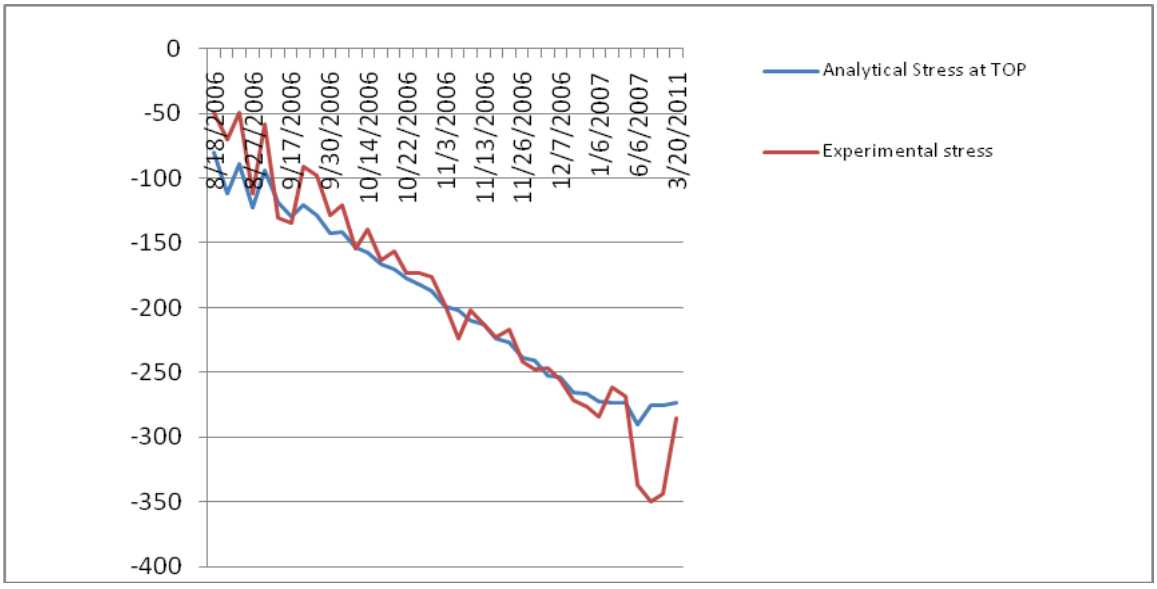

Fig 12.4 Experimental stress and analytical stress (kips /ft^2) at the top of segment 2806NB (Feng 2010)

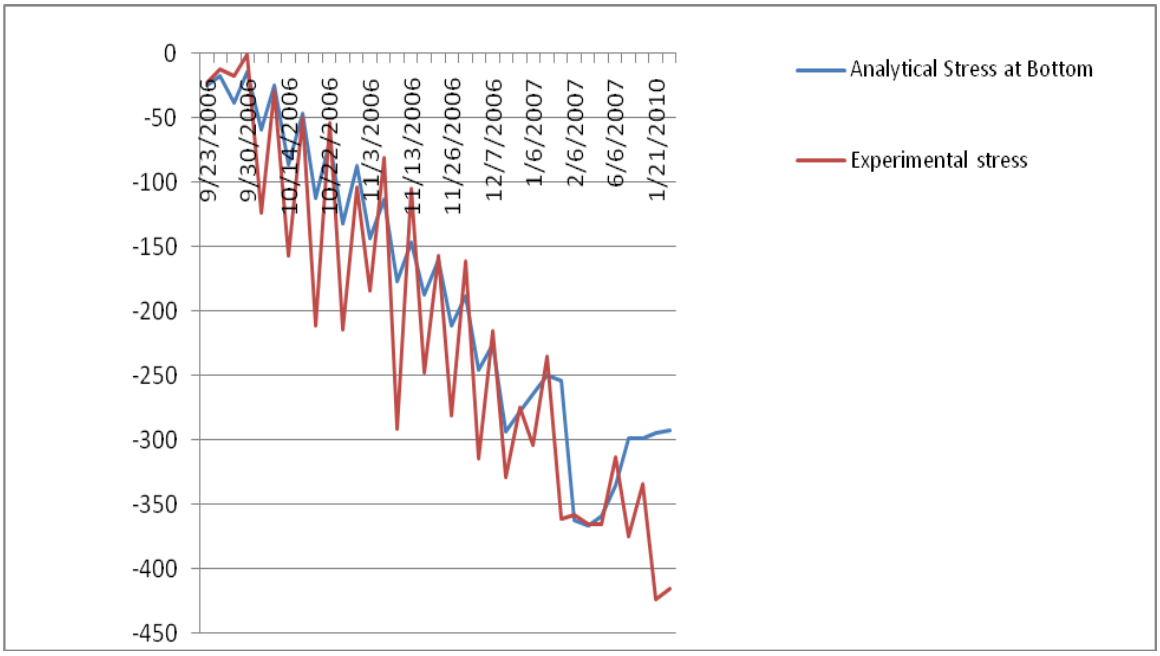

Fig 12.5 Experimental stress and analytical stress (kips /ft^2) at the bottom of segment 2828NB (Feng 2010)

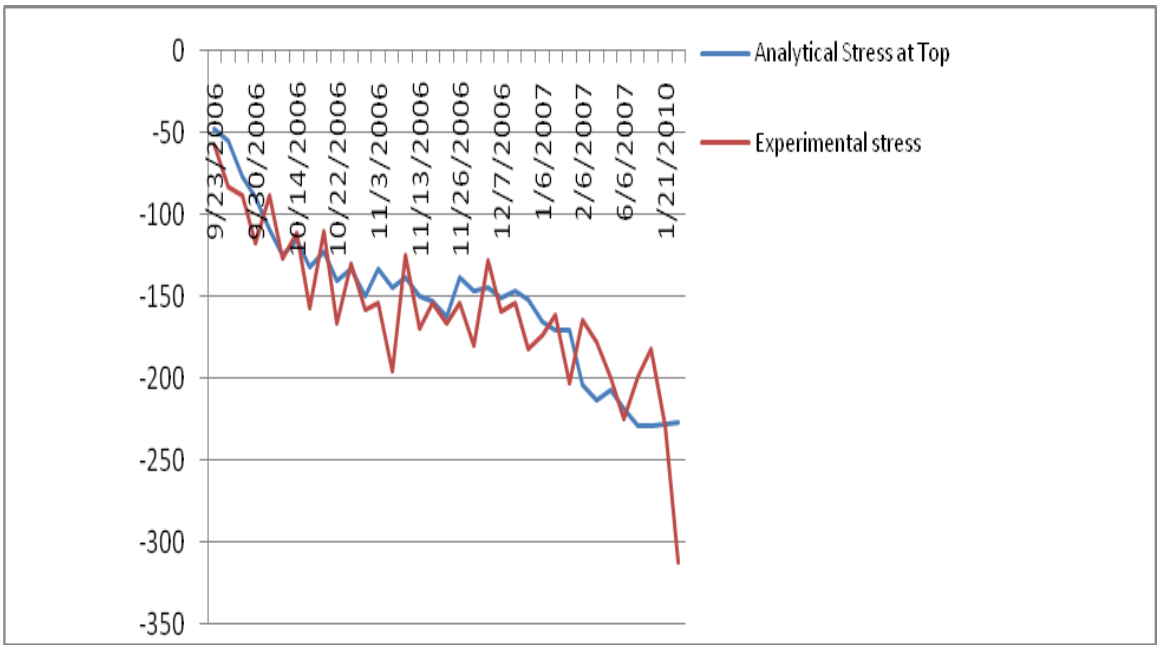

Fig 12.6 Experimental stress and analytical stress (kips /ft^2) at the top of segment 2828NB (Feng 2010)

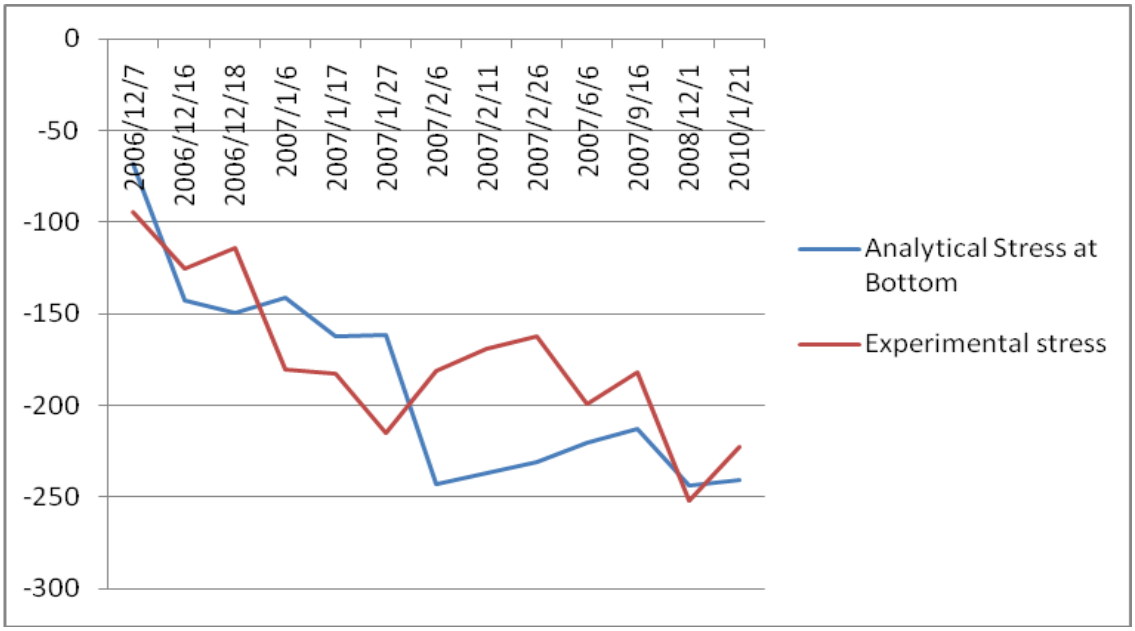

Fig 12.7 Experimental stress and analytical stress (kips /ft^2) at the bottom of segment 2704NB (Feng 2010)

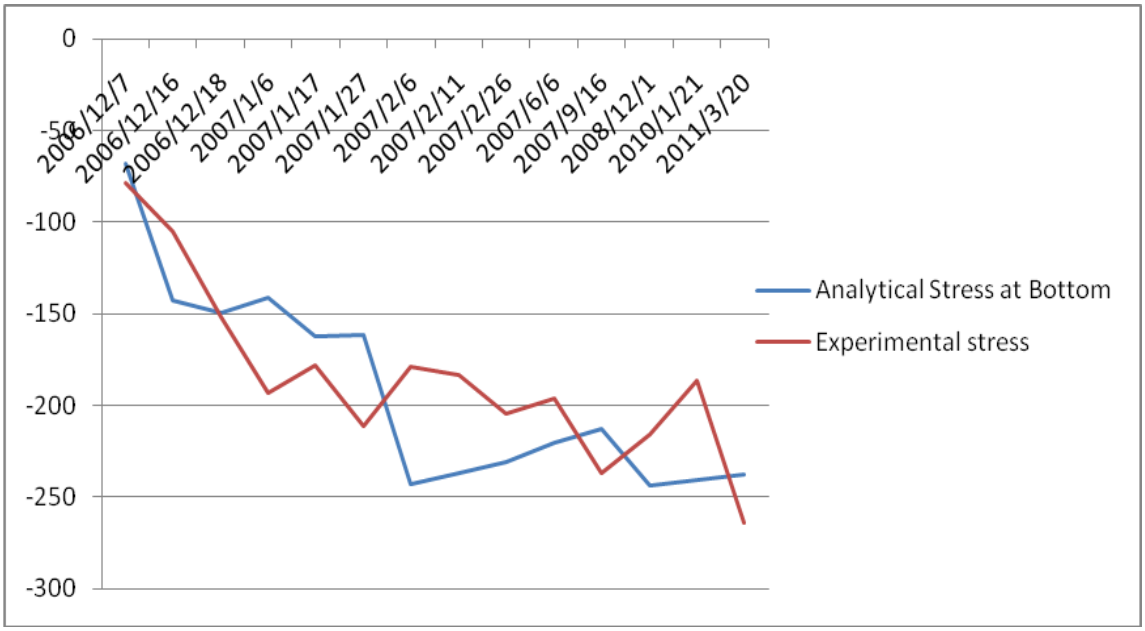

Fig 12.8 Experimental stress and analytical stress (kips /ft^2) at the bottom of segment 2704SB (Feng 2010)

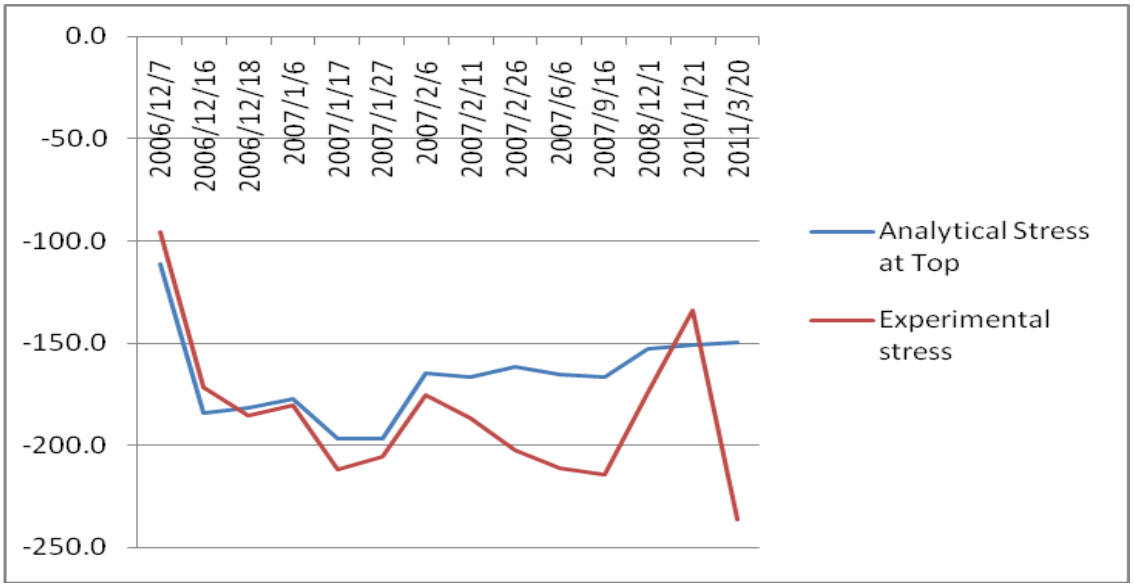

Fig 12.9 Experimental stress and analytical stress (kips /ft^2) at the top of segment 2704NB (Feng 2010)

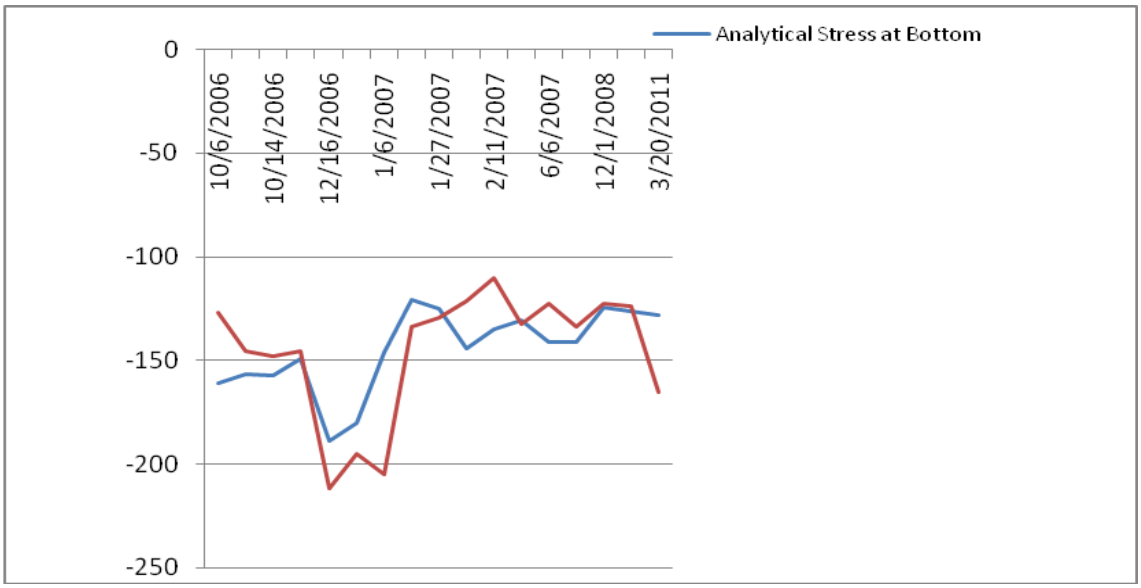

Fig 12.10 Experimental stress and analytical stress (kips /ft^2) at the bottom of segment 2741NB (Feng, 2010)

The stress comparisons at segment 2806 and segment 2828 show a good match in trend and a reasonable match in value.

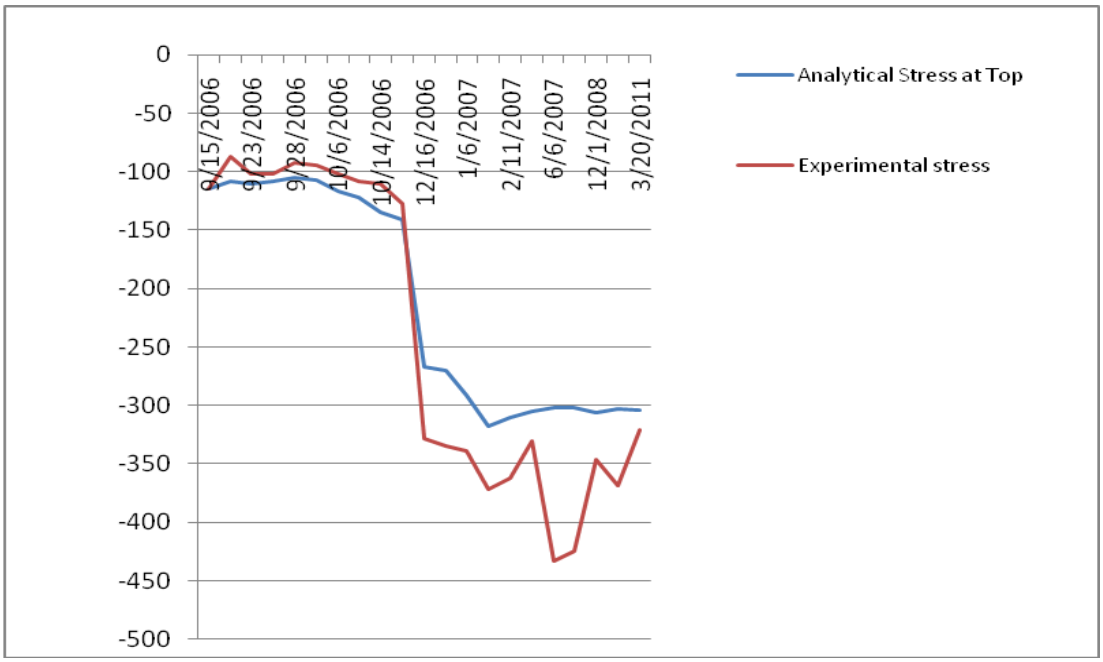

Fig 12.11 Experimental stress and analytical (kips /ft^2) stress at the top of segment 2741NB (Feng, 2010)

Segments 2704 and 2741 have few available experimental data during construction. But the experimental stress comparison between the northbound and southbound segments are a good match with each other and the experimental stresses present a good fit with analytical stress for BD2 model.

12.4 Summary of Results

This study verifies that the instrumented segments of VGCS behave as expected for the period studied.

References

1. Qiao C., 2009, "Analytical and Experimental Stress during Construction of the Veteran's Glass City Skyway" Master Thesis, The University of Toledo.

2. Feng X., 2010, “Nondestructive load testing of the Veteran’s Glass City Skyway” Master Thesis, The University of Toledo.

3. Branson, D., 1977, “Deformation of Concrete Structures”, McGraw-Hill.

4. IDS 2011, Interactive Design Systems, Inc., Bridge Designer II, http://www.ids-soft.com/

5. Yi G., 2011, “Long-term Behavior of the Veteran’s Glass City Skyway Cable Stayed Bridge” Master Thesis, The University of Toledo.

Chapter 13: Load Rating

13.1 Load Rating Procedure

In this study, the allowable stress (ASR) load rating method was used to evaluate the inventory load rating factor for analytical and experimental stresses. The following load-rating equation was used for the load rating of the concrete in each of the instrumented segments.

$$\text{Load Rating Factor} = \frac{\text{Allowable Capacity} - \text{Dead Load Effect}}{\text{Live Load Effect}} \qquad \text{(Eq. 13.1)}$$

Previous work done by Mr. Bosworth (2007) and Mr. Feng (2010)confirmed that the VGCS behaves symmetrically. This is illustrated in Figure 13.1.

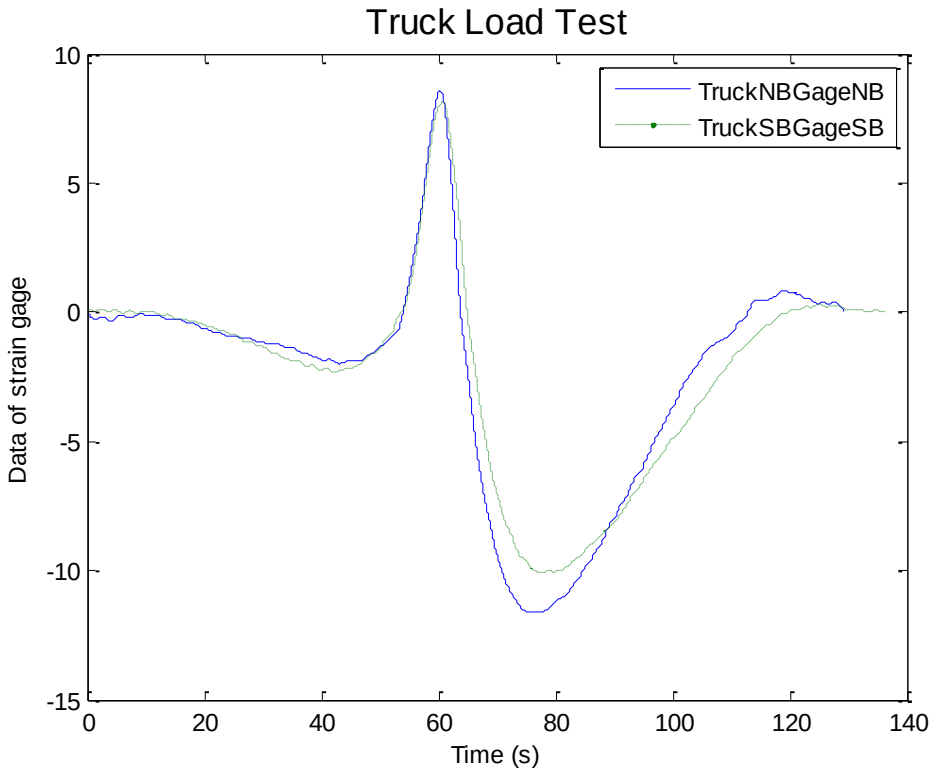

Fig 13.1 NBFL with Northbound loaded and SBFL with Southbound loaded

A good match of the strain comparison (Qiao, 2009) and good match of the stress comparison as shown in chapter 12 (Figures 12.3 thru 12.11) for each pair of segments throughout construction verified that dead load effects from the two sides of the bridge are similar during service (Feng, 2010).

Thus, because of the verified symmetry of the VGCS, this study only evaluates the live load effect for the northbound segments.

13.2 Development of the Unit Influence Line

To evaluate the live load effect for VGCS, the unit influence line (UIL) need to be generated by the finite element model (LARSA) and truck load tests. Here the unit influence line from the LARSA model with the unit influence line derived from the dynamic truck load test. In the following exercise, the unit load considered is the truck configuration.

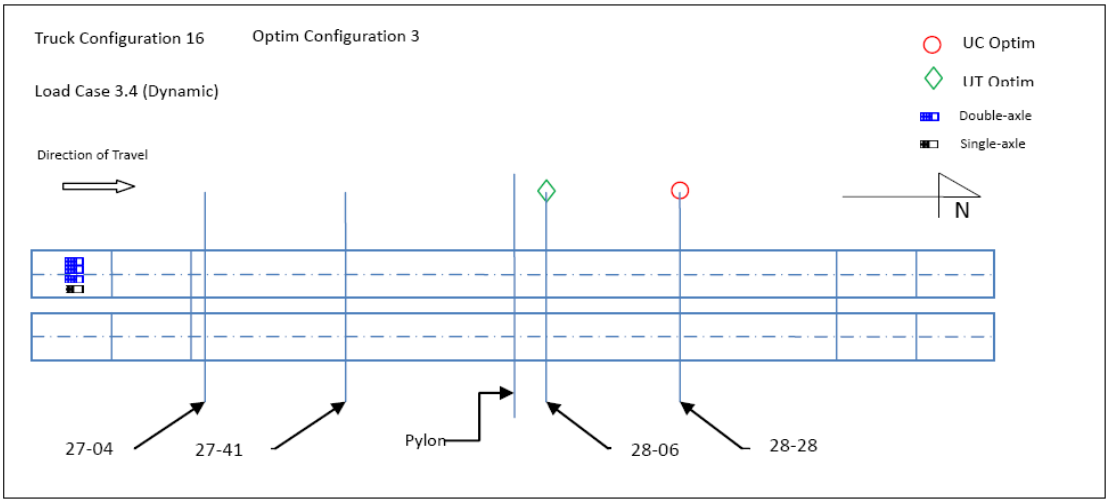

Fig 13.2 Second truck load test configuration 16

Fig 13.2 is configuration 16 of the second truck load test. (Four trucks moving north bound across the main span of VGCS).

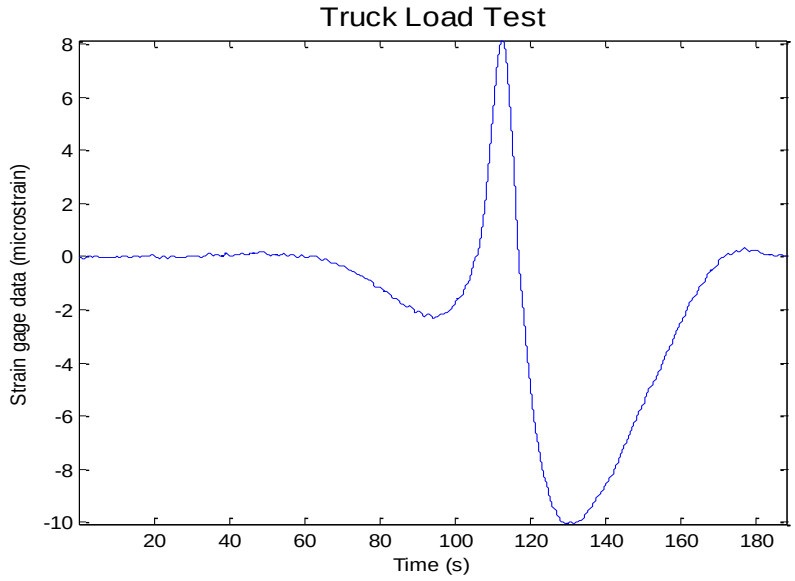

Fig 13.3 Data at segment 2806NB measured from the truck load test configuration 15

Figure 13.3 is the strain data for the gage embedded in the middle of the floor at segment 2806 measured from truck load test configuration 16.

The following equations are used to convert this curve to an influence line:

ε: Strain $$\varepsilon = \frac{\sigma}{E}$$ Eq. (13.2)

σ: Stress $$\sigma = \frac{My}{I_x}$$ Eq. (13.3)

M: Moment $$M = \frac{\varepsilon E I_x}{Wy}$$ Eq. (13.4)

Where,

y is the moment arm, or distance of the gage from the neutral axis of the segment

W is the total weight of truck loads

v is the velocity of the live loads in the truck load test

Table 13.1 Geometry properties of segment 2806 from LARSA model

Location	Element No.	Ix	Neutral axis(in)	Modulus of Elasticity (lb/in^2)
NBseg2806	20089	39885495	99.67	5098000

Table 13.2 Truck weight information for the four trucks used in second truck load test

Northbound				
Truck No.	T2643	T2580	T2840	T2739
Truck Type	Double Axle	Double Axle	Double Axle	Single Axle
Gross Weight (lb)	45480	47570	46540	27620

For truck load test, all the geometric properties of segment come from the LARSA model. By using the equations above, the strain time history can be converted to influence line.

Figure 13.4 is the influence line evaluated by strain data from truck load test; whereas figure 13.5 is the influence line obtained from LARSA model at segment 2806. These two curves show a good match. The maximum value of negative moment from Figure 13.4 is -17.56 kip-ft, and the maximum value of negative moment from Figure 13.5 is -19.00 kip-ft. The difference

between the maximum values of negative moment from Fig. 13.4 and Fig. 13.5 is 7.5%. Thus, the LARSA model is able to effectively to simulate the structure's response to live load.

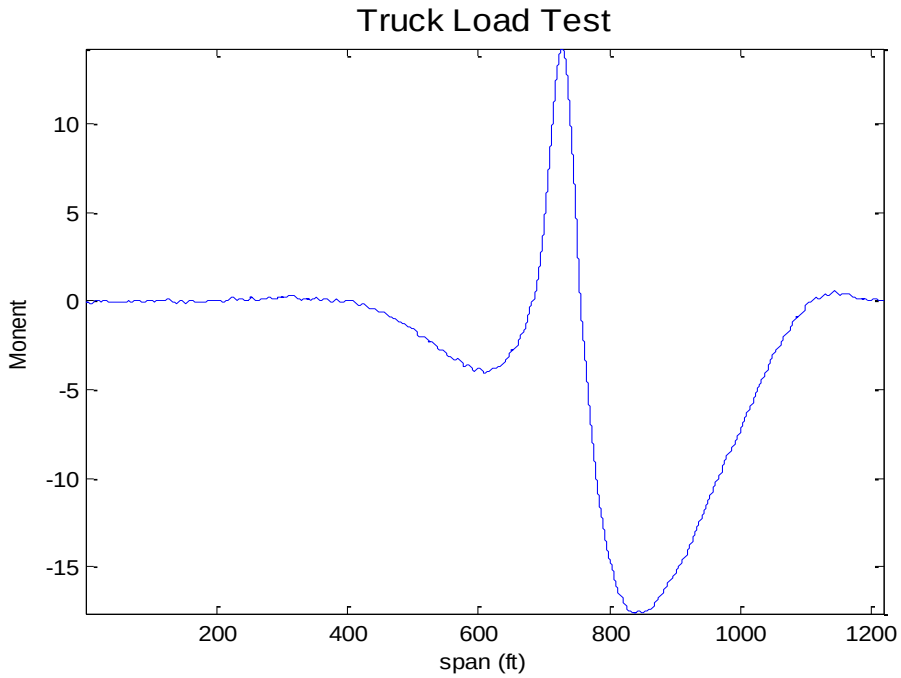

Fig 13.4 Converted influence line

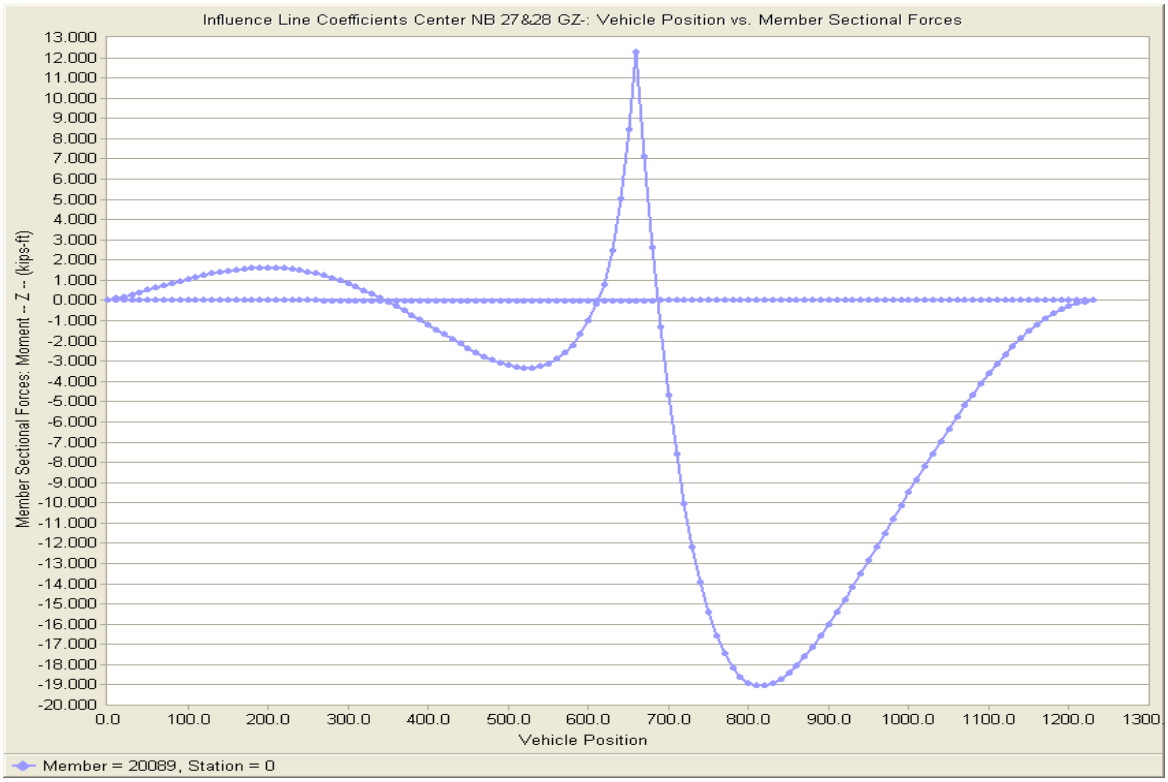

Fig 13.5 Influence line from LARSA for segment 2806

From configuration 5 and configuration 17 (figure 13.6 and 13.7 respectively) of second truck load test (Eight trucks across the main span of VGCS), the strain data can be converted to the experimental influence line and integrated with the analytical influence line.

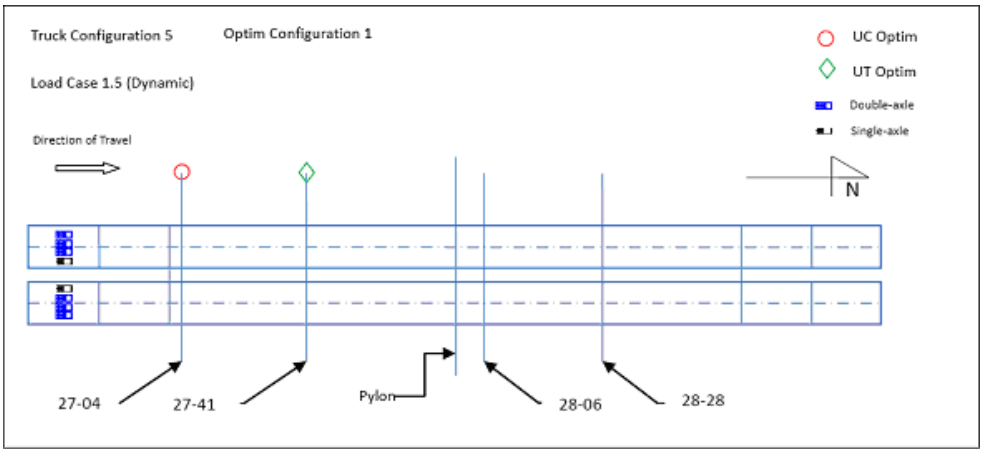

Fig 13.6 Second truck load test configuration 5

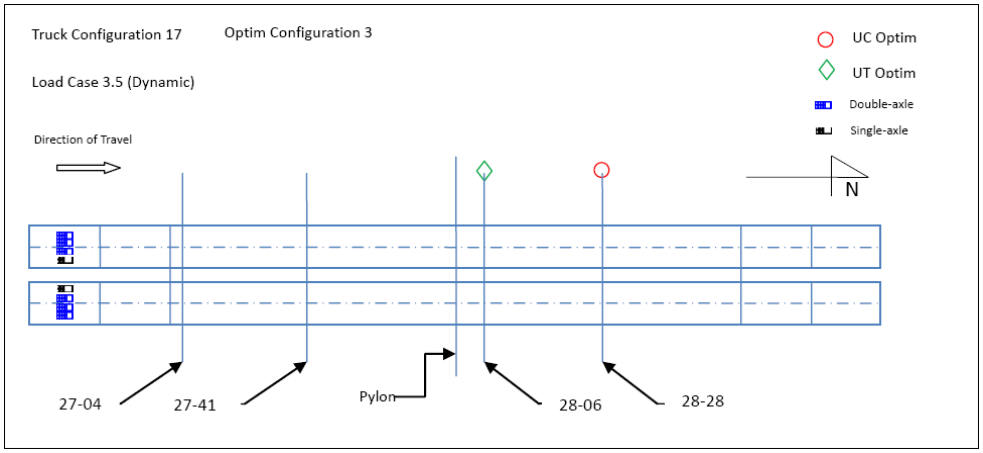

Fig 13.7 Second truck load test configuration 17

Figures 13.8~13.11 compares the analytical and experimental influence lines for each instrumented segment.

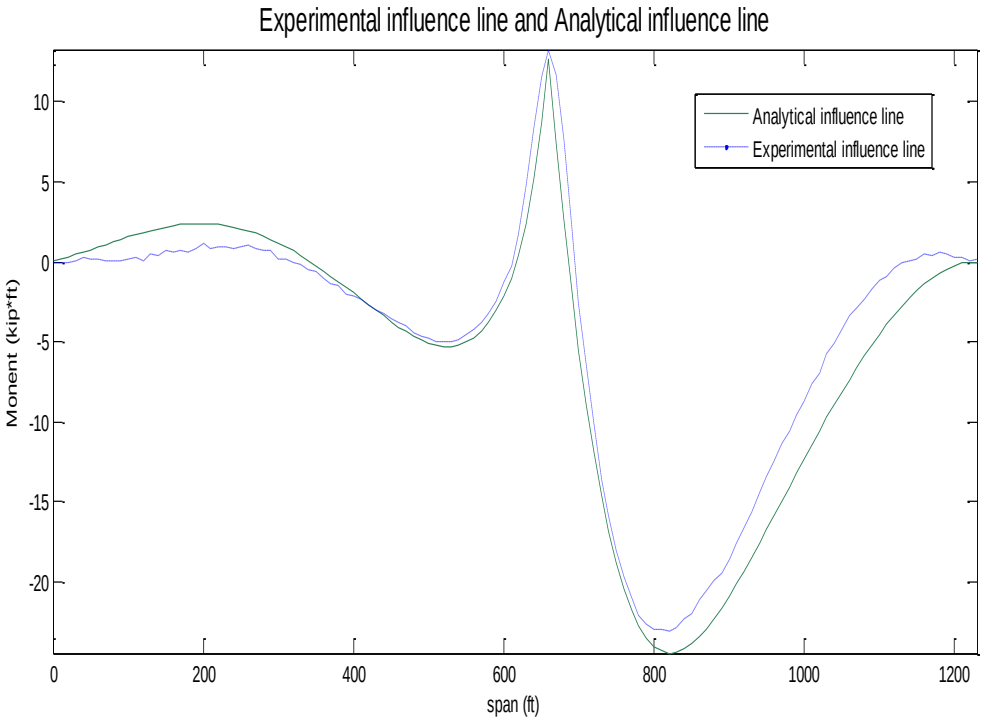

Fig 13.8 Integrate influence line for segment 2806

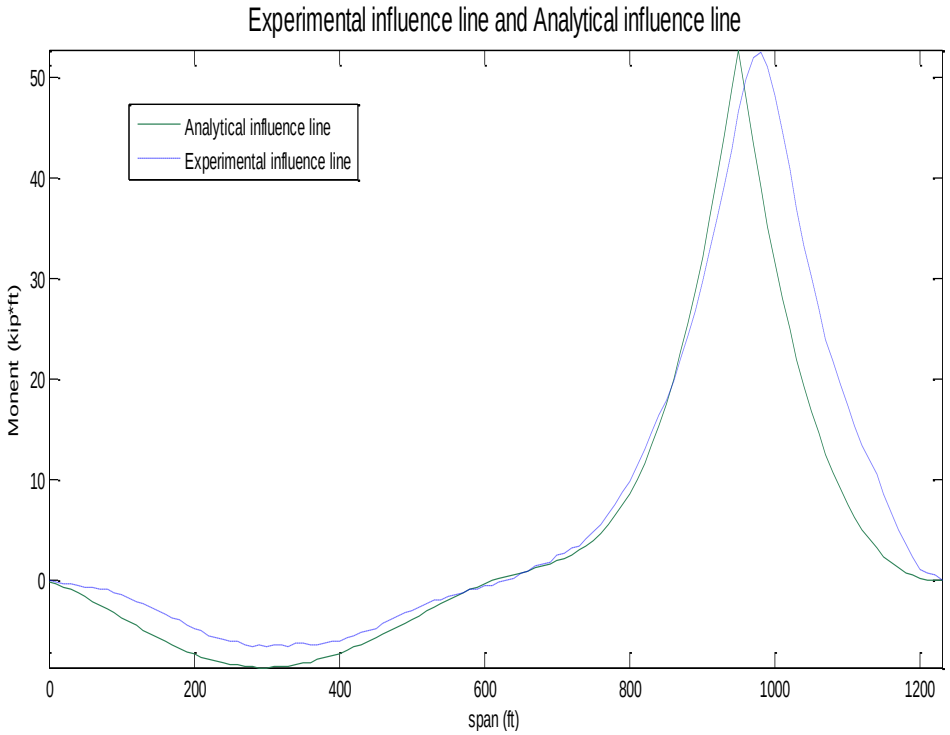

Fig 13.9 Integrate influence line for segment 2828

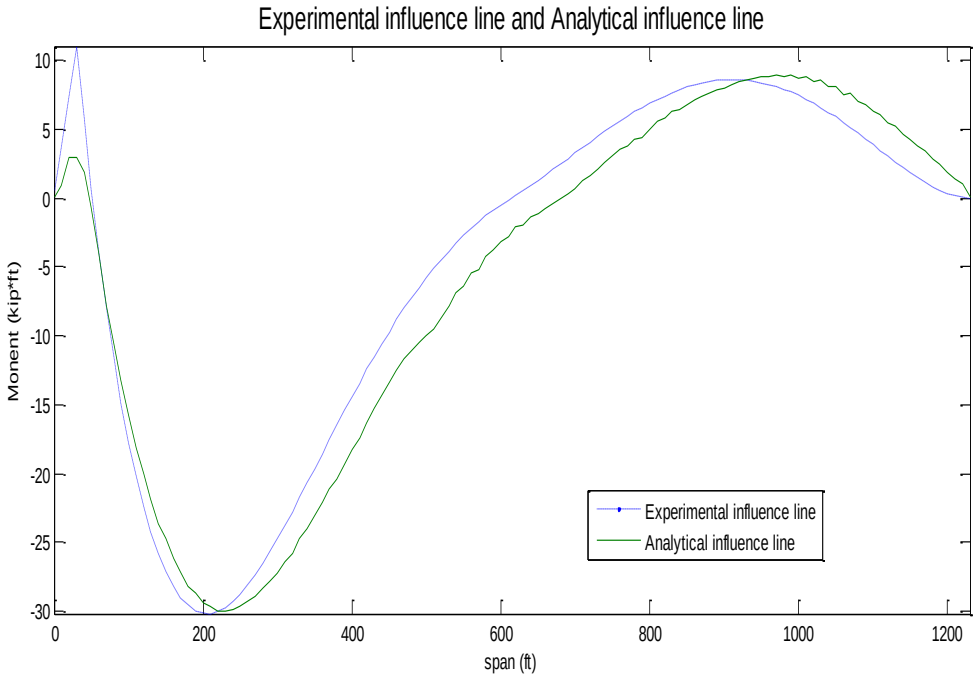

Fig 13.10 Integrate influence line for segment 2704

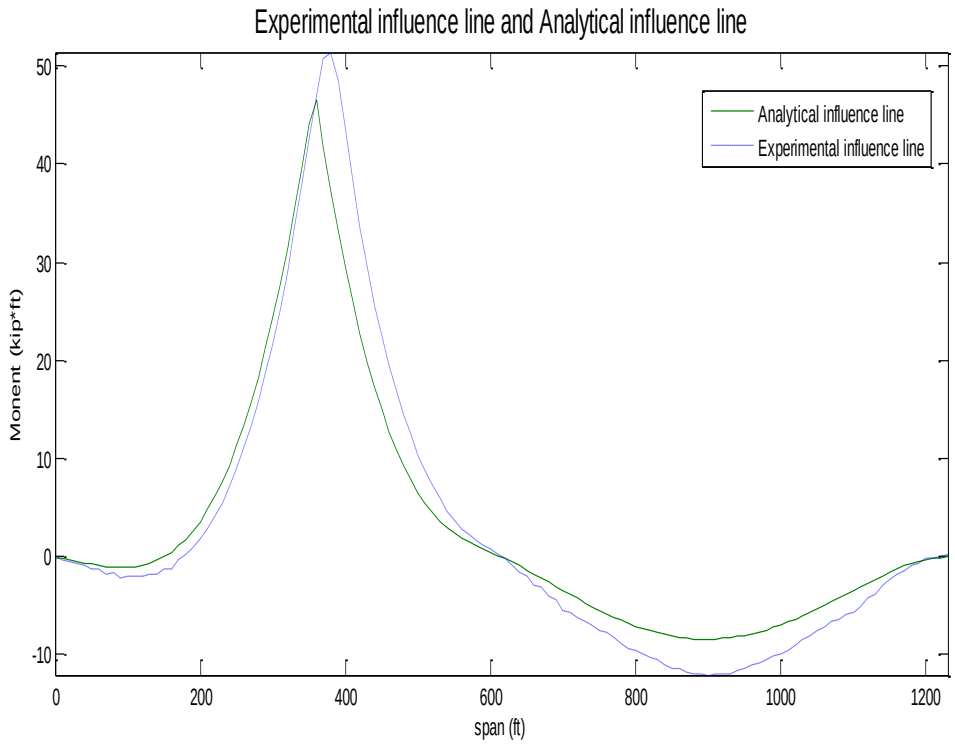

Fig 13.11 Integrate influence line for segment 2741

13.3 Live Load Effect

At inventory level, we just consider the design service live loads. The bridge was designed to handle HS25 live load, as well as two other loadings: Michigan grain truck II and III, one per traffic direction, (with HS25s in the other lanes), and single military. Following the AASHTO Bridge Design Manual, the HS25 lane load is suggested as 0.8 kip/ft^2 for each lane.

Table 13.3 HS-25 Truck Load Moment Effect for Segment 2806

Positive LL Moment			
span	Influence Line (kip-ft)	Axle load	Cumulative Truck Load Moment (HS-25×8) (kip-ft)
646	7.3	10	587
660	12.6	40	4632
674	5.5	40	6379
Negative LL Moment			
span	Influence Line (kip-ft)	Axle load	Cumulative Truck Load Moment (HS-25×8) (kip-ft)
806	-24.2	10	-1939
820	-24.5	40	-9772
834	-24.4	40	-17566

Table 13.4 Lane Load Effect for Segment 2806

Lane Load Moment (kip-ft)		Lane Load Moment × 8
Positive	716	5730
Negative	-6175	-49402

Tables 13.3 and Table 13.4 present the analytical HS-25 truck load effect and lane load effect for segment 2806 evaluated by the integration of the influence line.

According to AASHTO 17th edition (2002), Section 3.8.2.1, the impact factor for live loads shall be determined by the formula:

$$IM = 1 + \frac{50}{L + 125} \qquad \text{(Eq. 13.5)}$$

Where, IM : live load impact factor

L: the loaded length. For continuous spans: the length of span under consideration for positive moment, and the average of two adjacent loaded spans for negative moment.

The impact factor was calculated and reported in table 13.5 for northbound segments for both positive and negative moments.

Table 13.5 Impact Factor for Segments 2806, 2828, 2704, and 2741

Segment	Impact Factor (IM)	
	Positive Moment	Negative Moment
NB2806	1.07	1.07
NB2828	1.07	1.07
NB2704	1.07	1.1
NB2741	1.07	1.1

The lane load moment effect is shown in table 13.6 due to the lane load effect, while the adjusted truck moment is shown in table 13.7 due to the truck load effects.

Table 13.6 Lane Load Effect including Impact Factor for Segment 2806

Lane Load Moment (kip-ft)	Total Lane Load Moment (kip-ft) = Lane Load Moment × 8	Impact Factor (IM)	Total Lane Load Moment (kip-ft) × IM	
Positive	5730	1.07	Positive	6131
Negative	-49402	1.07	Negative	-52860

Table 13.7 Adjusted Truck Load Moment Effect including Impact Factor and Multiple Lane Factor (0.75) for Segment 2806

Truck Load Moment (kip-ft)	Cumulative Truck Load Moment (kip-ft) (table 13.3)	Impact Factor (IM)	Adjusted Truck Load Moment (kip-ft) = Cumulative Truck load Moment × IM × 0.75	
Positive	6379	1.07	Positive	5119
Negative	-17566	1.07	Negative	-14097

For maximum positive moment, only one concentrated load shall be used per lane, combined with as many spans loaded uniformly as are required to produce maximum moment. For the determination of maximum negative moment in the design of continuous spans, however, AASHTO Section 3.11.3 specifies that the lane load shown shall be modified by the addition of a second concentrated load of equal weight placed in one other span in the series in such position to produce the maximum effect.

Per AASHTO figure 3.7.6B, the additional concentrated load shall be 18 kips for HS20 loading. Since HS25 loading is being considered in this analysis, the 18 kips concentrated load

must be scaled up by 1.25 multiplier. Hence the proportioned 22.5 kips concentrated load is to be added to the lane load, plus another 22.5 kips concentrated load on other side of support for any sensor locations governed by negative moment. The total resulting positive and negative moments from a 22.5 kips point load, are shown in table 13.8 and 13.9 respectively.

Table 13.8 Point Load 22.5 kips Positive Effect at Maximum Influence Line of Two Adjacent Spans for Segment 2806

Positive LL Moment			
1st span	Influence Line (kip-ft)	Point load	Moment (22.5K×8) (kip-ft)
200	2.4	22.5	432
Positive LL Moment			
2nd span	Influence Line (kip-ft)	Point load	Moment (22.5K×8) (kip-ft)
660	12.6	22.5	2275
Total = Worst Case			2275

Table 13.9 Point Load 22.5 kips Negative Effect at Maximum Influence Line of Two Adjacent Spans for Segment 2806

Negative LL Moment			
1st span	Influence Line (kip-ft)	Point load	Moment (22.5K×8) (kip-ft)
530	-5.3	22.5	-954
Negative LL Moment			
2nd span	Influence Line (kip-ft)	Point load	Moment(22.5K×8) (kip-ft)
820	-24.5	22.5	-4406
Total = Add Both Cases			-5360

Per AASHTO Section 3.12.1, a reduction in load intensity may be considered where maximum stresses are produced in any member by loading a number of traffic lanes simultaneously; therefore, a 75 percent reduction of the live loads may be used for four lanes or more in view of the improbability of coincident maximum loading. Therefore, table 13.10 shows the application of a multiple lane factor equal to 0.75 and the segment corresponding impact factor (from table 13.5) to the cumulative moment effects of lane load and the 22.5 kips point load from table 13.8 and 13.9 respectively.

Table 13.10 Adjusted Lane Moment Effects of Lane Load plus a 22.5 kips Point Load including Impact Factor and Multiple Lane Factor (0.75) for Segment 2806

(a) Lane Load Moment (kip-ft)		(b) Lane Load Moment (kip-ft) × 8 lanes	(c) Point Load LL Moment (kip-ft)	(d) Cumulative Lane Moment = Lane Load Moment (b) + Point Load Moment (c) (kip-ft)	(e) Adjusted Lane Moment Effects = Cumulative Lane Moment (d) × IM × 0.75 (kip-ft)
Positive	716	5730	2275	8005	6424
Negative	-6175	-49402	-5360	-54762	-43947

Tables 13.11 shows the calculated stresses due to the adjusted lane moment effects due to the lane load and the point load from table 13.10. However, table 13.12 shows the calculated stresses due to adjusted truck load moment effect from table 13.7. By comparing the live lane load stresses (table 13.11) and the live truck load stresses (table 13.12) for Segment 2806; it is evident that the live lane load stresses are critical and govern in this case. This is also valid for the other three segments: 2828, 2704, and 2741.

Table 13.11 Live Lane Load Stresses for Segment 2806

Stresses due to Adjusted Lane Moment Effects (e) from table 13.10 (Segment 2806)				
	M (kips-in)	y (in)	Ix (in^4)	Stress (ksi)
Tension on bottom	77,092	100	39,885,495	0.19
Compression on bottom	-527,359	100	39,885,495	-1.32
Compression on top	77,092	46	39,885,495	-0.09
Tension on top	-527,359	46	39,885,495	0.61

Table 13.12 Live Truck Load Stresses for Segment 2806

Stresses due to Adjusted Truck Load Moment Effect from table 13.7 (Segment 2806)				
	M (kips-in)	Y (in)	Ix (in^4)	Stress (ksi)
Tension on bottom	76,549	100	39,885,495	0.15
Compression on bottom	-210,794	100	39,885,495	-0.42
Compression on top	76,549	46	39,885,495	-0.07
Tension on top	-210,794	46	39,885,495	0.20

13.4 Load Rating Procedure

Load rating defines the maximum live load capacity of a bridge. In this study, the experimental and analytical inventory load rating for the concrete in compression will be evaluated by the Allowable Stress Rating Method for concrete. The general idea for analytical load rating is: Load rating factor = (Allowable capacity - Dead load effect) / Live load effect.

- The allowable compressive stress of prestressed concrete is -691.2 kip/ft^2 (-4.80 ksi), which comes from design company Figg's database. The prestressed concrete was specified as f_c' = 8000 psi, which has allowable compressive stress of 0.6 f_c' and allowable tensile stress of $3\sqrt{f_c'}$ according to AASHTO Specification 9.15.2.1.
- For the experimental dead load effect, actual stress at day 2840 (03/20/2011) will be used from the long-term monitoring of VGCS (Yi, 2011).
- The influence line can describe the live load effect at each segment by the equation:

$$\sigma = \frac{My}{I_x} \qquad \text{(Eq. 13.6)}$$

Tables 13.13 thru 13.16 shows a load rating comparison among the design, analytical and experimental results.

Table 13.13 Analytical Load Rating and Experimental Load Rating for Segment 2806

Load Rating For Segment 2806 NB						
Stress	Seg. 2806NB	Location	Allowable Stress (ksi)	Dead Load Effect (ksi)	Live Load Effect (ksi)	Load Rating LR
Compression	Analytical	Bottom	-4.8	-1.2	-1.32	2.7
Compression	Analytical	Top	-4.8	-1.9	-0.09	32.7
Tension	Analytical	Bottom	1.03	-1.2	0.19	11.5
Tension	Analytical	Top	1.03	-1.9	0.61	4.8
Compression	Experimental	Bottom	-4.8	-1.5	-1.12	2.9
Compression	Experimental	Top	-4.8	-2	-0.08	34.2
Tension	Experimental	Bottom	1.03	-1.5	0.18	14.2
Tension	Experimental	Top	1.03	-2	0.52	5.9

Table 13.14 Analytical Load Rating and Experimental Load Rating for Segment 2828

Load Rating For Segment 2828 NB						
Stress	Seg. 2828NB	Location	Allowable Stress (ksi)	Dead Load Effect (ksi)	Live Load Effect (ksi)	Load Rating LR
Compression	Analytical	Bottom	-4.80	-2.00	-0.52	5.4
Compression	Analytical	Top	-4.80	-1.60	-0.72	4.5
Tension	Analytical	Bottom	1.03	-2.00	1.56	1.9
Tension	Analytical	Top	1.03	-1.60	0.24	10.9
Compression	Experimental	Bottom	-4.8	-2.9	-0.37	5.1
Compression	Experimental	Top	-4.8	-2.2	-0.88	3.0
Tension	Experimental	Bottom	1.03	-2.9	1.91	2.1
Tension	Experimental	Top	1.03	-2.2	0.17	18.8

Table 13.15 Analytical Load Rating and Experimental Load Rating for Segment 2704

Load Rating For Segment 2704 NB						
Stress	Seg. 2704NB	Location	Allowable Stress (ksi)	Dead Load Effect (ksi)	Live Load Effect (ksi)	Load Rating LR
Compression	Analytical	Bottom	-4.8	-1.7	-1.59	2.0
Compression	Analytical	Top	-4.8	-1	-0.26	14.6
Tension	Analytical	Bottom	1.03	-1.7	0.57	4.8
Tension	Analytical	Top	1.03	-1	0.73	2.8
Compression	Experimental	Bottom	-4.8	-1.5	-1.75	1.9
Compression	Experimental	Top	-4.8	-1.6	-0.24	13.4
Tension	Experimental	Bottom	1.03	-1.5	0.52	4.9
Tension	Experimental	Top	1.03	-1.6	0.81	3.3

Table 13.16 Analytical Load Rating and Experimental Load Rating for Segment 2741

Load Rating For Segment 2741 NB						
Stress	Seg. 2741NB	Location	Allowable Stress (ksi)	Dead Load Effect (ksi)	Live Load Effect (ksi)	Load Rating LR
Compression	Analytical	Bottom	-4.80	-0.9	-0.53	7.3
Compression	Analytical	Top	-4.80	-2.1	-0.58	4.7
Tension	Analytical	Bottom	1.03	-0.9	1.25	1.5
Tension	Analytical	Top	1.03	-2.1	0.24	12.8
Compression	Experimental	Bottom	-4.8	-1.1	-0.77	4.8
Compression	Experimental	Top	-4.8	-2.2	-0.66	3.9
Tension	Experimental	Bottom	1.03	-1.1	1.43	1.5
Tension	Experimental	Top	1.03	-2.2	0.35	9.1

13.5 Load Rating Summary

The analytical and experimental influence lines have a good fit. Therefore, the load rating values in the analytical and experimental results are in agreement. It is noteworthy to mention that there are slight differences in some load rating values when the peaks of analytical and experimental influence lines occur within several feet from each other in the same span; however, differences are hardly noticeable and are rather insignificant. The calculated load rating from the analytical and the experimental tests should be close to what was intended in the design.

References

1. Bosworth, K.J., 2007, "Health Monitoring of the Veterans' Glass City Skyway: Vibrating Wire Strain Gage Testing, Study of Temperature Gradients and a Baseline Truck Test." Master's Thesis, The University of Toledo.

2. Qiao C., 2009, "Analytical and Experimental Stress during Construction of the Veteran's Glass City Skyway" Master Thesis, The University of Toledo.

3. Feng X., 2010, "Nondestructive load testing of the Veteran's Glass City Skyway" Master Thesis, The University of Toledo.

4. AASHTO 17th edition (2002), Standard Bridge Design Manual.

5. IDS 2011, Interactive Design Systems, Inc., Bridge Designer II, http://www.ids-soft.com.

6. Yi G., 2011, "Long-term Behavior of the Veteran's Glass City Skyway Cable Stayed Bridge" Master Thesis, The University of Toledo.

Chapter 14 Stay Vibration

14.1 Introduction

This chapter focuses on the stay testing program that was employed on this project (Kangas, 2009). Several experiments were performed during various stages of construction to determine the capability of using traditional vibration techniques to estimate cable tensions with the non-traditional cable sheathing system of this structure. The stays on this bridge use a stainless steel cover pipe instead of a more traditional high density polyethylene (HDPE) sheath utilized on other stay bridges. Also, following recent trends, the stays at this bridge are built without the use of grout for the purposes of inspection and, if necessary, replacement. The cables are aligned in a single plane and use a semi-harp arrangement. The cables consist of 82 to 156 epoxy-coated strands which are enclosed within a stainless steel cover pipe. There are 40 cables on the bridge with cable lengths varying from 28 to 200 m. The stays are numbered from 1 to 20, starting at the tower and extending towards the abutment and labeled A for the approach span or B for the back span. Fig. 14.1 shows a basic overview for this bridge.

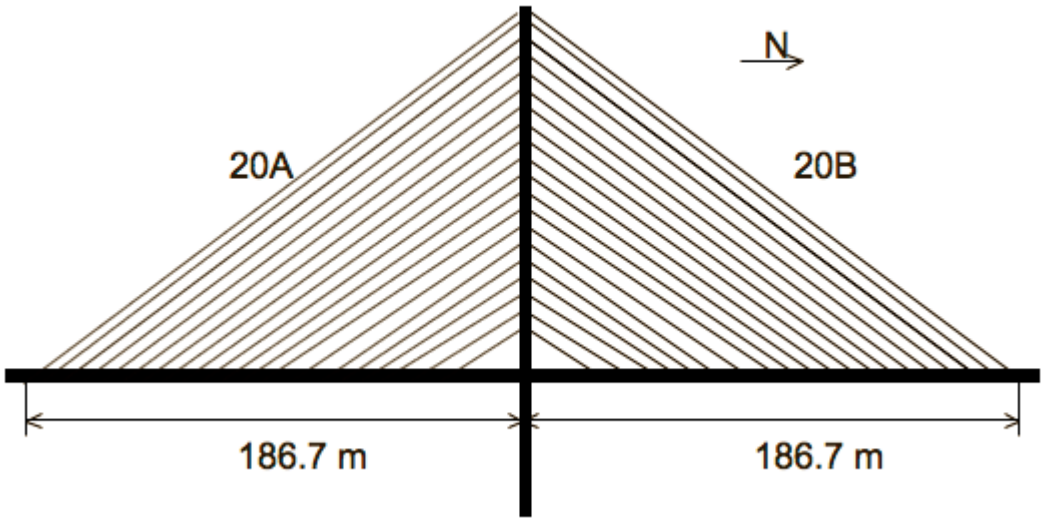

Figure 14.1 Plan View of VGCS Bridge (Kangas, 2009)

The cables at VGCS continuously pass through the pylon and terminate at the deck level. Although there are 20 total cables on this bridge, each span is considered to have unique cable motion resulting in 40 cable legs. This bridge is one of two cable-stayed bridges, along with the Penobscot Narrows Bridge, that uses this innovative cradle system to eliminate anchorages in the pylon (Figg, 2007). Each strand passes through its own individual stainless steel sleeve in the cradle assembly and is housed within stainless steel sheathing for its free length.

14.2 Cable Vibration and Force Estimation

To estimate cable force, cable vibrations are measured by placing accelerometers on the cable's protective cover pipe which is assumed to move in unison with the internal wire strands. The measured vibrations are used to create auto-correlation functions, calculated only using the positive time lags and therefore only retains information pertaining to the positive (stable) poles. These identified correlations are subsequently used as basis functions within a stochastic subspace identification algorithm to extract the eigenfrequencies of the cable's measured response. Figure 14.2 shows a typical measured cable acceleration and its corresponding auto-correlation used to identify cable resonant frequencies. To identify the resonant cable frequencies, the stochastic algorithm computes eigenfrequencies for varying model orders. The returned eigenfrequencies that are consistent for various model orders are selected for calculation of cable force. Figure 14.3 shows an example of the eigenfrequencies estimated by the subspace algorithm compared against the power spectrum created the positive correlation lags. The simplest model to describe a member under tension assumes it behaves like a taut string and is described by the following equation:

Taut String Equation:

$$f_n^s = \frac{n}{2L}\sqrt{\frac{T}{m}} \qquad \text{(Equation 14.1)}$$

where f^s_n is the n_{th} harmonic frequency of vibration (Hz), T, m and L are string tension (N), cable mass (kg/m), and cable free length (m), respectively.

This taut string approximation is not completely accurate for stay cables which have a degree of bending stiffness (EI), and cable sag associated with them, where sag is represented by

the parameter sag-extensibility (λ^2). Mehrabi (1998) accounted for these parameters within the following equation to describe the in-plane resonant frequencies:

$$\frac{f_n^{EI}}{f_n^s} = 1 + \frac{2}{\epsilon} + \frac{4 + n^2\pi^2/2}{\epsilon^2}$$

Stay with Sag Equation: (Equation 14.2)

$$\epsilon = L\sqrt{\frac{T}{EI}}$$

where: (Equation 14.3)

f^{EI}_n is the measured frequency of the n_{th} harmonic (Hz)

f^{S}_n is the equivalent-taut string frequency of the n_{th} harmonic (Hz)

ε is the dimensionless parameter related to the bending stiffness

The method for tension estimation implemented within this research follows the two-step method outlined by Peeters (2003) where non-linear least squares is used to simultaneously estimate ε and f^{S}_1 from the identified cable frequencies, which are assumed to behave like f^{EI}_n in Equation 14.2. Knowing the cable length (L) and mass per unit length (m), the estimate of f^{S}_1 can be used to calculate cable force according to Equation 14.1.

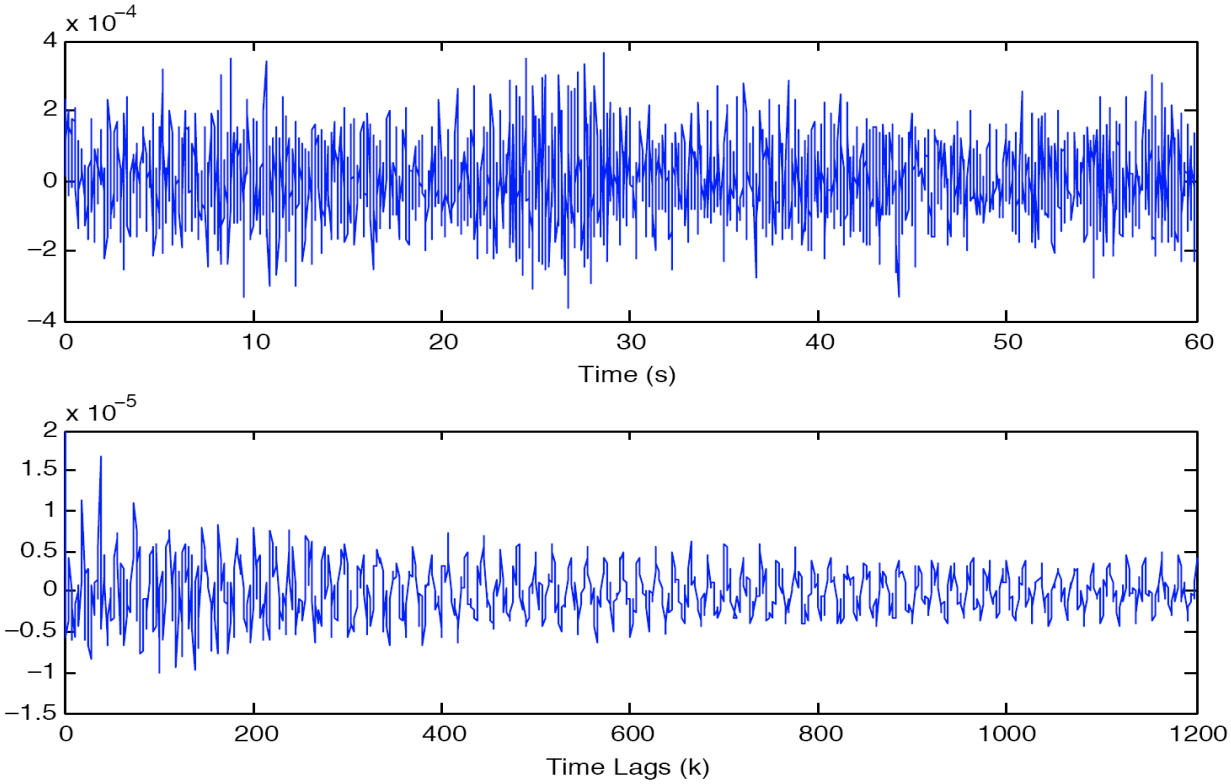

Figure 14.2 Acceleration (top) and auto-correlation (bottom) (Kangas, 2009)

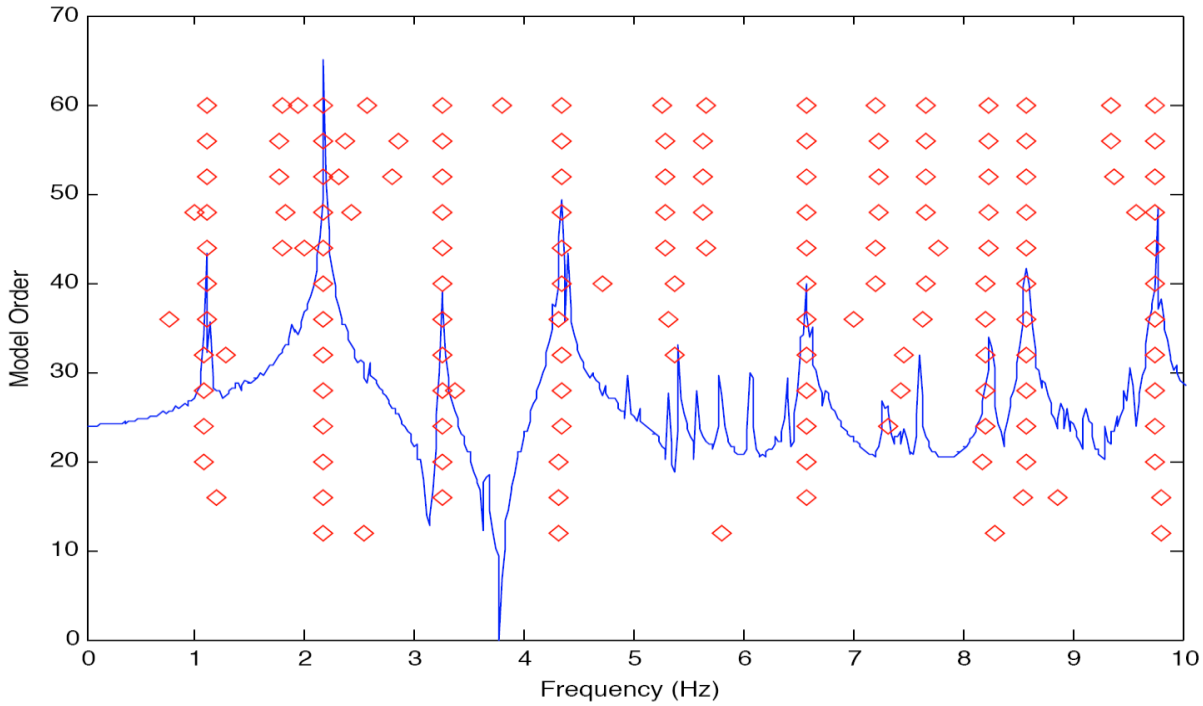

Figure 14.3 Cable eigenfrequencies (Kangas, 2009)

14.3 *Baseline Stay Tests before Installation of Cable Dampers - 3/12/2007*

Under contract with the Ohio Department of Transportation (ODOT), there was an ongoing mutual dialogue and data sharing agreement between the University of Cincinnati Infrastructure Institute (UCII) and the CTL Group. The results shown in this section are based on data recorded by the CTL Group and processed with algorithms developed by UCII. Tables 14.1 and 14.2 show the cable lengths, measured fundamental frequencies, lift-off forces supplied by the erection engineer and calculated forces assuming a uniformly distributed sheath for each of the 40 stays at VGCS. Lift-off measurements are typically employed during stay installation (or in later inspections) where each (or several) strand are hydraulically lifted off their anchorage in order to directly measure their tensile force. These calculated forces are as much as 40% lower than measured lift-off forces requiring sheath/strand interaction to again be quantified based on lift-off readings. Sheath participation factors were calculated for all the cables and these calculated sheath participation factors are also plotted against cable length in Figure 14.4. From this figure, it is apparent that the sheath participation factors decrease as the cable length increases (or as cable inclination decreases). These participation factors approach a value of one as cable length increases indicating that the distribution of sheath mass approaches a uniform distribution for the longer cables.

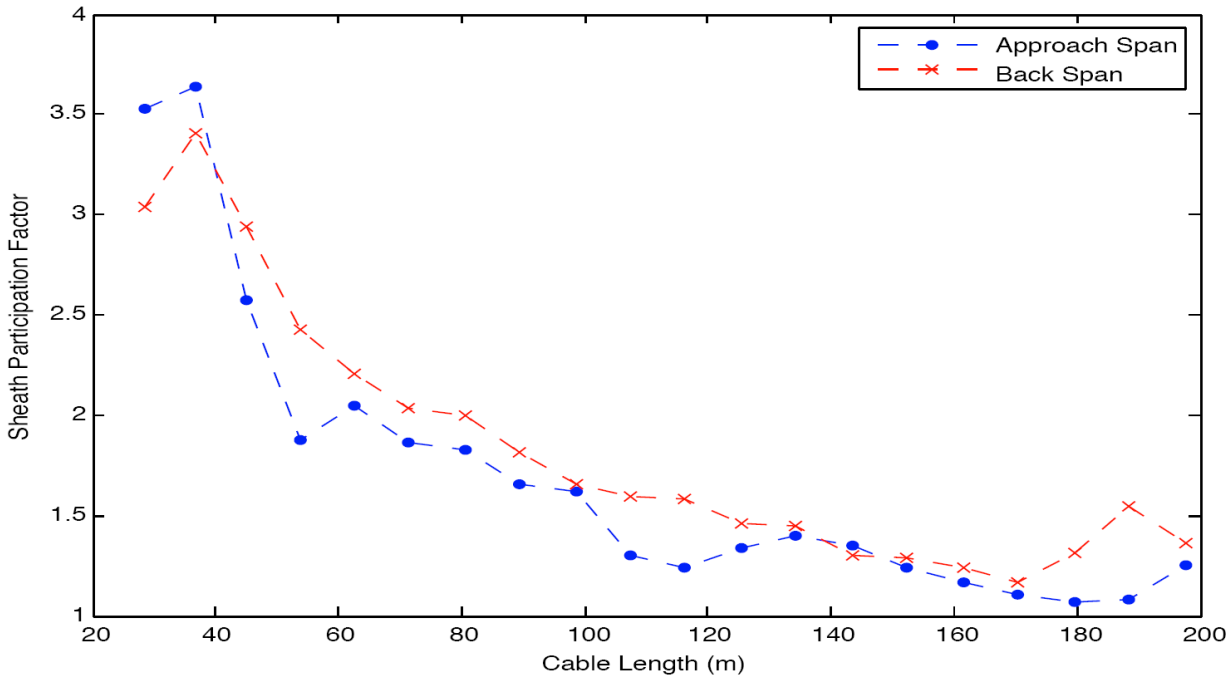

Figure 14.4 Sheath participation factors identified before damper installation (Kangas, 2009)

Cable	Length (m)	Fund Freq (Hz)	Lift-Off Forces (kN)	Calculated Forces (kN)	Diff (%)
1A	28.6	3.415	9017	5925	-34.29
2A	36.6	2.656	8096	4644	-42.64
3A	45.1	2.227	7962	5623	-29.38
4A	53.6	1.953	8096	6610	-18.35
5A	62.5	1.758	9857	7980	-19.04
6A	71.4	1.611	10863	9105	-16.18
7A	80.3	1.416	11921	9866	-17.24
8A	89.4	1.309	12602	10578	-16.06
9A	98.4	1.191	13162	11494	-12.67
10A	107.2	1.084	12744	11703	-8.17
11A	116.3	1.016	12869	12215	-5.08
12A	125.3	0.957	13812	12566	-9.02
13A	134.3	0.918	14919	13692	-8.23
14A	143.3	0.889	15809	14652	-7.32
15A	152.4	0.820	14821	14323	-3.36
16A	161.4	0.840	17388	16836	-3.17
17A	170.5	0.791	16654	16525	-0.77
18A	179.5	0.732	14990	14701	-1.93
19A	188.5	0.684	12668	12433	-1.86
20A	197.5	0.633	11797	10969	-7.02

Table 14.1 Frequencies & Forces for Approach Stays before damper installation (Kangas, 2009)

Cable	Length (m)	Fund Freq (Hz)	Lift-Off Forces (kN)	Calculated Forces (kN)	Diff (%)
1B	28.6	3.516	8509	6152	-27.70
2B	36.6	2.676	7913	4840	-38.84
3B	45.1	2.305	9003	6134	-31.87
4B	53.6	2.109	10342	7722	-25.33
5B	62.5	1.836	11116	8589	-22.73
6B	71.4	1.650	11801	9608	-18.58
7B	80.3	1.426	12539	10022	-20.08
8B	89.4	2.549	12989	11392	-12.29
9B	98.4	1.201	13718	11677	-14.88
10B	107.2	1.113	14087	12357	-12.28
11B	116.3	1.982	13887	12250	-11.79
12B	125.3	0.967	14212	13096	-7.85
13B	134.3	0.908	14741	13487	-8.51
14B	143.3	0.869	14924	13901	-6.85
15B	152.4	0.811	14599	13669	-6.37
16B	161.4	0.830	17255	16374	-5.10
17B	170.5	0.781	16441	15484	-5.82
18B	179.5	0.703	14132	13144	-6.99
19B	188.5	0.654	12993	11641	-10.41
20B	197.5	0.645	12749	11970	-6.11

Table 14.2 Frequencies & Forces for Back Stays before damper installation (Kangas, 2009)

14.4 *Baseline Stay Tests after Installation of Cable Dampers - 6/16/2009*

The preliminary tests performed at VGCS have shown the estimated tensions have been consistently underestimated as a result of a non-uniform distribution of sheath mass. This underestimation seems to be heavily influenced by cable angle; as the stay inclination decreases the sheath mass becomes more uniformly distributed and vibration-based tension estimates approach the values from lift-off readings. After installation of the cable dampers at VGCS, a final series of stay measurements were conducted. Lift-off tension readings were not available at the time of testing, so cable forces were assumed to be constant between these stays tests and the set of experiments before the dampers were installed.

Table 14.3 compares the fundamental frequency measured at each stay before and after dampers were installed. These cable frequencies are very close and there is a subtle upward shift in frequencies after the installation of the dampers (except for Cables 1A and 1B, which are the shortest cables with highest degree of cable inclination). Using the identified cable frequencies,

sheath participation factors were calculated and are shown in Figure 14.5. Unlike the previous experiments, from the measurements taken here a majority of the cables have a sheath participation factor close to unity. It is hypothesized that this reflects the change in cable state now that the stays are in their final configuration and the bridge is open to service; further, with the elimination of the temporary spacer, the distribution of sheath mass along the free length of the cable has approached a more uniform distribution.

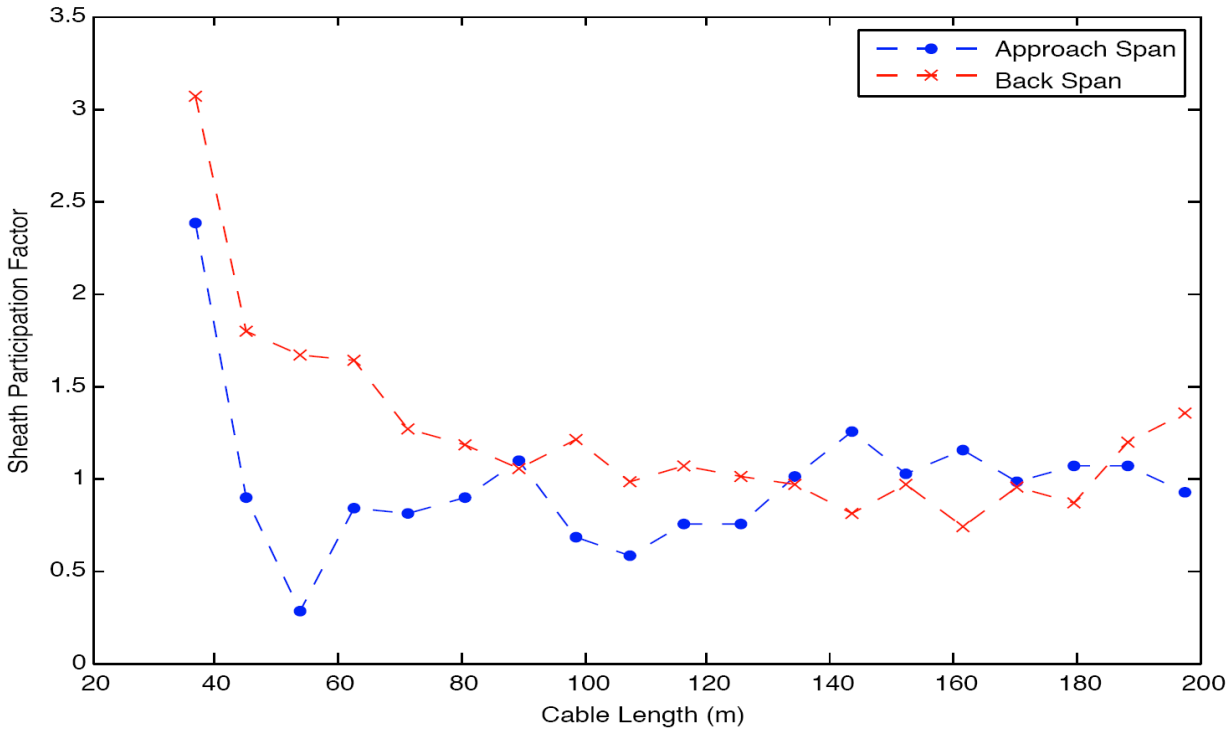

Figure 14.5 Sheath participation factors identified after damper installation (Kangas, 2009)

Cable	Fund Freq (Hz)		Cable	Fund Freq (Hz)	
	W/O Damper	W/ Damper		W/O Damper	W/ Damper
1A	3.415	5.371	1B	3.454	5.137
2A	2.654	2.969	2B	2.673	2.773
3A	2.224	2.656	3B	2.283	2.539
4A	1.951	2.363	4B	2.088	2.246
5A	1.756	1.992	5B	1.834	1.934
6A	1.610	1.797	6B	1.649	1.777
7A	1.415	1.582	7B	1.424	1.562
8A	1.317	1.406	8B	1.307	1.426
9A	1.190	1.328	9B	1.210	1.270
10A	1.093	1.191	10B	1.112	1.191
11A	1.015	1.074	11B	1.015	1.074
12A	0.966	1.035	12B	0.966	1.016
13A	0.917	0.957	13B	0.907	0.957
14A	0.888	0.898	14B	0.868	0.918
15A	0.820	0.840	15B	0.810	0.840
16A	0.839	0.840	16B	0.829	0.879
17A	0.790	0.781	17B	0.781	0.801
18A	0.742	0.742	18B	0.702	0.742
19A	0.683	0.684	19B	0.654	0.684
20A	0.634	0.664	20B	0.644	0.645

Table 14.3 Comparison of Stay Frequencies Before/After Damper Installation (Kangas, 2009)

14.5 Research Results and Conclusions

Stay vibration tests were performed during multiple stages of cable erection of the Veteran's Glass City Skyway Bridge. The stays at VGCS have unique structural characteristics that posed challenges to traditional vibration-based force estimation. Unlike the high density polyethylene sheathing system often incorporated on cable stayed bridges, the relative stiffness of the stainless steel cover pipe prevents the sheath and strands from making contact except at a limited number of locations. The sheath can account for approximately 25% of the total cable mass and its influence needed to be taken into account for accurate estimation of cable tension. After refining the cable force formulation based on field test observations, future vibration-based force estimations can be implemented in lieu of lift-off measurements.

References

1. Figg, 2007, Figg Bridge Engineers, Charles Pankow Award for Innovation, American Society of Civil Engineers (ASCE), April
2. S. Kangas, A. Helmicki, V. Hunt, R. Sexton, J. Swanson, "Identification of Cable Forces on Cable-Stayed Bridges: A Novel Extension of the MUSIC Algorithm", Experimental

Mechanics Journal, Society for Experimental Mechanics (SEM), Volume 50, Number 7, pp. 957-968, 2010.

3. S. Kangas, "Modeling and Ambient Vibration Monitoring of Cable-Stayed Bridges," Dissertation, University of Cincinnati, 2009.
4. Mehrabi, A., and Tabatabai, H. Unified finite difference formulation for free vibration of cables. *Journal of Structural Engineering 124*, 11 (1998), 1313–1322.
5. Peeters, B., Couvreur, G., Razinkov, O., Kundig, C., Der Auweraer, H. V., and Roeck, G. D. Continuous monitoring of the øresund bridge: System and data analysis. In *Proceedings of International Modal Analysis conference (IMAC)* (2003).
6. R. Sexton, S. Koganti, A. Helmicki, V. Hunt, and J. Swanson, "Aspects of Health Monitoring for Cable Stay Bridges," *Proceedings of ASNT Structural Materials Technology VI: An NDT Conference*, Columbus, OH, October, 2005.

Chapter 15 Modal Analysis

15.1 Introduction

This chapter focuses on the operational modal analysis program that was employed on this project (Chauhan, 2008). The magnitude and direction of structural vibrations may be monitored/measured at critical locations through the use of mounted accelerometers to identify the characteristic modal shapes and frequencies of the bridge. Monitoring structural vibrations at such locations for several long time periods (20-30 minutes) throughout the course of 1-2 days should be sufficient to capture important vibration response characteristics of the bridge. Sensors are easily mounted and the bridge is left open to traffic for the duration of the test. Live-load inputs from passing vehicles as well as the wind are used to induce structural vibration. Separate characterization of wind inputs to the structure are typically captured through synchronization with the weather station installed at the site.

From such data, it can be assessed whether vibration magnitude and/or frequency is of concern to the health or use of the bridge. Identification of vibration-critical regions in this manner may consequently provide information that can assist in assessing the performance of damping systems which, by reducing vibration contribute toward increasing the serviceable life of the structure. In addition, this vibrational data can be analyzed to characterize the dynamic mechanisms of bridge articulation. Such analysis is essential for a comprehensive calibration of FEM models.

15.2 Test Set-up, Data Acquisition and Data Processing

Figure 15.1 shows the test set-up layout. The sensor grid used for the test is much coarser in comparison to the one used for the US Grant Bridge and thus it is expected that some of the modes might appear to be similar (poor observability). A total of 10 sensors are used, 5 on each side of the parapet. The sensor lines extend from the back span side to the front span side with 8 sensors on one side of the pylon and 2 on the other as indicated. The sensor line extends 500m from Cable 14B on the back span to 6A on the front span. Note that notations *A* and *B* are for front and back spans respectively. Figure 15.2 shows one of the accelerometers glued on the

bridge superstructure. The data acquisition parameters for the test were set as following: sampling rate 40 Hz, frequency range 0 – 15 Hz, and test duration 20 minutes. The bridge was partially opened to public and one lane of traffic was open during the test.

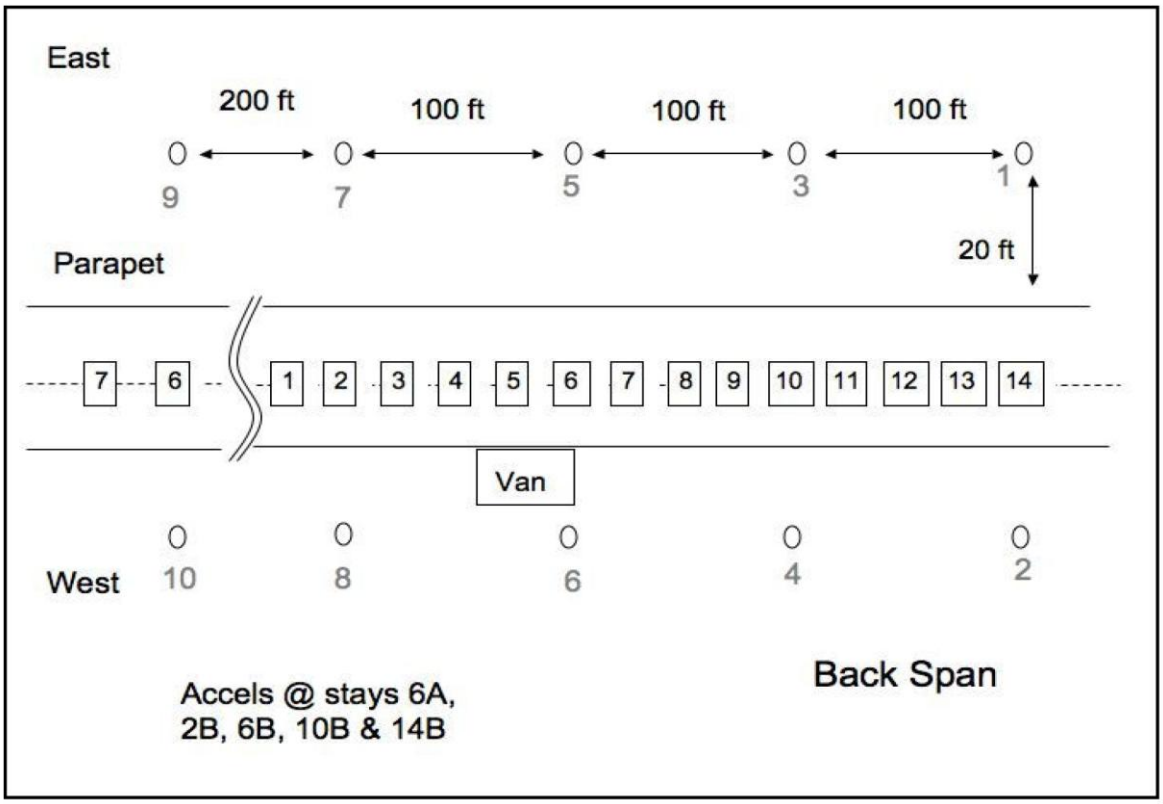

Figure 15.1 OMA Test Set-Up Layout for the VGCS Bridge (Chauhan, 2008)

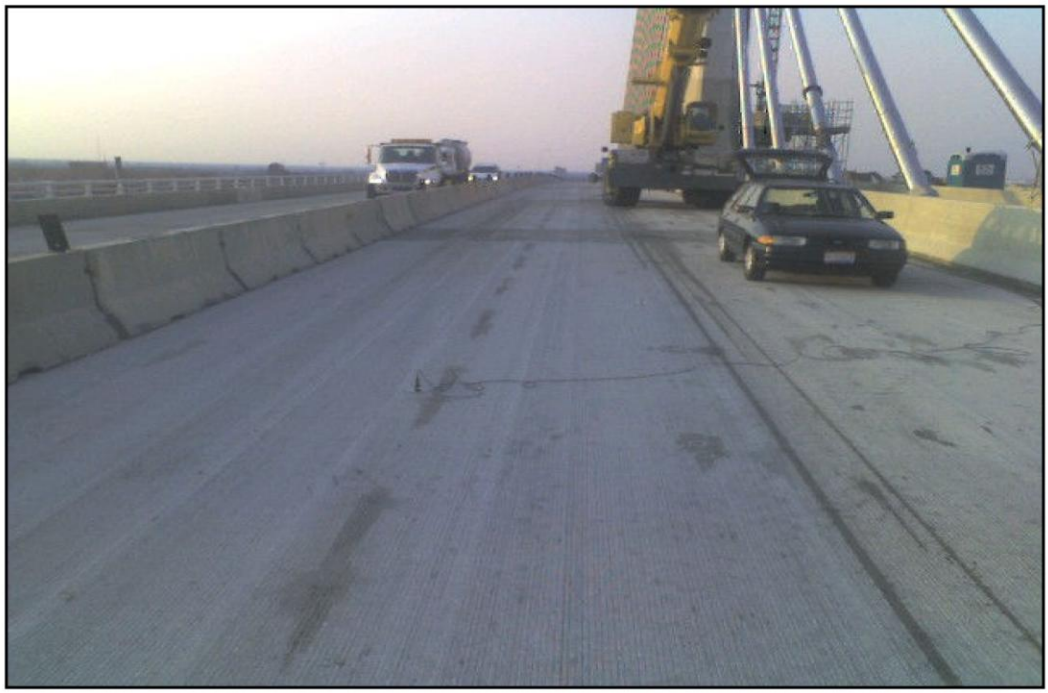

Figure 15.2 Typical accelerometer set up for the VGCS Bridge OMA test (Chauhan, 2008)

A block size of 2048, along with the application of Hanning window and 66.67 % overlap was used for processing the output time histories to obtain the power spectra. The autopower plot of individual channels is shown in Figure 15.3. The plot indicates the presence of at least 6 modes below 1.4 Hz frequency range. Further analysis also indicated the presence of two close modes around 1 Hz in addition to the modes indicated by the Autopower plot.

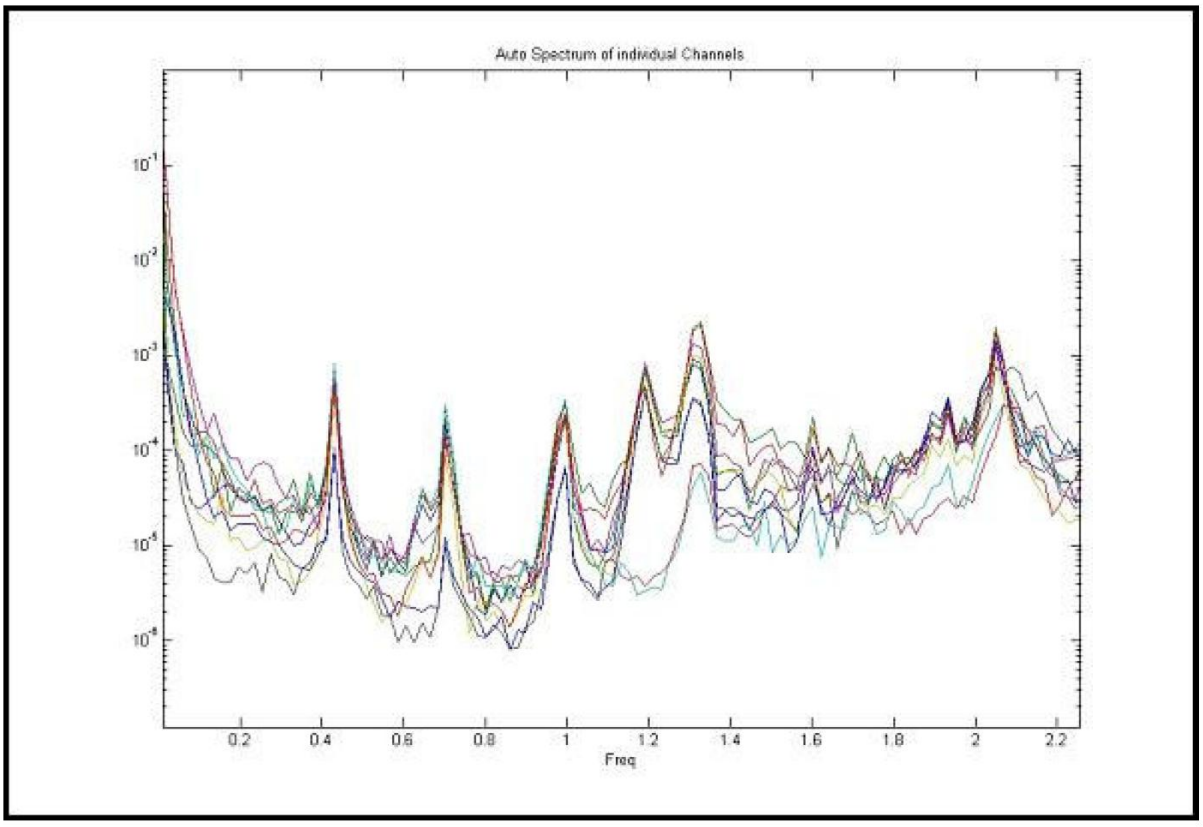

Figure 15.3 Autopower spectrum of individual channels (VGCS Bridge) (Chauhan, 2008)

15.3 Modal Parameter Estimation

Table 15.1 shows the modal parameters obtained using custom algorithms developed at the University of Cincinnati. The modal frequencies obtained using two algorithms match well. However, the damping estimates differ due to their dependence on a number of factors which are algorithm specific. Damping for the mode at 1.66 Hz (highlighted in green) is not estimated using the Enhanced Frequency Domain Decomposition (EFDD) algorithm as its spectral bell curve could not be identified properly at this frequency.

OMA-EMIF		EFDD	
Modal Freq (Hz)	Damping (%)	Modal Freq (Hz)	Damping (%)
0.4340	2.6277	0.4342	1.6064
0.6444	3.5642	0.6490	3.2492
0.7083	1.8282	0.7095	1.4179
0.9851	1.2470	0.9895	1.1213
0.9921	1.1892	0.9914	1.2432
1.1876	1.6644	1.1910	1.1651
1.3116	1.3653	1.3107	1.4484
1.5177	2.4909	1.5048	1.3426
1.6168	0.8962	1.6012	0.5292
1.6671	2.1747	1.6894	-
1.9462	1.8112	1.9307	0.8183
2.0528	1.2576	2.0534	0.9176
2.0994	1.2064	2.0699	0.5118
2.2993	1.7047	2.2869	0.8706
2.4204	1.6692	2.4206	0.3266

Table 15.1 Modal Parameter Estimates (VGCS Bridge) (Chauhan, 2008)

15.4 Finite Element (FE) Model Comparison

A finite element model of the bridge was developed and analyzed to compute the modal frequencies and the mode shapes. The modal frequencies and the mode shapes are listed in Table 15.2 along with the corresponding operational modal analysis results. It should be noted that most of these modes are vertical bending modes. Thus, the sensor layout for the final superstructure test was chosen in a manner that ensured the observation of these critical modes. Note that most of the early flexural modes for the FE model have been validated by field tests.

Mode No	FEM	OMA	Mode Type
4	0.38	0.44	Flex
6	0.63	N/A	Flex
7	0.65	0.7	Flex
8	0.96	0.99	Torsional
9	1.02	1.16	Torsional
11	1.14	1.17	Flex
12	1.24	1.3	Flex

Table 15.2 Frequency Comparison of OMA and FEM Results (VGCS Bridge) (Chauhan, 2008)

15.5 Research Results and Conclusions

In past, operational modal analysis has been shown to give good results with both analytical and lab based experimental data. In this study, the performance of these algorithms has been further analyzed by means of studies conducted on a cable stayed bridge. The modal parameter estimates obtained are shown to have comparative results with respect to at least two algorithms. In certain cases, the mode shapes appear to be similar. One of the reasons for this is the limited spatial resolution, which gives rise to observability related issues. However, with the help of the available knowledge in terms of the FE model, all the important modes have been estimated properly. Thus the study underlines the two key points of modal analysis in general that 1) its always good to have some a priori information available, and 2) the importance of good test planning, set up and good data acquisition because the parameter estimation algorithm is only as good as the data collected.

References

1. S. Chauhan, "Parameter Estimation and Signal Processing Techniques for Operational Modal Analysis," Dissertation, University of Cincinnati, 2008.
2. S. Chauhan, A. Helmicki, V. Hunt, J. Swanson, J. Saini, S. Kangas, D. Nims, R. Allemang, "Application of OMA-EMIF Algorithm to Cable Stayed Bridges," *Proceedings of International Seminar on Modal Analysis (ISMA)*, Leuven, Belgium, 2008.
3. R. Sexton, S. Koganti, A. Helmicki, V. Hunt, and J. Swanson, "Aspects of Health Monitoring for Cable Stay Bridges," *Proceedings of ASNT Structural Materials Technology VI: An NDT Conference*, Columbus, OH, October, 2005.

Chapter 16 Website Design and Documentation

16.1 Introduction

This chapter focuses on the long term instrumentation package, data collection system and web site which is used to monitor and evaluate the long term environmental effects on the structure. This system provided ODOT, UT and UCII the ability to plot strain and temperature information about the bridge in a data-form which can easily be plotted over periods of time for multiple locations. (1)

The system starts with sensors installed in specific locations on the bridge which all attach to a central data logger located near the bridges tower in a protected, temperature controlled metal cabinet. This data logger collects and stores the sensor readings for collection from a data processing system. A computer in the UCII laboratory was setup with customized data-logger software to make scheduled downloads of this sensor data. These scheduled processes trigger various sets of programs to then load the collected data into a database for further analysis or plotting from web sites. With the data loaded into a database, ODOT, UT and UCII can plot sensor information from any web accessible device via a simple web browser. The ability to run programs on recently collected sensor data also provides the ability to alert the authorities of events if necessary. A diagram of the overall system described above is shown in Figure 16.1.

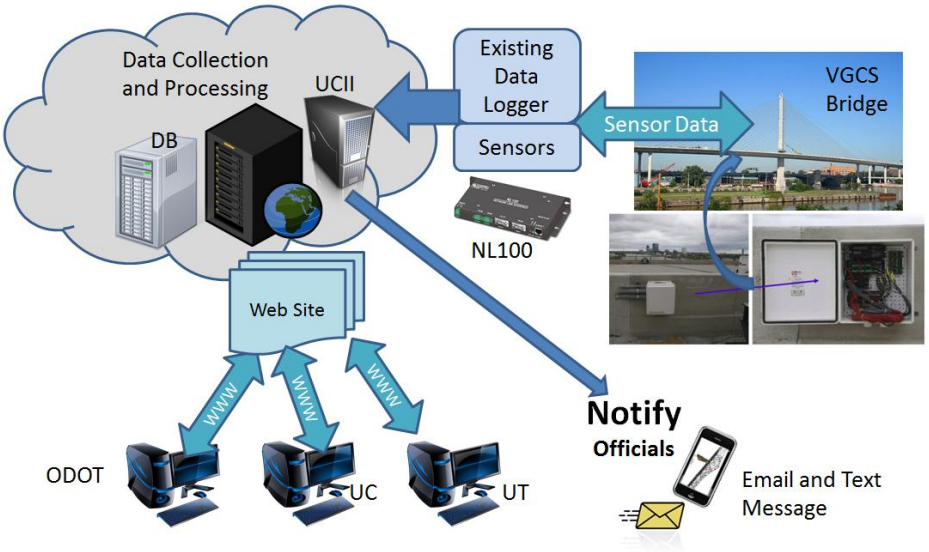

Figure 16.1: Complete Monitor System Diagram

16.2 Instrumentation

The current system contains a Campbell Scientific (2) CR10X data-logger, AM16/32 Relay Multiplexers, an NL100 Network Link interface, a Geokon Vibrating Wire Digital Signal Processor (DSP) interface and 64 Geokon (3) Vibrating Wire Gages (VWG) embedded in the concrete.

A total of 64 vibrating wire embedded strain gages are installed, 8 for each lane as shown in Figure 16.2 (16 at each location) and 4 locations. Figure 16.2 is a schematic showing the gage layout inside one lane of each of the 4 locations on the bridge where sensors are installed.

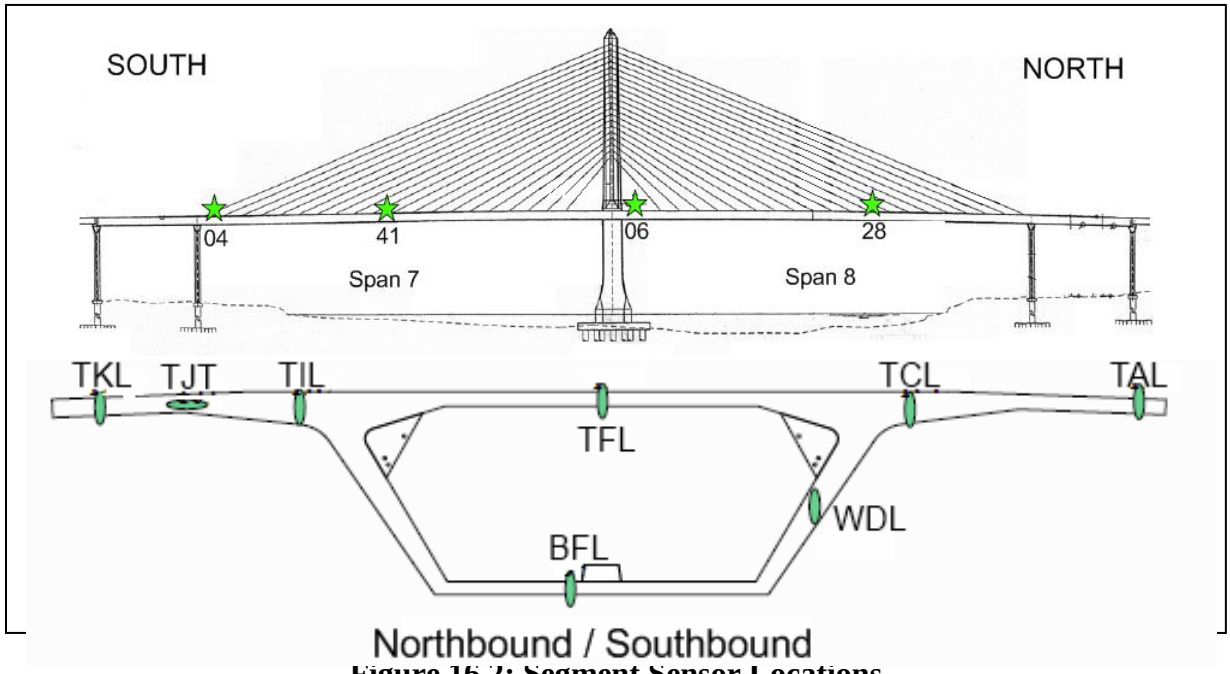

Figure 16.2: Segment Sensor Locations

16.3 Data Collection

The data collection and storage portion of the monitoring system is setup to take measurements every 30 minutes and store that information for download. Once stored by the data logger, the data is then ready for collection which can be carried out various ways. The remote collection of data from the bridge is done using a dedicated computer with a dedicated internet connection which links to the NL100 device located at the bridge. Scheduling the automatic collection of the data is done using the LoggerNet software provided by Campbell Scientific.

The bridge health monitor incorporates a standard process for formatting and warehousing the collected data from the bridge. In order for the data downloaded from the CR10X to integrate into a database, some custom programs were developed for pushing the sensor data into a MySQL (4) database. This custom program gets initiated by LoggerNet and also archives the raw sensor data collected from the CR10X data-logger.

Making the collected data accessible via the web means warehousing the data in a database. This not only makes the data accessible but also makes sections or slices of specific data easily attainable. The database design was based on requirements of typical requests of the sensor data and how to respond most efficiently and quickly. The database resides on servers at the UCII laboratory which run the MySQL database server software. Since the data is pushed immediately after each collection sequence, the database always maintains the latest sensor data and can be used for real time monitoring of the bridge.

16.4 Website

The front door of this project is the web site which provides the tool for monitoring the bridge's health. Not only does the site provide the health monitoring but also provides information about all the equipment used and locations of installed sensors. To make navigating the site easy for the targeted audience, its design was based on the ODOT home page (5). The web site's main sections include equipment information, information on the installation of the equipment and the monitoring system hardware. The navigation through the site is accomplished with a standard set of links on the left side that are always present. These links take you to the main sections of the web site and back to the main description page. The entire website is inaccessible by the general public and requires authorization by a username and password. Since the website is part of an ODOT funded project and was developed for UT and UCII researchers and ODOT staff to view, the website is limited to those personnel.

The monitor section of the web site is the most interactive and important section of the monitor and allows for plotting and analysis of sensor readings. The goal here was to provide a user-friendly interface to plot the strain readings but also includes a schematic of gage locations, a user input page, and an interactive plotting utility.

Figure 16.2 shows the schematic used on the monitor page and Figure 16.3 is a screen shot of the rest of the monitor page where the user interaction takes place. As shown the sensors installed on the bridge are listed on the left, which can be selected for plotting on a graph during a specified time frame. Temperature can also be plotted by selecting the check box next to it instead of Stress or Strain. The Strain vs. Temperature can be plotted for a particular gage but for this type of plot only one gage can be selected at a time. Once all of the desired parameters are chosen, the "Graph" button is selected to produce the plot based these selections. A maximum of eight sensors can be plotted and each is plotted in different colors. You can also export the data to a file which is formatted using the comma separated value (CSV) format for use in other programs, such as Microsoft™ Excel by selecting the "Export" button.

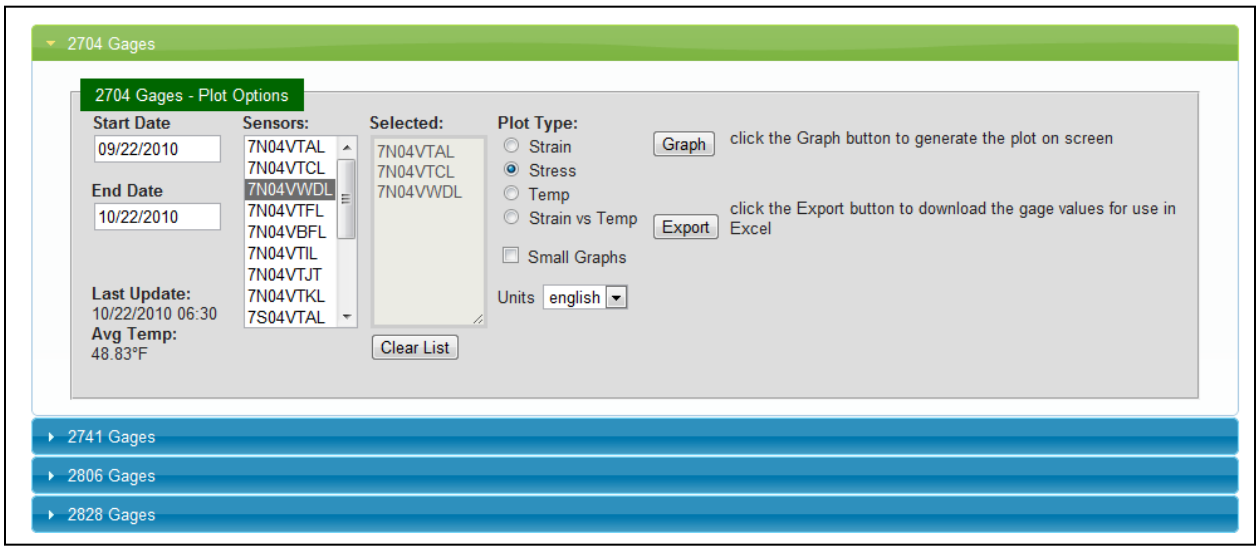

Figure 16.3: Monitor Web Site

Figure 16.4 are plots from the web site showing on the left a strain plot and on the right a temperature plot. Both plots are for two sensors which as can be seen in the temperature plot read the same temperature values.

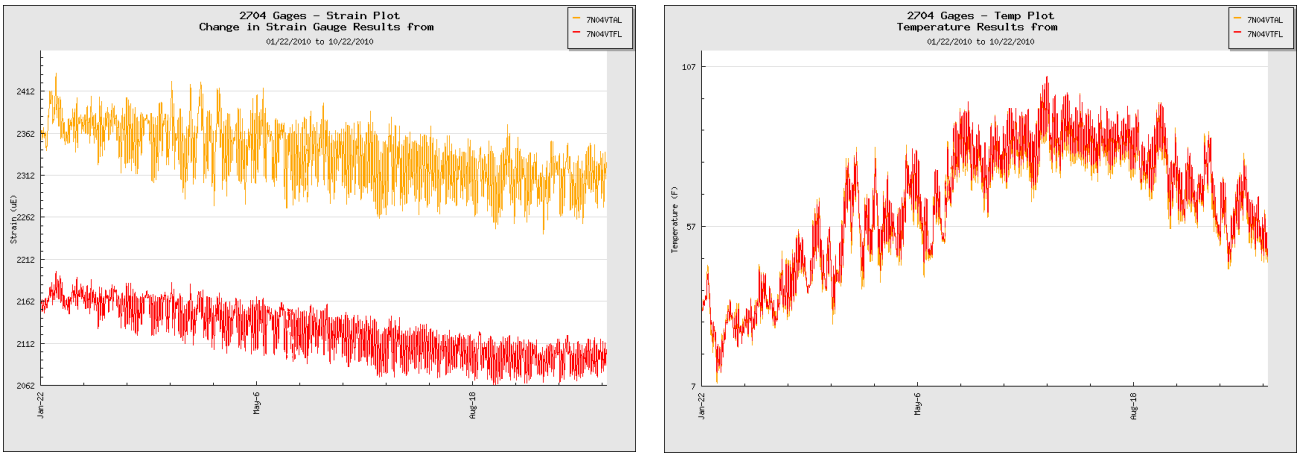

Strain (µE) **Temperature (°F)**

Figure 16.4: Web Monitor Sample Plots

16.5 Conclusion

This automated long-term health monitoring system is customizable and modular thus making it possible to add additional gages or other data driven devices. One main reason is the utilization of the existing manufacturer's software (in this case Campbell Scientific) in a customized fashion. The use of open-source software and web standards also makes the system open and easy for future customizations and additions. Currently the system consists of the following modules: data measurement, data collection and storage, and the web interface.

The data collection and warehousing of gage readings means not only can officials do further analysis of the bridges health but a historical archive of bridge performance is recorded. Plotting of strain data for multiple sensors over varying time frames means ODOT, UT and UCII can further analyze the health of certain sections or the bridge as a whole over seasonal changes. High speed connectivity allows for more frequent data collection which enables close to real time monitoring of the bridge and conditions like cold weather or icing. This also allows for a close to real time model of the bridge for possible fault detection and the ability to automatically send warning notifications.

References

1. G. Kimmel, J. Kumpf, V. Hunt, J. Swanson, A. Helmicki, "Automated Health Monitoring of an Aged and Deteriorated Truss," *Proceedings of ASNT Fall Conference and Quality Testing Show*, Columbus, OH, October, 2009.
2. *Campbell Scientific: dataloggers, data acquisition systems, weather stations*, Campbell Scientific Inc, 2012, http://www.campbellsci.com/.

3. *Geokon Instrumentation*, Geokon Inc., 2012, http://geokon.com/.
4. *MySQL:: The world's most popular open source database*, Oracle Corporation, 2012, http://mysql.com/.
5. *The Ohio Department of Transportation*, The Ohio Department of Transportation, 2010, http://www.dot.state.oh.us/.

Chapter 17: Conclusions and Future Work

This project has focused on the instrumentation, monitoring and testing of the main span unit of the VGCS, one of Ohio's first long-span, cable-stayed bridges and one of only a few dozen such bridges in service in the nation. This effort looked at five main areas: (1) health monitoring; assessment of the changes in force distribution and bridge condition during erection and early service, (2) verification of design assumptions during erection, (3) investigation of the unique design features which have been incorporated into the VGCS, (4) investigation into the unique erection features and sequencing which will be used during its construction, and (5) investigation of stay cable vibration which is a general, unresolved issue for bridges of this type.

Based on the findings discussed in the previous chapters of this report, specific conclusions and recommendations can be offered as follows.

A health monitoring system for the bridge was designed, planned, and implemented for the Veteran's Glass City Skyway bridge, with data collection and archival throughout its construction and ultimately an automated, user-friendly interface on a dedicated website. The primary criteria for selecting the segments to be instrumented was the predicted stresses and rating factors using the analytical data provided by the designer. An addendum to the plans was prepared to document the items to be installed by the contractor (e.g., conduit, junction boxes, main data cabinet, phone service, power outlets, etc.), the general plan for instrumentation and testing, the required access to the site and casting yard by the university research team (URT), the requirements for notification during construction, and the protection of instrumentation, wiring, and data acquisition equipment. Once gages were installed on the rebar cage of the segments, the lead wires were routed to the inside parapet and protected from the elements by using trash bags and a white NEMA 4 box. Initially, each segment was handled independently (e.g., in the casting yard), but ultimately both northbound and southbound segments were combined at one multiplexer after their installation on the bridge. As per the plans, the contractor installed conduit along the length of the parapet, mounted the white boxes to the side of the parapet, installed the main data cabinet near the pylon, and connected all

these together to enable one common architecture for the health monitoring system. This will be facilitated by the web application which will provide the ability to check the status, plot and access all sensor data from the instrumentation backbones. This will also provide the research group the information needed to assess the equipment and system performance and validate any research findings or conclusions.

An extensive component of the project involved the use and development of analytical and FE models of the structure for a variety of reasons. Since a cable stayed bridge may exhibit a complex nonlinear behavior, it necessitates that all the assumptions made during the design stage be verified. Above all, if the cable stayed bridges is made of concrete segments whose behavior is inherently time dependent it adds to the problem of predicting a response. It was concluded from the literature that assumptions and choices like the kind analytical precision required, that is 2D or 3D analysis, use of particular type of finite element for elements like segments and cables, material property representation in the model and assumption regarding the way the bridge is going to behave at the connections go a long way towards determining the validity of the model. These assumption might speed up the analysis and may be acceptable at the design stage but they need to be verified before they could be use to generate quantitative data to be used for maintenance. For the proposed study, reviewing previous literature research efforts have yielded significant information that will used to develop initial models in such a way that they will require minimum changes afterwards to calibrate them. Also keeping in mind that the instrumentation suite employed for VGCS is a sparse one, it was decided to progressively calibrate the model, that is, make changes to the model parameters such as stiffness and support conditions so that the model output correlates well with the measured data even for intermediate stages of construction. This was done to instill confidence in the use of the model as a maintenance tool.

Another component of the project involved the installation of gaging whose data was used, in part, to track stresses and loadings developed during construction/erection. Total 64 vibrating wire strain gages were installed in eight segments at four cross sections to monitor the long-term behavior of this bridge. Data from these gages has been collected since the casting date of each segment. A method of assembling the time line

was developed, a Matlab program was written to combine the strain time history line for the data of one strain gage, and the experimental stresses were compared to analytical stresses calculated by the contractor.

From the sample study of the time history line from 28NB28BFL, a good match between construction events from the construction log and health monitoring strain gage data was observed. Other gages' data also showed a good fit to construction events. These good matches indicated that the gages worked properly during construction, and the data from these gages is an accurate reflection of the actual strains in the bridge.

By checking the gages at the same elevation located in the same longitudinal position, the assumption of a two dimensional model, where there is little bending about the vertical axis was verified. Based on this verification, information from one top and bottom gage in each cross section is concluded to be representative for the local load condition.

The next step was using the strain gage data to derive experimental stress time histories to compare them to the construction finite element analyses. To calculate converted stress time histories, the initial strain and modulus of elasticity are required. The initial strain for each gage can be obtained from the strain time history on the casting date. The modulus of elasticity can be assumed to be a constant because the construction procedure did not take too long time and thus influence the modulus of elasticity much.

By following this research procedure, the comparisons between analytical stress and experimental stress for selected gages were done.

Above all, this work supplied a convincing confirmation of both the accuracy of the gage monitoring process and the finite element analysis used in the design and construction of the VGCS.

The following actions are recommended for further data review:

- The modulus of elasticity as a time dependent coefficient should be studied in the future to generate a more accurate experimental stress time history line for a long time comparison and prediction.

- The continuous database of collected strain needs to be updated to the current time. Based on this database, the long-term monitoring, the future load condition prediction, and load rating can be correlated with the contractor's or another model.

- The zero strain estimate for each strain gage is inherently uncertain. The method of determining the zero strain should be more fully developed to minimize the uncertainty

- Other factors, such as temperature and geometry, which could influence the reduction of the strain gage data needs to be studied in the future to get a more accurate result.

Based on future truck testing and improving the accuracy of the long term strain data reduction, improved estimates of the short term and long term stresses can be made. These estimates of live load and dead load stresses can be used to establish an experimental load rating.

Temperature gradients in the VGCS were also studied with two main goals: to preliminarily assess if the bridge behaves as the AASHTO Code predicts, and to lay the foundation for future studies of temperature gradients. Results of the maximum and minimum temperature gradients in Segment 26NB14 were plotted for October, November, December of 2005 and January, February, March, April and September of 2006. It should be noted that the accuracy of the thermistors is +/- 0.5ºC, or +/- 0.9ºF. This amount of error could have a significant effect on the shape of the temperature gradients, as will be seen in the following figures, as often the range of temperatures for a temperature gradient was at most 8ºF. Depending on which way the individual thermistors err, the range of 8ºF could easily decrease to almost 6ºF or increase to nearly 10ºF.

Plots of the Positive Temperature Gradients were fairly consistent for most of the eight months of collected data. This consistency was in the shape of the gradient, while the actual temperatures varied. Consistency, however, was not the only attribute to observe from the temperature gradients; comparison of the actual gradients to the design gradient was done as well. It was found by inspecting the plots that the actual gradients follow and typically fall within the design gradient. One interesting similarity in the positive temperature gradient plots is that one or two of the upper gages, Gage VTHL and VTHT, was consistently colder than the bottom slab gage VBEL. This anomaly could be explained by the gage being located in a spot where it is surrounded by more concrete than other gages and that at the time of the maximum positive temperature gradient occurring the concrete immediately surrounding the gage did not have sufficient time to warm up as did gage VBEL. Lastly, the upper-most gages all fell within the design code, reaching upwards of 8ºF warmer than gage VBEL, while the design code temperature difference is 11ºF for the cross section at the height of those gages.

Plots of the negative temperature gradients were not as consistent as the positive temperature gradients, however, they were still insightful. Plots for two of the eight months of negative temperature gradients followed the general idea of the top slab being colder than the bottom slab, while the other six months actually were positive temperature gradients, indicating that negative temperature gradients never occurred during those months. Looking at the temperature difference in December between the coldest top slab gage and gage VBEL, it was found that this value was within the specified code value of 3.3ºF. However, in November, the gradient was not a maximum between the top-most gage and gage VBEL, it was between the one upper gage and the top-most gage. This could be explained in a similar way as in the positive temperature gradients when the gage is takes longer to be affected by temperature changes since it is embedded deeper in concrete than other gages.

Based on the results from the small set of data used, it can be said that the VGCS behaves within reason to the AASHTO Design Code. Sometimes the gradient didn’t follow the code so well, as seen with the variability in even the well-behaved positive temperature gradients, or the two negative temperature gradients that occurred. However,

taking into consideration the error of the thermistors, the variability of temperature cycles, the fast-changing weather patterns of northwest Ohio and the small data set available, the results were reasonable enough to say that the study of temperature gradients is a valuable pursuit. Based on the confirmation of the thermistors and the preliminary results from eight months of temperature data, it is recommended that temperature gradients in the instrumented bridge segments are studied for long periods of time, on the order of years.

The fact that only two of the eight months produced negative temperature gradients underlines the importance of studying temperature gradients and analyzing several years' worth of data versus several months and that negative temperature gradients do not occur very often.

A series of two sets of truckload tests was conducted on the structure. These were planned and run with two main goals in mind. One goal was to obtain baseline readings of the bridge so that future load tests could be run and the two sets of data could be compared. Comparing the data sets will be useful when assessing the health of the bridge, as increased levels of strain could indicate a loss of structural integrity such as excessive concrete cracking, or post-tensioning strand deterioration. The other main goal of the Truck Test was to confirm the Larsa model. By comparing the influence lines with the dynamic loading data, the model was confirmed. This confirmed model can be used in the future to predict stresses, strains or moments for any load configurations for future truck tests. The model could also be calibrated in the future to account for structural deficiencies found during future truck tests. With a model calibrated for structural deficiencies, it would be possible to look at any point in the bridge and determine if there were any sections which were overstressed, or could potentially become overstressed if further deterioration occurred. Thus, the health of the bridge could be monitored over time and structural repairs could be suggested based on any deterioration found either through visual inspection or by increases in strains from a truck load test.

During the first phase of this project a delta frame was instrumented and monitored. A sparse array of instrumentation concentrated in areas of high strain was

used to resolve uncertainties in modeling of a complex element of a cable stayed bridge. After calibration, the element model was used to verify that there was no cracking before service. Finally, the calibrated model of the element can be placed confidently in a model of the overall bridge. Also, the VGCS delta frames were heavily post tensioned during construction, inducing tension in the bottom chord. This could have potentially lead to development of cracks. Therefore, the bottom chord of VGCS delta frame 18B was instrumented in a few critical locations with the highest expected tensile strains to verify strain levels corresponding to critical post tensioning events. A relatively inexpensive sparse instrument array was installed and the measured response against the post tensioning events was used to develop a calibrated component model of the delta frame. First the model was calibrated against initial post tensioning and then used to generate surface strains for the initial post tensioning plus self weight. These strains were then checked against the cracking strain. Then this calibrated model was fit into a complex model of the cross section and the calibration was verified at this stage against measured response from final post tensioning. Surface strain levels at this stage were also checked against cracking. It was found that at both stages of post tensioning the surface strains were well below the cracking level. Since the final loading of the delta frame is stay stressing which induces compression in the delta frame bottom chord, it can be concluded that the bottom chord of the delta frame did not crack due to construction loads. This conclusion was also supported by the visual inspection of the delta frame done during construction.

Since the VGCS Bridge is instrumented for long term monitoring, the calibrated model of the delta frame which showed good correlation to measured response during the second post-tensioning was now ready to be used as a component of the full bridge model. Therefore, this work also contributes towards developing long term maintenance planning of VGCS. Though the efforts were directed towards expected problems at the VGCS, the verification of delta frame behavior under various construction arrangements will, provide more support for their use in this future.

In the initial phase of this work, the foundation for performing progressive calibration was laid. It assured the quality of the data collected. It verified the design

assumptions of linearity and symmetry. Since the project employed a sparse array of instrumentation, achieving these objectives was important to prove that the instrumentation array was sufficient for carrying out model calibration.

The uniqueness was in the progressively calibrated model of the bridge. The design models available for bridges were underlain by design assumptions, predicted responses to construction procedures and loads. Such design efforts satisfied the code requirements and had been found to be sufficient enough to ensure the service life and safety of the structure. But they lack the sophistication and accuracy required to be useful for maintenance purposes. Whereas a model developed and calibrated progressively is more responsive to changes since it is fine tuned with changing geometry, stiffness and against a variety of loading conditions. Satisfactory verification against all monitored construction stages instills confidence in its future use for inspection and maintenance purposes.

Transverse bending of the bottom slab was monitored in order to reconcile discrepancies in finite element analyses performed by the construction and design engineers. Vibrating wire strain gages were installed in the bottom slab of segments to monitor transverse bending. Data was collected during construction, as well as during the truck load test prior to opening the VGCS to traffic.

Two research studies focused on investigating the concentration of strain in the bottom slab of the delta frame by comparing the results of the experimental data to the analysis results provided by the design engineer.

Wright investigated strain concentrations in the bottom slab of the VGCS caused by the post-tensioning tendons used to hold the delta frames in place. Results of the research monitoring strain levels immediately behind the delta frame tension block following the tensioning of the DF4 tendon indicated that the strain magnitudes attenuated quickly when moving away from the zone of predicted response**.**

Ward studied the transverse bending behavior of the bottom slab by monitoring the slab prior to installation and after the bridge was completed and opened to traffic. Experimental results at a construction stage prior to stressing stay 8 were compared with analysis provided by the designer. Experimental results were higher than predicted by the design engineer, but less than those predicted by the construction engineer. Strains approaching the yield for reinforcement (approximately 2000με) were not observed at any point during construction. Strain magnitudes did not exceed 300με for any of the gages installed on the bottom slab.

Visual inspection following installation of the instrumented segments, as well as subsequent segments did not reveal any cracking in the bottom slab in the regions where large strains were predicted. Strain magnitudes from the gages installed on the bottom slab of segments 28SB15 and 28SB25 have been independently verified to be accurate by performing lab calibration of the actual gages used in the field.

In addition, data recorded during live load tests including the crane withdrawal and full scale truckload tests confirms the assertion that dead load bending behavior dominates the transverse bending capacity of the bottom slab.

Dead load effects caused by the self-weight of the segments and delta frames are the predominant factor in determining the capacity of the bottom slab in transverse bending of the bottom slab.

In this chapter, the analytical and experimental stresses from the time of stay stressing through service life up to the present time are compared. Time history of the analytical stresses in the contractor's as-built finite element model for staged construction (BD2) is compared to the time history of the stresses based on the strain data collected. Representative plots for the comparison are presented.

Stay cable stressing events eave a clear signature in the time history line and the exact time of each event is recorded in the stay cable stressing log. This study can verifies that the instrumented segments of VGCS behave as expected for the period studied

In another aspect of this study, the allowable stress (ASR) load rating method was used to evaluate the inventory load rating factor for analytical and experimental stresses. This work utilized results obtained from both models, long term monitoring results and truckload testing.

Stay vibration tests were also performed during multiple stages of cable erection of the Veteran's Glass City Skyway Bridge. The stays at VGCS have unique structural characteristics that posed challenges to traditional vibration-based force estimation. Unlike the high density polyethylene sheathing system often incorporated on cable stayed bridges, the relative stiffness of the stainless steel cover pipe prevents the sheath and strands from making contact except at a limited number of locations. The sheath can account for approximately 25% of the total cable mass and its influence needed to be taken into account for accurate estimation of cable tension. After refining the cable force formulation based on field test observations, future vibration-based force estimations can be implemented in lieu of lift-off measurements.

In past, operational modal analysis has been shown to give good results with both analytical and lab based experimental data. In this study, the performance of these algorithms has been further analyzed by means of studies conducted on a cable stayed bridge. The modal parameter estimates obtained are shown to have comparative results with respect to at least two algorithms. In certain cases, the mode shapes appear to be similar. One of the reasons for this is the limited spatial resolution, which gives rise to observability related issues. However, with the help of the available knowledge in terms of the FE model, all the important modes have been estimated properly. Thus the study underlines the two key points of modal analysis in general that 1) its always good to have some a priori information available, and 2) the importance of good test planning, set up and good data acquisition because the parameter estimation algorithm is only as good as the data collected.

This automated long-term health monitoring system for bridges is highly customizable and modular thus making it possible to add additional gages or other data driven divices. One main reason is the utilization of the existing manufacturer's software

in a customized fashion. The most important and potential stopping point for such a system is remote connectivity but with modern devices such as cell phones even fairly remote locations can be connected. The use of open-source software and web standards also makes the system more apt to future customizations and additions. Currently the system consists of the following modules: data collection, data analysis and storage, and the web interface.

The data collection and warehousing of gage readings means not only can officials do further analysis of the bridges health but a historical archive of bridge performance is recorded. Plotting of strain data for multiple sensors over varying time frames means ODOT and UCII can further analyze the health of certain sections or the bridge as a whole over seasonal changes. High speed connectivity allows for more frequent data collection which enables close to real time monitoring of the bridge and conditions like cold weather or icing. This also allows for a close to real time model of the bridge for possible fault detection and warning.

To summarize, based on the discussion above, this project sought to implement and operate an appropriate instrumentation and field testing program to support management of the VGCS through construction and on into its service life. This program augments the traditional visual inspection program to provide objective, quantitative data for use by ODOT in assessing the status of the structure. There is value in continuing to collecting, archive and analyze the strain data from the bridge. The data will give insight into how the bridge is ageing and ascertain that the actual long term behavior is that expected during design.